2009

The role of water stress in plant disease resistance and the impact of water stress on the global transcriptome and survival mechanisms of the phytopathogen *Pseudomonas syringae*

Brian Carl Freeman
Iowa State University

The role of water stress in plant disease resistance and the impact of water stress on the global transcriptome and survival mechanisms of the phytopathogen *Pseudomonas syringae*

by

Brian C. Freeman

A dissertation submitted to the graduate faculty
in partial fulfillment of the requirements for the degree of

DOCTOR OF PHILOSOPHY

Major: Plant Pathology

Program of Study Committee:
Gwyn A. Beattie, Major Professor
Larry J. Halverson
Edward J. Braun
Thomas J. Baum
Lynn G. Clark

Iowa State University

Ames, Iowa

2009

Dedication

To my parents, who inspired me to dream about the stars,
and to my wife, who helped me reach them.

Table of Contents

Abstract

Leaf water status may play a significant role in determining the outcome of bacterial-plant interactions based on changes in leaf hydration as well as the molecular and physiological changes that occur in bacterial cells when responding to such stresses. In this study, we characterized localized changes in leaf hydration of *Arabidopsis thaliana* that occurred in response to challenge with the ubiquitous bacterial plant pathogen *Pseudomonas syringae*. We found that *A. thaliana* resistance to *P. syringae* pv. tomato DC3000 cells expressing *avrRpm1* involved virtually complete cessation of vascular water movement into the infection site coupled with water loss through the stomata. Interestingly, suppression of bacterial growth during AvrRpm1-mediated resistance was prevented by physically blocking leaf water loss through the stomata or by incubating plants at high relative humidity. Collectively, these results indicate that gene-for-gene resistance in *A. thaliana* requires at least a localized loss of water for effective suppression of *P. syringe* growth, suggesting that this water loss either directly starves the invading bacteria of water or induces other components of the hypersensitive response that suppress bacterial growth. To understand the responses of *P. syringae* to low water availability and if these responses vary among strains, we performed a transcriptome analysis of the closely related strains *P. syringae* pv. tomato DC3000 and pv. syringae B728a exposed to water stress. We found significant differences in gene expression between the two strains. For example, certain osmoadaptation genes were induced more strongly in B728a than in DC3000, including those for alginate biosynthesis and osmoprotectant transporters. In addition, many genes involved with pathogenicity and virulence, including genes in the HrpL regulon, were suppressed in DC3000 but not altered or even induced in B728a. Lastly, to better understand the ecological importance of the major compatible solute trehalose in *P. syringae*, we examined three putative trehalose biosynthetic operons in DC3000. Mutants lacking any of the operons were more sensitive to the effects of osmotic stress than wild-type DC3000. In addition, mutants lacking all three operons exhibited decreased survival compared to that of the wild type when grown on host and non-host plants. These results indicate that trehalose biosynthesis plays an important role in protecting *P. syringae* cells from osmotic stress and contributes to survival of this important pathogen when growing in association with host and non-host plants.

General introduction

Bacteria are ubiquitous in the phyllosphere where many species are able to colonize leaf surfaces and influence plant health. Many foliar bacterial plant pathogens are able to establish large epiphytic populations that can invade leaves and cause disease. The leaf surface is a harsh environment where low water availability is a constant threat to resident microbes, and bacteria that are able to colonize this habitat must be able to endure desiccation and osmotic stress brought about as surface water evaporates and the remaining dissolved solutes become highly concentrated. Epiphytic population sizes are often strongly correlated with disease incidence and severity, and differences in bacterial stress tolerance may significantly influence these populations during periods of water stress. Furthermore, changes in leaf hydration are known to occur during both disease and plant defense responses, and may influence the outcome of bacterial-plant interactions; this outcome may also be influenced by the response of a bacterial pathogen to water limitation. In the present study, we evaluated changes in leaf physiology and water content in plants following infection (challenge) with pathogenic and non-pathogenic bacterial strains, as well as the subsequent impact of these changes on bacterial population sizes. In addition, we performed a transcriptome analysis of two closely related strains of the bacterial pathogen *Pseudomonas syringae* exposed to water stress in order to better understand the impact of changes in gene expression on abiotic stress responses and bacterial survival. When faced with water stress, many bacteria accumulate compatible solutes, including the disaccharide trehalose, in order to restore cellular osmotic balance. The contribution of trehalose accumulation to survival of leaf-associated bacteria in the phyllosphere is poorly understood. Osmotolerance is among several fitness traits predicted to contribute to the ability of bacterial pathogens such as *P. syringae* to colonize leaf surfaces, and trehalose clearly protects bacterial cells from osmotic stress. Therefore, trehalose accumulation may contribute to bacterial survival on leaf surfaces as well as pathogen survival within endophytic sites of susceptible host plants. Trehalose biosynthetic pathways have not been characterized for many foliar plant pathogens including *P. syringae*. In this study, we elucidated the putative trehalose biosynthetic pathways in *P. syringae*. In addition, we characterized the role of trehalose accumulation in survival of *P. syringae* in high osmolarity growth media as well as in association with both host and non-host plants.

Dissertation organization

This dissertation is divided into five chapters. The first chapter provides a review of the literature on bacterial-plant interactions and the influence of water status on plant health and bacterial survival. The second chapter presents studies on the changes in leaf water status that occur when plants are challenged with pathogenic and non-pathogenic bacterial strains, as well as the effects these changes have on bacterial population sizes. The third chapter presents transcriptional profiling of two closely related strains of the leaf-associated bacterial species *P. syringae* in response to osmotic water stress to better understand the influence of gene expression changes on abiotic stress responses and bacterial survival. The fourth chapter characterizes the trehalose biosynthetic pathways present in *P. syringae* and the influence of trehalose accumulation on survival of this organism when exposed to water stress and when growing in association with host and non-host plants. The fifth chapter contains my general conclusions and possible future directions.

Chapter 1. Literature review

The leaf as a habitat for bacterial colonization

Microbes are natural inhabitants of above-ground plant parts, a habitat referred to as the phyllosphere. Bacteria that colonize aerial plant surfaces are called epiphytes (Leben 1965; Hirano and Upper 1983), and they can be found in numbers as high as 10^6 to 10^7 cells per cm^2 (Beattie and Lindow 1995; Andrews and Harris 2000; Hirano and Upper 2000). Culturable bacterial communities isolated from leaves appear to differ substantially from those isolated from bulk soil or the rhizosphere (Fokkema and van de Heuvel 1986; Beattie and Lindow 1995; Lindow and Brandl 2003). Microbial communities on leaves appear to be dominated by a few culturable genera (Dickinson et al. 1975; Ercolani 1983; Thompson et al. 1993; Jacques et al. 1995), with bacterial diversity lowest during the warmest and driest months of the season and highest during the cooler wet months (Ercolani 1991). Epiphytic populations differ significantly in size between plants of the same species, as well as over short time scales or throughout the entire growing season (Hirano and Upper 1989).

The leaf surface is a hostile environment where bacterial colonists are exposed to rapid fluctuations in temperature, relative humidity, solar radiation, and the intermittent presence of available free water. Low water availability may be the most significant obstacle faced by resident microbes on leaf surfaces, as epiphytic populations generally increase in the presence of water but decrease when leaves are dry (Hirano and Upper 1983; Hirano and Upper 1990). Bacteria that are able to colonize this habitat must be able to endure desiccation and osmotic stress brought about as surface water evaporates and remaining dissolved solutes become highly concentrated. Many foliar plant pathogens are able to colonize leaf surfaces and establish large populations (Crosse 1959) where they can invade leaves and cause disease (Hirano and Upper 1983). The sizes of epiphytic populations of plant pathogens such as *Pseudomonas syringae* are strongly correlated with disease incidence and severity (Lindemann et al. 1984; Rouse et al. 1985). Therefore, characterizing the traits necessary for epiphytic survival and colonization are important because this knowledge could help researchers develop more effective disease control

measures. In this study, we test the hypothesis that leaf water availability plays a critical role in determining bacterial population sizes in the phyllosphere.

Bacteria are not found uniformly scattered across the leaf surface. Leaf imprints have demonstrated that bacteria are often located in "protected sites", including the base of trichomes (Leben 1969; Bashan et al. 1982; Mew and Vera Cruz 1986; Mansvelt and Hattingh 1989), stomata and stomatal pits (Miles et al. 1977; Roos and Hattingh 1983; Mew and Vera Cruz 1986; Timmer et al. 1987; Mansvelt and Hattingh 1989), epidermal cell wall junctions (Leben 1969; Blakeman 1985; Davis and Brlansky 1991), leaf vein grooves (Leben 1988; Mansvelt and Hattingh 1989), and hydathodes (Mew et al. 1984). These regions likely represent areas where water and nutrients are more freely available and the bacteria can escape the harsh effects of solar radiation. The ability to access these protected sites and escape environmental stresses is conferred on bacteria, in part, by flagellar motility, an important fitness trait (Kennedy and Ercolani 1978; Haefele and Lindow 1987) that also allows phytopathogenic bacteria to access the leaf interior of susceptible host plants where they can reproduce and cause disease (Panopoulos and Schroth 1974; Bayot and Ries 1986; Hattermann and Ries 1989).

Bacteria are able to actively modify the leaf surface habitat in order to make conditions more favorable for growth. For example, bacteria can increase the wettability of leaves by secreting surfactants (Bunster et al. 1989; Hutchison and Johnstone 1993). The water films created by these biosurfactants may help hydrate epiphytic bacterial cells and facilitate movement of bacteria to more favorable sites (Lindow and Brandl 2003). Bacteria also modify their local environment by producing exopolymeric substances (EPS). Scanning electron micrographs reveal strands of material emanating from bacterial cells on leaves (Miles et al. 1977; Roos and Hattingh 1983; Timmer et al. 1987; Mansvelt and Hattingh 1989; Davis and Brlansky 1991). EPS may anchor bacterial cells to the leaf surface and prevent desiccation by encapsulating cells in a hygroscopic matrix (Wilson et al. 1965; Takahashi and Doke 1984). Synthesis of alginate, a component of EPS, is stimulated by desiccation stress in *P. syringae* (Singh et al. 1992; Keith and Bender 1999) and contributes to epiphytic fitness of this organism on dry leaves (Yu et al. 1999). High cell densities induce the expression of particular genes (Pierson et al. 1998; Bassler 1999) and contribute to epiphytic fitness (Monier and Lindow 2003)

via quorum sensing cell-cell signals. Leaf-associated bacteria often differ significantly in their ability to establish large epiphytic populations. Expression levels of genes coding for important epiphytic traits such as alginate production and flagellar motility could play a critical role in determining epiphytic fitness. In this study, we conducted a transcriptome analysis between two closely related pathovars of *P. syringae* that differ in their ability to colonize leaf surfaces in order to determine whether differences in gene expression may influence bacterial responses to water stress.

Osmotolerance is important for epiphytic survival, as osmosensitive mutants of *P. syringae* exhibit reduced survival on drying leaf surfaces (Lindow et al. 1993; Beattie and Lindow 1994; Beattie and Lindow 1994). Other fitness traits that contribute to epiphytic survival of *P. syringae* include UV-mediated mutagenic repair (Sundin et al. 1996; Sundin and Murillo 1999), a functional type III secretion system (Hirano et al. 1999), surface attachment via type IV pili (Roine et al. 1998), and secretion of plant hormones (Mazzola and White 1994).

Cellular water movement and bacterial adaptation to water stress

The movement of water is a thermodynamic process governed by both water pressure gradients and concentration gradients. Water tends to move spontaneously from areas of high to low pressures and concentrations, and as it does so, it releases free energy due to increased entropy. The potential energy of a given volume of water, or "water potential", is measured in units of energy (joules/m^3) or units of pressure (megapascals, or MPa, or bars). Water potential (Ψ_w) is a relative value, with pure water at 1 atm having a water potential of 0 MPa. As water moves down pressure or concentration gradients, free energy is released and the water potential is represented as a negative value. For example, water containing 1M sucrose has a water potential of -0.244 MPa, while water containing 1M NaCl has a water potential of -0.488 (double that of sucrose due to the presence of *two* moles of dissolved ions).

The water status of plant and bacterial cells is governed by several factors, including the osmotic (Ψ_s) and matric (Ψ_m) water potentials of both the cell and its environment, and cell turgor pressure (Ψ_p). Osmotic potential is measured as the availability of water when dissolved

solutes are present. Water containing dissolved solutes is less “available” to a living cell than pure water because fewer water molecules are actually present in a given volume due to the presence of the added solute molecules. When water forms thin films on surfaces only a few molecules thick, water molecules exhibit a natural attraction for the surface through a complex interaction of forces. This phenomenon is measured as the “matric” potential of water and commonly occurs in soil and other dry habitats where water is present but not freely available for living cells. Differences in water potential between a cell and its environment are the driving forces for water accumulation in living cells; water is not transported into cells by energetic pumps. The semi-permeable lipid membranes of living cells allow water to move somewhat freely into and out of cells while restricting the movement of dissolved solutes, particularly large molecules and charged ions, in a process called osmosis. As a result, water tends to move spontaneously into cells when the internal osmolarity is high, and out of cells when the internal osmolarity is low. In order to grow and maintain a well hydrated cytoplasm, both bacteria and plant cells must accumulate cytosolic osmolytes in concentrations higher than the external medium in order to force water to flow down the concentration gradient and into the cell.

The water status of an organism is perhaps the most important determinant of overall health and likely plays a significant role in determining the outcome of bacterial-plant interactions. Well-hydrated bacterial and plant cells exhibit a strong turgor pressure as the cytoplasm pushes out against the semi-rigid cell wall. Small changes in water content can lead to large changes in turgor pressure. In bacteria, hypoosmotic shock generally results in only small increases in cell volume due to the rigidity of the cell wall (Stock et al. 1977), although extreme hypoosmotic shock can lead to cell lysis. Hyperosmotic shock, in contrast, results in plasmolysis, a rapid efflux of water from the cell and a resultant shrinkage in cytoplasmic volume (Koch 1984; Miller et al. 1986). The kinetics and magnitude of plasmolysis are determined by the osmolarity of the external medium, not the nature of the dissolved solutes, provided that the cell membrane is impenetrable to these compounds. As a result, molecules such as glycerol and ethanol, which can freely diffuse across lipid membranes, do not cause plasmolysis (Mitchell and Moyle 1956).

Mild hyperosmotic shock causes only transient plasmolysis as cells typically undergo osmotic adjustment via the accumulation of cytoplasmic osmoprotectants in order to restore osmotic equilibrium. The steady-state cytoplasmic volume continues to be dependent on the external osmolarity following osmoadaptation, however, such that cytoplasmic volume decreases with increasing external osmolarity (Csonka 1989). Sudden plasmolysis inhibits a variety of essential cellular processes including nutrient uptake and DNA replication (Roth et al. 1985; Roth et al. 1985; Walter et al. 1987) as the rapid increase in cytoplasmic molecular concentrations begin to inhibit enzymatic processes and ions reach potentially toxic levels. Bacteria generally respond to hyperosmotic stress by accumulating compatible solutes, cytoplasmic osmoprotectants that can accumulate to high levels without disrupting cellular machinery. These compounds can include K^+ ions, the amino acids glutamate, glutamine, proline, γ-aminobutyrate and alanine, the quaternary amines glycine betaine and other amino acid derivatives including NAGGN, and the sugars sucrose, trehalose, and glucosylglycerol (Flowers et al. 1977; Yancey et al. 1982; Imhoff 1986; Reed et al. 1986). Bacteria can accumulate these compounds through *de novo* synthesis or via uptake of osmoprotectants from the external environment (Csonka and Hanson 1991). Osmoprotectants such as glycine betaine can function directly as compatible solutes, or they can serve as precursors, such as choline, which is converted to glycine betaine after uptake. Uptake is generally favored because it requires far less energy and nutrient resources than *de novo* synthesis. The contribution of compatible solute accumulation to survival of bacteria in the phyllosphere is poorly understood, yet it likely plays a significant role considering that low water availability is one of the most important obstacles faced by leaf-associated bacteria. In this study, we characterized the contribution of trehalose to survival of *P. syringae* in hyperosmotic growth media as well as growing in association with host and non-hot plants.

P. syringae pv. tomato strain DC3000 is distinct from most bacterial species in deriving greater osmoprotection from exogenous choline than from glycine betaine (Chen and Beattie 2007). Choline and phosphorylcholine are ubiquitous in plants whereas glycine betaine is produced in detectable amounts by some plant species but not others (Storey and Jones 1975). *P. syringae* has likely developed mechanisms to exploit plant-derived compounds as part of its adaptive response to low water availability and other stresses that are common in the

phyllosphere. The superior osmoprotection derived from choline is the result of the BetT transporter, a secondary transporter in the betaine-choline-carnitine transporter (BCCT) family that rapidly transports choline when present in high concentrations (Chen and Beattie 2008). BetT activity is induced in response to hyperosmolarity but can mediate significant uptake under low-osmolarity conditions, suggesting dual roles in both osmotic stress adaptation and catabolism. In addition to the BCCT family, DC3000 possesses transporters in the ATP-binding cassette (ABC) family, including OpuC, which functions as the primary transporter for glycine betaine and as one of multiple transporters for choline under high osmolarity. The BccVWX transporter is another ABC transporter and is a homolog of the *E. coli* ProU transporter that does not appear to be regulated by hyperosmolarity (Chen and Beattie 2007). In this study, we conducted a transcriptome analysis between two closely related pathovars of *P. syringae* that differ in their osmotolerance in order to determine whether differences in gene expression may influence bacterial responses to water stress.

Disease mechanisms of Pseudomonas syringae

Pseudomonas syringae is a widespread and economically significant gram-negative bacterial pathogen that has become a model organism for the study of plant-pathogen interactions. *P. syringae* is divided into over 50 pathovars based on host specificity, and some pathovars are further divided into races based on the ability to cause disease on specific differential cultivars. The typical infection cycle begins with pathogen colonization of external plant parts and establishment of epiphytic populations. Next, *P. syringae* enter leaves through open stomata (Melotto et al. 2006), hydathodes (Bretschneider et al. 1989), cracks in the cuticle (Mansvelt and Hattingh 1989), or in wounds including broken trichomes (Schneider and Grogan 1977; Pohronczny K. et al. 1992). Once inside, bacterial populations begin to grow. *P. syringae* commonly causes leaf spots, chlorosis, and necrosis on susceptible species but can elicit a hypersensitive response on resistant and non-host species. On susceptible hosts, disease symptoms typically develop after several days following bacterial growth in the intercellular spaces of plant tissues, while the hypersensitive response can occur within 24 hours in plant cells that are in physical contact with the pathogen (Richael and Gilchrist 1999). Eventually, endophytic populations egress through lesions and open stomata, allowing the bacteria to spread to healthy plant tissue via rain splash or contaminated seeds.

Pathogenicity and virulence genes determine the host range and disease severity of phytopathogenic bacteria. In *P. syringae*, some of these genes are organized into discreet clusters called pathogenicity islands (PAIs). *P. syringae*, like many bacterial pathogens, relies on protein effectors secreted directly into plant cells via a type III secretion system (T3SS) where they modulate host signaling pathways and promote disease. The T3SS acts as a molecular "syringe" by translocating effectors directly across the host cell membrane. Following contact with a host cell, *P syringae* forms a T3SS complex that penetrates the plant cell wall and translocates effectors directly into the cytoplasm, possibly through a pore in the host plasmalemma. Many gram-negative bacterial pathogens employ type III secretion systems, including animal pathogens in the genera *Yersinia*, *Salmonella*, *Shigella*, and *Escherichia,* and plant pathogens in the genera *Pseudomonas*, *Erwinia (Pantoea)*, *Xanthomonas*, and *Ralstonia* (Hueck 1998; Galan and Collmer 1999). Phytopathogenic bacteria that employ this system are able to colonize the intercellular spaces of plant tissues where they (eventually) cause plant cell death. Genes that encode the T3SS system were originally called *hrp* genes, for hypersensitive response and pathogenicity (He 1998).

At least nine genes of the type III secretion system are conserved among a wide range of plant and animal pathogens (Bogdanove et al. 1996). These genes encode an outer-membrane protein, an outer-membrane associated lipoprotein, five inner-membrane proteins, and two cytoplasmic proteins, including a putative ATPase (Bogdanove et al. 1996). These structural core components are also known as *hrc* (HR-conserved) genes and they share strong homology with the *fli/flh* genes of *E. coli* and other bacteria that encode components of bacterial flagella. Although the minimal number of *hrp* genes required for pathogenesis has not been defined, mutational analysis has demonstrated that a number of *hrp/hrc* gene products are required for secretion of disease effectors by *P. syringae*, including HrcU, HrcC, HrpE, HrpZ and HrpA (Huang et al. 1995). HrpA is the major structural component of the T3SS pilus and acts as a positive regulator of T3SS activity (Yuan and He 1996).

Regulation of the *hrp* system is complex and the environmental signals that induce *hrp* gene expression are specific for each bacterial species. In general, *hrp* genes are induced in

plants and minimal nutrient media but repressed in complex media (Lindgren 1997). Expression is influenced by carbon and nitrogen sources, pH, osmolarity, temperature, and plant signal molecules. Identification of these conditions has led to the development of *hrp*-inducing media that may mimic the conditions found in the plant apoplast and are used for the *in vitro* expression of the *hrp* regulon. One of the best characterized regulatory systems is the *P. syringae* HrpR/S/L multicomponent transcriptional regulatory system. The HrpR/S system is related to the NtrB/C class of two-component nitrogen-sensing regulatory systems (Xiao et al. 1994). The system consists of a sensor kinase (HrpS) that detects the specific environmental conditions of the apoplast and subsequently activates a response regulator (HrpR) via phosphorylation. HrpR activates transcription of the HrpL transcriptional regulator by binding to the *hrpL* promoter. *hrpL* also contains a conserved σ^{54} binding motif in its promoter region that is recognized by the alternative sigma factor RpoN, and RpoN is required for induction of *hrpL* in some bacterial species (Lindgren 1997). Once induced, HrpL, a sigma factor, induces the expression of a number of T3SS-related genes by facilitating RNA polymerase binding to promoter regions that contain the consensus sequence GGAACCNA-N_{14}-CCACNNA, also known as the *hrp*- or *avr*-box (Xiao and Hutcheson 1994).

Recent advances in genomics and bioinformatics have allowed researchers to identify dozens of putative effectors in the *P. syringae* genome by identifying promoters that contain *hrp*-boxes (Greenberg and Vinatzer 2003). These effectors are commonly referred to as *hop* (*hrp*-dependent outer protein) or *avr* (avirulence) genes, with the latter name referring to the role of some in triggering the resistance (*R*) gene-mediated hypersensitive response. Effector repertoires vary in size and composition among strains. Only 13 effectors are shared between three fully sequenced strains of *P. syringae* pathovars tomato (strain DC3000), syringae (strain B728a) and phaseolicola (strain 1448a), with the remaining 40 additional effectors unique to one strain or shared between only two strains (Collmer et al. 2000). Unlike the *hrp/hrc* T3SS core components, many *P. syringae* effectors are not organized into clusters on the bacterial chromosome. For example, more than half of the effector genes in *P. syringae* DC3000 occur in ten clusters of two or more genes (nine on the chromosome and a tenth on plasmid A) while the other half seem to exist as orphans.

The targets of most effectors are not known. Mutational analysis has demonstrated that most effectors only contribute a small, quantitative role in promoting bacterial growth and disease (Alfano and Collmer 1996), and often do so, in part, by suppressing host defenses. Targets for suppression via T3SS effectors include the hypersensitive response, defense gene expression, cell wall–based defenses, jasmonate signaling, the plant proteasome system, and stomatal closure (Hauck et al. 2003; Cui et al. 2005; Abramovitch et al. 2006; Janjusevic et al. 2006; Rigano et al. 2007). DC3000 secretes several effectors involved with suppressing basal defense, including AvrPto (Hauck et al. 2003), AvrRpt2 and AvrRpm1 (Kim et al. 2005). Transgenic *Arabidopsis thaliana* plants expressing any one of these proteins are severely compromised in their ability to express basal defenses, as detected by an inability to deposit callose in their cell walls when challenged with non-pathogenic DC3000 *hrcC* mutants (Hauck et al. 2003). AvrRpt2 and AvrRpm1 act on the host protein RPM1-INTERACTING PROTEIN-4 (RIN4), a negative regulator of basal defense (Kim et al. 2005). Other effectors that suppress basal defense include HopPtoM and AvrE (DebRoy et al. 2004). In addition to suppressing basal defenses, AvrRpt2 also acts to suppress the HR and disease resistance induced by AvrRpm1 (Ritter and Dangl 1996). A number of other DC3000 effectors also suppress the HR in non-host plants, including AvrPtoB, AvrPphE, AvrPpiB1, AvrPto, HopPtoD2, HopPtoE, HopPtoF, and HopPtoN (Abramovitch et al. 2003; Bretz et al. 2003; Espinosa et al. 2003; Jamir et al. 2004; Kang et al. 2004; Lopez-Solanilla et al. 2004; Lin and Martin 2005).

Bacterial effectors also appear to modulate plant hormone signaling in order to promote disease. The DC3000 effector AvrPtoB stimulates abscisic acid (ABA) production in host plants leading to suppression of host defenses and increased susceptibility (de Torres-Zabala et al. 2007). AvrRpt2 modulates host auxin levels and increases susceptibility (Chen et al. 2007). In *Xanthamonas* spp. but not *Pseudomonas* spp., some effectors may even act as transcription factors. The effector AvrBs3 secreted by *Xanthomonas campestris* pv. vesicatoria localizes to the plant nucleus where it binds to the promoters of cell size regulators and causes hypertrophy (Kay et al. 2007), and the AvrBs3-like effector PthA from the citrus canker pathogen *X. axonopodis* pv. citri causes cell enlargement and may also act as a transcription factor (Shiotani et al. 2008).

In addition to type III secretion, pathovars of *P. syringae* produce a variety of phytotoxins that contribute significantly to disease; these include coronatine, syringomycin, syringopeptin, tabtoxin, and phaseolotoxin. Coronatine, produced by strain DC3000, which was widely used in my studies, is a polyketide mimic of the plant octadecanoid signaling hormone methyl jasmonate that antagonizes salicylic acid-mediated defense signaling and induces chlorosis, hypertrophy, inhibition of root elongation, and stimulation of ethylene production (Gnanamaickam et al. 1982; Völksch et al. 1989; Kenyon and Turner 1992). Coronatine has also been shown to act on guard cells and reopen stomata during basal defense, perhaps as a mechanism to allow bacteria to evade stomatal closure and enter the leaf apoplast (Melotto et al. 2006). Syringomycins and syringopeptins, produced by strain B728a, a focus of Chapter 3, are cyclic lipodepsinonapeptides and lipodepsipeptides, respectively, which forms cation pores directly in lipid bilayers, resulting in deadly transmembrane fluxes of K^+, H^+ and Ca^{2+} (Backman and DeVay 1971; Iacobellis et al. 1992). Tabtoxin, produced by *P. syringae* pv. tabaci strains, is a dipeptide that irreversibly inhibits glutamine synthetase, halting glutamine synthesis and resulting in the accumulation of toxic levels of ammonia in plant tissues (Thomas et al. 1983). Phaseolotoxin, produced by *P. syringae* pv. phaseolicola, is a sulfodiaminophosphinyl peptide that inhibits ornithine carbamoyl transferase (OCTase), a critical enzyme in the urea cycle. Inhibition of OCTase causes an accumulation of ornithine and a deficiency in intracellular pools of arginine, leading to chlorosis (Mitchell and Bieleski 1977). For the strains employed in this study, the phytotoxins generally act as virulence factors and are involved in the production of disease symptoms but they are not required for pathogenicity.

Plant defenses against bacterial pathogens

Plants have developed multiple layers of sophisticated surveillance mechanisms that are capable of recognizing potentially dangerous pathogens and rapidly responding before the induction of disease. As a result, very few bacterial species are pathogens of plants. Plant surveillance systems are linked to specific pre-programmed defense responses that fall into two broad categories, basal resistance and the hypersensitive response. Basal resistance, also called innate immunity (Nurnberger and Brunner 2002) or local induced resistance (Dow et al. 2000; Klement et al. 2003), is a “first line” of defenses that protect plants against entire groups of pathogens. Basal resistance includes both pre-formed and inducible physical barriers and

antimicrobial agents. Inducible defenses are triggered by both pathogens and non-pathogens that possess so-called microbe-associated molecular patterns (MAMPs). These MAMPs include conserved regions of bacterial flagellin (Felix et al. 1999), cold-shock protein (Felix and Boller 2003), bacterial elongation factor Tu (Kunze et al. 2004) and lipopolysaccharides (Felix et al. 1999; Dow et al. 2000; Felix and Boller 2003). Basal resistance is localized to the site of infection and is accompanied by several changes in host tissue, including the production of callose (β-1,3-glucan)-rich papillae in cell walls, a transient oxidative burst accompanied by increased levels of peroxidases, the production of phenolic compounds, and synthesis of hydroxyproline-rich glycoproteins (Lovrekovich and Farkas 1965; Klement et al. 1999). MAMP recognition triggers signaling events and transcriptional reprogramming in affected cells. MAPK cascades signal MAMP-recognition to the plant cell (Asai et al. 2002), followed by the rapid induction of genes that encode transcription factors, proteins involved in protein degradation, hormone biosynthesis, phosphatases, and protein kinases associated with LRR-receptor-like kinases (RLKs) (Navarro et al. 2004; Thilmony et al. 2006; Truman et al. 2006). As previously mentioned, a large number of type III effectors secreted by pathogenic bacteria suppress basal resistance.

Pathogens that are able to circumvent a host's basal resistance system may trigger a more radical phenomenon, the hypersensitive response (HR). The HR is characterized by deliberate programmed plant cell death that is localized to the site of infection. A variety of microbes can elicit the HR, including oomycetes, fungi, bacteria, and viruses. Accordingly, the physiological, molecular and phenotypic characteristics can vary tremendously depending upon the specific plant-pathogen interaction (Mur et al. 2008). The HR is triggered when resistance (*R*) gene products in the host "recognize" the presence of specific avirulence (*avr*) effectors introduced by the pathogen, a so-called "gene-for-gene" interaction (Flor 1956).

Once initiated, the HR is characterized by the production of a flurry of signal molecules including reactive oxygen species (ROS), Ca^{2+}, nitric oxide (NO), and salicylic acid (SA). The production of ROS, including superoxide (O_2^-) and hydrogen peroxide (H_2O_2), is part of a so-called "oxidative burst" that is one of the earliest cellular responses to pathogen recognition. Plant cells typically produce low levels of reactive oxygen molecules as a natural byproduct of

cellular metabolism, but the combined action of scavenging enzymes including superoxide dismutase and catalase convert these molecules into water and oxygen. During pathogen recognition, and particularly the hypersensitive response, plant cells generate superoxide radicals and peroxides by the action of NADPH oxidase and peroxidases present in the plant cell membrane and cell wall, respectively. This oxidative burst is a requirement for HR induction, and treatment of plant tissues with catalase can suppress formation of HR necrosis. The free-radicals generated during the HR cause peroxidation of lipids and partial depolarization of the cell membrane, resulting in an influx of Ca^{2+} (Levine et al. 1996; Blume et al. 2000) and an efflux of potassium and other electrolytes. NO is another signal molecule produced during pathogen recognition, and it is required in conjunction with the oxidative burst to initiate hypersensitive cell death and trigger disease resistance (Delledonne et al. 1998). SA is a plant signaling molecule involved in local and systemic defense responses to pathogen attack (Durrant and Dong 2004). ROS stimulate SA production (Leon et al. 1995), and SA levels increase dramatically in cells surrounding infection sites (Enyedi et al. 1992). SA accumulation can down-regulate ROS scavenging systems in cells adjacent to HR lesions that can contribute to increased overall ROS levels following pathogen recognition (Klessig et al. 2000).

Following these signaling events, an infected plant cell is irreversibly destined for death. The plasmalemma pulls away from the cell wall (Heath 2000; Naton et al. 1996), followed by the formation of large vacuoles reminiscent of autophagy (Bestwick et al. 1995; Liu et al. 2005). As the cytoplasm shrinks, organelles including the mitochondria and chloroplasts begin to break down (Seo et al. 2000; Lam et al. 2001). Photosynthesis ceases as PSII reaction centers are damaged by protein degradation (Almeras et al. 2003). Nuclear chromatin condenses and the DNA breaks up into fragments (Kiba et al. 2006), followed by cell membrane lysis. Induction of a local HR leads to the activation of systemic acquired resistance (SAR), a phenomenon associated with increased resistance to a wide range of pathogens for days or weeks following activation (Narusaka et al. 1999).

Surprisingly, the physiological mechanisms directly responsible for *P. syringae* growth restriction during the HR remain poorly understood. Whereas plant cell death may play a direct role in inhibiting obligate biotrophs that require living host tissue for survival, the role of cell

death in inhibiting hemibiotrophic or necrotrophic pathogens is less clear because these pathogens do not require living host tissue. Preformed antimicrobial compounds such as phytoalexins have been shown to inhibit some pathogens but not others (Osbourn 1996). Phytoalexins are low molecular weight compounds produced during incompatible pathogen challenge with clear antimicrobial activity *in vitro*. *Arabidopsis thaliana* produces the phytoalexin camalexin, and a number of phytoalexin mutants have been identified. However, these mutants are still capable of restricting avirulent strains of *P. syringae*, suggesting that camalexin is not required for resistance to this pathogen (Glazebrook and Ausubel 1994). Reactive oxygen molecules may function directly as antimicrobial agents, but the level of toxicity depends upon the sensitivity of the pathogen and the ROS concentration (Levine et al. 1994). The micromolar concentrations of ROS measured in some plants during the HR are sufficient to inhibit bacterial growth *in vitro* (Wu et al. 1995), but determining a causal relationship *in planta* has proven problematic. Callose production in cells adjacent to HR lesions can block plasmodesmata and impede cell-to-cell movement of some viruses (Beffa et al. 1996), but the role of callose in preventing bacterial infection is less well known.

Previous studies found that *P. syringa*e strain DC3000 encountered inhibitory levels of water stress during the hypersensitive response in *A. thaliana* (Wright and Beattie 2004). We hypothesize that low water availability in the apoplast may directly restrict endophytic bacterial populations by starving invading cells of water. In the present study, we evaluate changes in *A. thaliana* leaf water content that occur during the HR and characterize the physiological mechanisms responsible for leaf water loss, including changes in stomatal activity, leaf transpiration, and vascular water flow. We then evaluate the impact of leaf water loss on populations of *P. syringae*. If our hypothesis is correct, the synthesis of compatible solutes such as trehalose should influence survival of invading *P. syringae* cells. Thus, we also examine the role of trehalose production on the survival of *P. syringae* in association with living plants. In addition, we perform transcriptional profiling of two closely related strains of *P. syringae* in response to osmotic water stress to better understand the influence of gene expression changes on abiotic stress responses and bacterial survival.

References

Abramovitch, R. B., Janjusevic, R., Stebbins, C. E. and Martin, G. B. 2006. Type III effector AvrPtoB requires intrinsic E3 ubiquitin ligase activity to suppress plant cell death and immunity. Proc. Natl. Acad. Sci. U.S.A 103:2851-2856.

Abramovitch, R. B., Kim, Y. J., Chen, S., Dickman, M. B. and Martin, G. B. 2003. *Pseudomonas* type III effector AvrPtoB induces plant disease susceptibility by inhibition of host programmed cell death. EMBO J. 22:60-69.

Alfano, J. R. and Collmer, A. 1996. Bacterial pathogens in plants: Life up against the wall. Plant Cell 8:1683-1698.

Almeras, E., Stolz, S., Vollenweider, S., Reymond, P., Mene-Saffrane, L. and Farmer, E. E. 2003. Reactive electrophile species activate defense gene expression in *Arabidopsis*. Plant J. 34:205-216.

Andrews, J. H. and Harris, R. F. 2000. The ecology and biogeography of microorganisms on plant surfaces. Annu. Rev. Phytopathol. 38:145-180.

Asai, T., Tena, G., Plotnikova, J., Willmann, M. R., Chiu, W. L., Gomez-Gomez, L., Boller, T., Ausubel, F. M. and Sheen, J. 2002. MAP kinase signalling cascade in *Arabidopsis* innate immunity. Nature 415:977-983.

Backman, P. A. and DeVay, J. E. 1971. Studies on the mode of action and biogenesis of the phytotoxin syringomycin. Physiol. Plant Pathol. 1:215-234.

Bashan, Y., Diab, S. and Okon, Y. 1982. Survival of *Xanthomonas campestris* pv. vesicatoria in pepper seeds and roots in symptomless and dry leaves in non-host plants in the soil. Plant Soil 68:161-170.

Bassler, B. L. 1999. How bacteria talk to each other: regulation of gene expression by quorum sensing. Curr. Opin. Microbiol. 2:582-587.

Bayot, R. G. and Ries, S. M. 1986. Role of motility in apple blossom infection by *Erwinia amyiovora* and studies of fire blight control with attractant and repellent compounds. Phytopathology 76:441-445.

Beattie, G. A. and Lindow, S. E. 1994. Comparison of the behavior of epiphytic fitness mutants of *Pseudomonas syringae* under controlled and field conditions. Appl. Environ. Microbiol. 60:3799-3808.

Beattie, G. A. and Lindow, S. E. 1994. Survival, growth, and localization of epiphytic fitness mutants of *Pseudomonas syringae* on leaves. Appl. Environ. Microbiol. 60:3790-3798.

Beattie, G. A. and Lindow, S. E. 1995. The secret life of foliar bacterial pathogens on leaves. Annu. Rev. Phytopathology 33:145-172.

Beffa, R. S., Hofer, R. M., Thomas, M. and Meins, F., Jr. 1996. Decreased susceptibility to viral disease of [beta]-1,3-glucanase-deficient plants generated by antisense transformation. Plant Cell 8:1001-1011.

Bestwick, C. S., Bennett, M. H. and Mansfield, J. W. 1995. Hrp mutant of *Pseudomonas syringae* pv. phaseolicola induces cell wall alterations but not membrane damage leading to the hypersensitive reaction in lettuce. Plant Physiol. 108:503-516.

Blakeman, J. P. 1985. Ecological succession of leaf surface microorganisms in relation to biological control. In *Biological Control on the Phylloplane*, ed. C.E. Windels, S.E. Lindow. pp. 6-30. St. Paul, MN: American Phytopathological Society

Blume, B., Nurnberger, T., Nass, N. and Scheel, D. 2000. Receptor-mediated increase in cytoplasmic free calcium required for activation of pathogen defense in parsley. Plant Cell 12:1425-1440.

Bogdanove, A. J., Beer, S. V., Bonas, U., Boucher, C. A., Collmer, A., Coplin, D. L., Cornelis, G. R., Huang, H. C., Hutcheson, S. W., Panopoulos, N. J. and Van Gijsegem, F. 1996. Unified nomenclature for broadly conserved *hrp* genes of phytopathogenic bacteria. Mol. Microbiol. 20:681-683.

Bretschneider, K. E., Gonella, M. P. and Robeson, D. J. 1989. A comparative light and electron microscopical study of compatible and incompatible interactions between *Xanthomonas campestris* pv. campestris and cabbage (*Brassica oleracea*). Physiol. Mol. Plant Pathol. 34:285-297.

Bretz, J. R., Mock, N. M., Charity, J. C., Zeyad, S., Baker, C. J. and Hutcheson, S. W. 2003. A translocated protein tyrosine phosphatase of *Pseudomonas syringae* pv. tomato DC3000 modulates plant defence response to infection. Mol. Microbiol. 49:389-400.

Bunster, L., Fokkema, N. J. and Schippers, B. 1989. Effect of surface-active *Pseudomonas* spp. on leaf wettability. Appl. Environ. Microbiol. 55:1340-1345.

Chen, C. and Beattie, G. A. 2008. *Pseudomonas syringae* BetT is a low-affinity choline transporter that is responsible for superior osmoprotection by choline over glycine betaine. J. Bacteriol. 190:2717-2725.

Chen, C. L. and Beattie, G. A. 2007. Characterization of the osmoprotectant transporter OpuC from *Pseudomonas syringae* and demonstration that cystathionine-beta-synthase domains are required for its osmoregulatory function. J. Bacteriol. 189:6901-6912.

Chen, Z., Agnew, J. L., Cohen, J. D., He, P., Shan, L., Sheen, J. and Kunkel, B. N. 2007. *Pseudomonas syringae* type III effector AvrRpt2 alters *Arabidopsis thaliana* auxin physiology. Proc. Natl. Acad. Sci. U.S.A. 104:20131-20136.

Collmer, A., Badel, J. L., Charkowski, A. O., Deng, W. L., Fouts, D. E., Ramos, A. R., Rehm, A. H., Anderson, D. M., Schneewind, O., van Dijk, K. and Alfano, J. R. 2000. *Pseudomonas syringae* Hrp type III secretion system and effector proteins. Proc. Natl. Acad. Sci. U.S.A. 97:8770-8777.

Crosse, J. E. 1959. Bacterial canker of stonefruits. IV. Investigation of a method for measuring the innoculum potential of cherry trees. Ann. Appl. Biol. 47:306-317.

Csonka, L. N. 1989. Physiological and genetic responses of bacteria to osmotic stress. Microbiol. Rev. 53:121-147.

Csonka, L. N. and Hanson, A. D. 1991. Prokaryotic osmoregulation: genetics and physiology. Annu Rev Microbiol 45:569-606.

Cui, J., Bahrami, A. K., Pringle, E. G., Hernandez-Guzman, G., Bender, C. L., Pierce, N. E. and Ausubel, F. M. 2005. *Pseudomonas syringae* manipulates systemic plant defenses against pathogens and herbivores. Proc. Natl. Acad. Sci. U.S.A. 102:1791-1796.

Davis, C. L. and Brlansky, R. H. 1991. Use of immunogold labelling with scanning electron microscopy to identify phytopathogenic bacteria on leaf surfaces. Appl. Environ. Microbiol. 57:3052-3055.

de Torres-Zabala, M., Truman, W., Bennett, M. H., Lafforgue, G., Mansfield, J. W., Rodriguez Egea, P., Bogre, L. and Grant, M. 2007. *Pseudomonas syringae* pv. tomato hijacks the *Arabidopsis* abscisic acid signalling pathway to cause disease. EMBO J. 26:1434-1443.

DebRoy, S., Thilmony, R., Kwack, Y. B., Nomura, K. and He, S. Y. 2004. A family of conserved bacterial effectors inhibits salicylic acid-mediated basal immunity and promotes disease necrosis in plants. Proc. Natl. Acad. Sci. U.S.A. 101:9927-9932.

Delledonne, M., Xia, Y., Dixon, R. A. and Lamb, C. 1998. Nitric oxide functions as a signal in plant disease resistance. Nature 394:585-588.

Dickinson, C. H., Austin, B. and Goodfellow, M. 1975. Quantitative and qualitative studies of phylloplane bacteria from *Lolium perenne*. J. Gen. Microbiol. 91:157–166.

Dow, M., Newman, M. A. and von Roepenack, E. 2000. The induction and modulation of plant defense responses by bacterial lipopolysaccharides. Annu. Rev. Phytopathol. 38:241-261.

Durrant, W. E. and Dong, X. 2004. Systemic acquired resistance. Annu. Rev. Phytopathol. 42:185-209.

Enyedi, A. J., Yalpani, N., Silverman, P. and Raskin, I. 1992. Localization, conjugation, and function of salicylic acid in tobacco during the hypersensitive reaction to tobacco mosaic virus. Proc. Natl. Acad. Sci. U.S.A. 89:2480-2484.

Ercolani, G. L. 1983. Variability among isolates of *Pseudomonas syringae* pv. savastanoi from the phylloplane of the olive. J. Gen. Microbiol. 129:901-916.

Ercolani, G. L. 1991. Distribution of epiphytic bacteria on olive leaves and the influence of leaf age and sampling time. Microb. Ecol. 21:35–48.

Espinosa, A., Guo, M., Tam, V. C., Fu, Z. Q. and Alfano, J. R. 2003. The *Pseudomonas syringae* type III-secreted protein HopPtoD2 possesses protein tyrosine phosphatase activity and suppresses programmed cell death in plants. Mol. Microbiol. 49:377-387.

Felix, G. and Boller, T. 2003. Molecular sensing of bacteria in plants. The highly conserved RNA-binding motif RNP-1 of bacterial cold shock proteins is recognized as an elicitor signal in tobacco. J. Biol. Chem. 278:6201-6208.

Felix, G., Duran, J. D., Volko, S. and Boller, T. 1999. Plants have a sensitive perception system for the most conserved domain of bacterial flagellin. Plant J. 18:265-276.

Flor, H. 1956. The complementary genic systems in flax and flax rust. Advances in Genetics 8:29-54.

Flowers, T. J., Troke, P. R. and Yeo, A. R. 1977. The mechanism of salt tolerance in halophites. Annu. Rev. Plant Physiol. 28:89-121.

Fokkema, N. J. and van de Heuvel, J. 1986. Microbiology of the phyllosphere. Cambridge; New York, Cambridge University Press.

Galan, J. E. and Collmer, A. 1999. Type III secretion machines: bacterial devices for protein delivery into host cells. Science 284:1322-1328.

Glazebrook, J. and Ausubel, F. M. 1994. Isolation of phytoalexin-deficient mutants of *Arabidopsis thaliana* and characterization of their interactions with bacterial pathogens. Proc. Nat. Acad. Sci. U.S.A. 91:8955-8959.

Gnanamaickam, S. S., Starratt, A. N. and Ward, E. W. B. 1982. Coronatine production in vitro and in vivo and its relation to symptom development in bacterial blight of soybean. Can. J. Bot. 60:645-650.

Greenberg, J. T. and Vinatzer, B. A. 2003. Identifying type III effectors of plant pathogens and analyzing their interaction with plant cells. Curr. Opin. Microbiol. 6:20-28.

Haefele, D. M. and Lindow, S. E. 1987. Flagellar motility confers epiphytic fitness advantages upon *Pseudomonas syringae*. Appl. Environ. Microbiol. 53:2528-2533.

Hattermann, D. R. and Ries, S. M. 1989. Motility of *Pseudomonas syringae* pv. glycinea and its role in infection. Phytopathology 79:284-289.

Hauck, P., Thilmony, R. and He, S. Y. 2003. A *Pseudomonas syringae* type III effector suppresses cell wall-based extracellular defense in susceptible *Arabidopsis* plants. Proc. Natl. Acad. Sci. U.S.A. 100:8577-8582.

He, S. Y. 1998. Type III protein secretion systems in plant and animal pathogenic bacteria. Annu. Rev. Phytopathol. 36:363-392.

Heath, M. C. 2000. Hypersensitive response-related death. Plant Mol. Biol. 44:321-334.

Hirano, S. S., Charkowski, A. O., Collmer, A., Willis, D. K. and Upper, C. D. 1999. Role of the Hrp type III protein secretion system in growth of *Pseudomonas syringae* pv. syringae B728a on host plants in the field. Proc. Natl. Acad. Sci. U.S.A. 96:9851-9856.

Hirano, S. S. and Upper, C. D. 1983. Ecology and epidemiology of foliar bacterial plant pathogens. Annu. Rev. Phytopathol. 21:243-269.

Hirano, S. S. and Upper, C. D. 1989. Diel variation in population size and ice nucleation activity of *Pseudomonas syringae* on snap bean leaflets. Appl. Environ. Microbiol. 55:623-630.

Hirano, S. S. and Upper, C. D. 1990. Population biology and epidemiology of *Pseudomonas syringae*. Ann. Rev. Phytopathol. 28:155-177.

Hirano, S. S. and Upper, C. D. 2000. Bacteria in the leaf ecosystem with emphasis on *Pseudomonas syringae*-a pathogen, ice nucleus, and epiphyte. Microbiol. Mol. Biol. Rev. 64:624-653.

Huang, H. C., Lin, R. H., Chang, C. J., Collmer, A. and Deng, W. L. 1995. The complete hrp gene cluster of *Pseudomonas syringae* pv. syringae 61 includes two blocks of genes required for harpin Pss secretion that are arranged colinearly with *Yersinia ysc* homologs. Mol. Plant-Microbe Interact. 8:733-746.

Hueck, C. J. 1998. Type III protein secretion systems in bacterial pathogens of animals and plants. Microbiol. Mol. Biol. Rev. 62:379-433.

Hutchison, M. L. and Johnstone, K. 1993. Evidence for the involvement ofthe surface active properties of the extracellular toxin tolaasin in the manifestation of brown blotch disease symptoms by *Pseudomonas tolaasii* on *Agaricus bisporus*. Physiol. Mol. Plant Pathol. 42:373–384.

Iacobellis, N. S., Lavermicocca, P., Grgurina, I., Simmaco, M. and Ballio, A. 1992. Phytotoxic properties of *Pseudomonas syringae* pv. syringae toxins. Physiol. Mol. Plant Pathol. 40:107-116.

Imhoff, J. F. 1986. Osmoregulation and compatible solutes in eubacteria. FEMS Microbiol. Rev. 39:57-66.

Jacques, M., Kinkel, L. L. and Morris, C. E. 1995. Population sizes, immigration, and growth of epiphytic bacteria on leaves of different ages and positions of field-grown endive (*Cichorium endivia* var. latifolia). Appl. Environ. Microbiol. 61:899-906.

Jamir, Y., Guo, M., Oh, H. S., Petnicki-Ocwieja, T., Chen, S., Tang, X., Dickman, M. B., Collmer, A. and Alfano, J. R. 2004. Identification of *Pseudomonas syringae* type III effectors that can suppress programmed cell death in plants and yeast. Plant J. 37:554-565.

Janjusevic, R., Abramovitch, R. B., Martin, G. B. and Stebbins, C. E. 2006. A bacterial inhibitor of host programmed cell death defenses is an E3 ubiquitin ligase. Science 311:222-226.

Kang, L., Tang, X. and Mysore, K. S. 2004. *Pseudomonas* type III effector AvrPto suppresses the programmed cell death induced by two nonhost pathogens in *Nicotiana benthamiana* and tomato. Mol. Plant-Microbe Interact. 17:1328-1336.

Kay, S., Hahn, S., Marois, E., Hause, G. and Bonas, U. 2007. A bacterial effector acts as a plant transcription factor and induces a cell size regulator. Science 318:648-651.

Keith, L. M. and Bender, C. L. 1999. AlgT (sigma22) controls alginate production and tolerance to environmental stress in *Pseudomonas syringae*. J. Bacteriol. 181:7176-7184.

Kennedy, B. W. and Ercolani, G. L. 1978. Soybean primary leaves as a site for epiphytic multiplication of *Pseudomonas glycinea*. Phytopathology 68:1196-1201.

Kenyon, J. S. and Turner, J. G. 1992. The stimulation of ethylene synthesis in *Nicotiana tabacum* leaves by the phytotoxin coronatine. Plant Physiol. 100:219-224.

Kiba, A., Takata, O., Ohnishi, K. and Hikichi, Y. 2006. Comparative analysis of induction pattern of programmed cell death and defense-related responses during hypersensitive cell death and development of bacterial necrotic leaf spots in eggplant. Planta 224:981-994.

Kim, H. S., Desveaux, D., Singer, A. U., Patel, P., Sondek, J. and Dangl, J. L. 2005. The *Pseudomonas syringae* effector AvrRpt2 cleaves its C-terminally acylated target, RIN4, from *Arabidopsis* membranes to block RPM1 activation. Proc. Natl. Acad. Sci. U.S.A. 102:6496-6501.

Kim, M. G., da Cunha, L., McFall, A. J., Belkhadir, Y., DebRoy, S., Dangl, J. L. and Mackey, D. 2005. Two *Pseudomonas syringae* type III effectors inhibit RIN4-regulated basal defense in *Arabidopsis*. Cell 121:749-759.

Klement, Z., Bozso, Z., Kecskes, M. L., Besenyei, E., Arnold, C. and Ott, P. G. 2003. Local early induced resistance of plants as the first line of defense against bacteria. Pest Manag. Sci. 59:465-474.

Klement, Z., Bozso, Z., Ott, P. G., Kecskes, M. L. and Rudolph, K. 1999. Symptomless resistant response instead of the hypersensitive reaction in tobacco leaves after infiltration of heterologous pathovars of *Pseudomonas syringae*. J. Phytopathol. 147:467–475.

Klessig, D. F., Durner, J., Noad, R., Navarre, D. A., Wendehenne, D., Kumar, D., Zhou, J. M., Shah, J., Zhang, S., Kachroo, P., Trifa, Y., Pontier, D., Lam, E. and Silva, H. 2000. Nitric oxide and salicylic acid signaling in plant defense. Proc. Nat. Acad. Sci. U.S.A. 97:8849-8855.

Koch, A. L. 1984. Shrinkage of growing *Escherichia coli* cells by osmotic stress. J. Bacteriol. 159:919-924.

Kunze, G., Zipfel, C., Robatzek, S., Niehaus, K., Boller, T. and Felix, G. 2004. The N terminus of bacterial elongation factor Tu elicits innate immunity in *Arabidopsis* plants. Plant Cell 16:3496-3507.

Lam, E., Kato, N. and Lawton, M. 2001. Programmed cell death, mitochondria and the plant hypersensitive response. Nature 411:848-853.

Leben, C. 1965. Epiphytic microorganisms in relation to plant disease. Annu. Rev. Phytopathol. 3:209-230.

Leben, C. 1969. Colonization of soybean buds by bacteria: observations with the scanning electron microscope. Can. J. Microbiol. 15:319-320.

Leben, C. 1988. Relative humidity and the survival of epiphytic bacteria with buds and leaves of cucumber plants. Phytopathology 78:179-185.

Leon, J., Lawton, M. A. and Raskin, I. 1995. Hydrogen peroxide stimulates salicylic acid biosynthesis in tobacco. Plant Physiol. 108:1673-1678.

Levine, A., Pennell, R. I., Alvarez, M. E., Palmer, R. and Lamb, C. 1996. Calcium-mediated apoptosis in a plant hypersensitive disease resistance response. Curr. Biol. 6:427-437.

Levine, A., Tenhaken, R., Dixon, R. and Lamb, C. 1994. H_2O_2 from the oxidative burst orchestrates the plant hypersensitive disease resistance response. Cell 79:583-593.

Lin, N. C. and Martin, G. B. 2005. An avrPto/avrPtoB mutant of *Pseudomonas syringae* pv. tomato DC3000 does not elicit Pto-mediated resistance and is less virulent on tomato. Mol. Plant-Microbe Interact. 18:43-51.

Lindemann, J., Arny, D. C. and Upper, C. D. 1984. Use of an apparent infection threshold population of *Pseudomonas syringae* to predict incidence and severity of brown spot of bean. Phytopathology 74:1334–1339.

Lindgren, P. B. 1997. The role of hrp genes during plant-bacterial interactions. Annu. Rev. Phytopathol. 35:129-152.

Lindow, S. E., Andersen, G. and Beattie, G. A. 1993. Characteristics of insertional mutants of *Pseudomonas syringae* with reduced epiphytic fitness. Appl. Environ. Microbiol. 59:1593-1601.

Lindow, S. E. and Brandl, M. T. 2003. Microbiology of the phyllosphere. Appl. Environ. Microbiol. 69:1875-1883.

Liu, Y., Schiff, M., Czymmek, K., Talloczy, Z., Levine, B. and Dinesh-Kumar, S. P. 2005. Autophagy regulates programmed cell death during the plant innate immune response. Cell 121:567-577.

Lopez-Solanilla, E., Bronstein, P. A., Schneider, A. R. and Collmer, A. 2004. HopPtoN is a *Pseudomonas syringae* Hrp (type III secretion system) cysteine protease effector that suppresses pathogen-induced necrosis associated with both compatible and incompatible plant interactions. Mol. Microbiol. 54:353-365.

Lovrekovich, L. and Farkas, G. L. 1965. Induced protection against wildfire disease in tobacco leaves treated with heat-killed bacteria. Nature 205:823–824.

Mansvelt, E. L. and Hattingh, M. J. 1989. Scanning electron microscopy of invasion of apple leaves and blossoms by *Pseudomonas syringae* pv. syringae. Appl. Environ. Microbiol. 55:533-538.

Mazzola, M. and White, F. F. 1994. A mutation in the indole-3-acetic acid biosynthesis pathway of *Pseudomonas syringae* pv. syringae affects growth in *Phaseolus vulgaris* and syringomycin production. J. Bacteriol. 176:1374-1382.

Melotto, M., Underwood, W., Koczan, J., Nomura, K. and He, S. Y. 2006. Plant stomata function in innate immunity against bacterial invasion. Cell 126:969-980.

Mew, T. W., Mew, I. C. and Huang, J. S. 1984. Scanning electron microscopy of virulent and avirulent strains of *Xanthomonas campestris* pv. oryzae on rice leaves. Phytopathology 74:635-641.

Mew, T. W. and Vera Cruz, C. M. 1986. Epiphytic colonization of host and non-host plants by phytopathogenic bacteria. Microbiology of the Phyllosphere, ed. N.J. Fokkema, J. van den Heuvel Press, Cambridge University. pp. 269-282.

Miles, W. G., Daines, R. H. and Rue, J. W. 1977. Presymptomatic egress of *Xanthomonas pruni* from infected peach leaves. Phytopathology 67:895-897.

Miller, K. J., Kennedy, E. P. and Reinhold, V. N. 1986. Osmotic adaptation by gram-negative bacteria: possible role for periplasmic oligosaccharides. Science 231:48-51.

Mitchell, P. and Moyle, J. 1956. Osmotic function and structure in bacteria. Symp. Soc. Gen. Microbiol. 6:150-180.

Mitchell, R. E. and Bieleski, R. L. 1977. Involvement of phaseolotoxin in halo blight of beans: Transport and conversion to functional toxin. Plant Physiol. 60:723-729.

Monier, J. M. and Lindow, S. E. 2003. Differential survival of solitary and aggregated bacterial cells promotes aggregate formation on leaf surfaces. Proc. Natl. Acad. Sci. U.S.A. 100:15977-15982.

Mur, L. A. J., Kenton, P., Lloyd, A. J., Ougham, H. and Prats, E. 2008. The hypersensitive response; the centenary is upon us but how much do we know? J. Exp. Bot. 59:501-520.

Narusaka, Y., Narusaka, M., Horio, T. and Ishii, H. 1999. Comparison of local and systemic induction of acquired disease resistance in cucumber plants treated with benzothiadiazoles or salicylic acid. Plant Cell Physiol. 40:388-395.

Naton, B., Hahlbrock, K. and Schmelzer, E. 1996. Correlation of rapid cell death with metabolic changes in fungus-infected, cultured parsley cells. Plant Physiol. 112:433-444.

Navarro, L., Zipfel, C., Rowland, O., Keller, I., Robatzek, S., Boller, T. and Jones, J. D. 2004. The transcriptional innate immune response to Flg22. Interplay and overlap with *avr* gene-dependent defense responses and bacterial pathogenesis. Plant Physiol. 135:1113-1128.

Nurnberger, T. and Brunner, F. 2002. Innate immunity in plants and animals: emerging parallels between the recognition of general elicitors and pathogen-associated molecular patterns. Curr. Opin. Plant Biol. 5:318-324.

Osbourn, A. E. 1996. Preformed antimicrobial compounds and plant defense against fungal attack. Plant Cell 8:1821-1831.

Panopoulos, H. I. and Schroth, M. N. 1974. Role of flagellar motility in the invasion of bean leaves by *Pseudomonas phaseolicola*. Phytopathology 64:1389-1397.

Pierson, L. S., 3rd, Wood, D. W. and Pierson, E. A. 1998. Homoserine lactone-mediated gene regulation in plant-associated bacteria. Annu. Rev. Phytopathol. 36:207-225.

Pohronczny K., Hewitt M., Infante J. and L., D. 1992. Wind and wind-generated sand injury as factors in infection of pepper by *Xanthomonas campestris* pv. vesicatoria. Plant Dis. 76:1036-1039.

Reed, R. H., Borowitzka, L. J., Mackay, M. A., Chudek, J. A., Foster, R., Warr, S. C. R., Moore, D. J. and Stewart, W. D. P. 1986. Organic solute accumulation in osmotically stressed cyanobacteria. FEMS Microbiol. Rev. 39:51-56.

Richael, C. and Gilchrist, D. 1999. The hypersensitive response: a case of hold or fold? Physiol. Mol. Plant Pathol. 55:5–12.

Rigano, L. A., Payette, C., Brouillard, G., Marano, M. R., Abramowicz, L., Torres, P. S., Yun, M., Castagnaro, A. P., El Oirdi, M., Dufour, V., Malamud, F., Dow, J. M., Bouarab, K. and Vojnov, A. A. 2007. Bacterial cyclic beta-(1,2)-glucan acts in systemic suppression of plant immune responses. Plant Cell 19:2077-2089.

Ritter, C. and Dangl, J. L. 1996. Interference between two specific pathogen recognition events mediated by distinct plant disease resistance genes. Plant Cell 8:251-257.

Roine, E., Raineri, D. M., Romantschuk, M., Wilson, M. and Nunn, D. N. 1998. Characterization of type IV pilus genes in *Pseudomonas syringae* pv. tomato DC3000. Mol. Plant-Microbe Interact. 11:1048-1056.

Roos, I. M. M. and Hattingh, M. J. 1983. Scanning electron microscopy of *Pseudomonas syringae* pv. morsprunorum on sweet cherry leaves. Phytopathology 108:18-25.

Roth, W. G., Leckie, M. P. and Dietzler, D. N. 1985. Osmotic stress drastically inhibits active transport of carbohydrates by *Escherichia coli*. Biochem. Biophys. Res. Commun. 126:434-441.

Roth, W. G., Porter, S. E., Leckie, M. P., Porter, B. E. and Dietzler, D. N. 1985. Restoration of cell volume and the reversal of carbohydrate transport and growth inhibition of osmotically upshocked *Escherichia coli*. Biochem. Biophys. Res. Commun. 126:442-449.

Rouse, D. I., Nordheim, E. V., Hirano, S. S. and Upper, C. D. 1985. A model relating the probability of foliar disease incidence to the population frequencies of bacterial plant pathogens. Phytopathology 75:505-509.

Schneider, R. W. and Grogan, R. G. 1977. Tomato leaf trichomes, a habitat for resident populations of *Pseudomonas tomato*. Phytopathology 67:898-902.

Seo, S., Okamoto, M., Iwai, T., Iwano, M., Fukui, K., Isogai, A., Nakajima, N. and Ohashi, Y. 2000. Reduced levels of chloroplast FtsH protein in tobacco mosaic virus-infected tobacco leaves accelerate the hypersensitive reaction. Plant Cell 12:917-932.

Shiotani, H., Yoshioka, T., Yamamoto, M. and Matsumoto, R. 2008. Susceptibility to citrus canker caused by *Xanthomonas axonopodis* pv. citri depends on the nuclear genome of the host plant. J. Gen. Plant Pathol. 74:1345-2630.

Singh, S., Koehler, B. and Fett, W. F. 1992. Effect of osmolarity and dehydration on alginate production by fluorescent pseudomonads. Curr. Microbiol. 25:335–339.

Stock, J. B., Rauch, B. and Roseman, S. 1977. Periplasmic space in *Salmonella typhemurium* and *Escerichia coli*. J. Biol. Chem. 252:7850-7861.

Storey, R. and Jones, R. G. W. 1975. Betaine and choline levels in plants and their relationship to NaCl stress. Plant Sci. Lett. 4:161-168.

Sundin, G. W., Kidambi, S. P., Ullrich, M. and Bender, C. L. 1996. Resistance to ultraviolet light in *Pseudomonas syringae*: sequence and functional analysis of the plasmid-encoded *rulAB* genes. Gene 177:77-81.

Sundin, G. W. and Murillo, J. 1999. Functional analysis of the *Pseudomonas syringae rulAB* determinant in tolerance to ultraviolet B (290-320 nm) radiation and distribution of rulAB among *P. syringae* pathovars. Environ. Microbiol. 1:75-87.

Takahashi, T. and Doke, N. 1984. A role of extracellular polysaccharides of *Xanthomonas campestris* pv. cirri in bacterial adhesion to citrus leaf tissues in preinfectious stage. Annu. Phytopathol. Soc. Jpn. 50.

Thilmony, R., Underwood, W. and He, S. Y. 2006. Genome-wide transcriptional analysis of the *Arabidopsis thaliana* interaction with the plant pathogen *Pseudomonas syringae* pv. tomato DC3000 and the human pathogen *Escherichia coli* O157:H7. Plant J. 46:34-53.

Thomas, M. D., Langston-Unkefer, P. J., Uchytil, T. F. and Durbin, R. D. 1983. Inhibition of glutamine synthetase from pea by tabtoxinin beta-lactam. Plant Physiol. 71:912-915.

Thompson, I. P., Bailey, M. J., Fenlon, J. S., Fermor, T. R., Lilley, A. K., Lynch, J. M., McCormack, P. J., McQuilken, M. P. and Purdy, K. J. 1993. Quantitative and qualitative seasonal changes in the microbial community from the phyllosphere of sugar beet (*Beta vulgaris*). Plant Soil 150:177–191.

Timmer, L. W., Marois, J. J. and Achor, D. 1987. Growth and survival of xanthomonads under conditions nonconducive to disease development. Phytopathology 77:1341-1345.

Truman, W., de Zabala, M. T. and Grant, M. 2006. Type III effectors orchestrate a complex interplay between transcriptional networks to modify basal defence responses during pathogenesis and resistance. Plant J. 46:14-33.

Völksch, B., Bublitz, F. and Fritsche, W. 1989. Coronatine production by *Pseudomonas syringae* pathovars: screening method and capacity of product formation. J. Basic Microbiol. 29:463-468.

Walter, R. P., Morris, J. G. and Kell, D. B. 1987. The roles of osmotic stress and water activity in the inhibition of the growth, glycolysis and glucose phosphotransferase system of *Clostridium pasteurianum*. J. Gen. Microbiol. 133:259-266.

Wilson, H. A., Lilly, V. G. and Leach, J. G. 1965. Bacterial polysaccharides IV. Longevity of *Xanthomonas phaseoli* and *Serratia marcescens* in bacterial exudates. Phytopathology 55:1135-1138.

Wright, C. A. and Beattie, G. A. 2004. *Pseudomonas syringae* pv. *tomato* cells encounter inhibitory levels of water stress during the hypersensitive response of *Arabidopsis thaliana*. Proc. Natl. Acad. Sci. U.S.A. 101:3269-3274.

Wu, G., Shortt, B. J., Lawrence, E. B., Levine, E. B., Fitzsimmons, K. C. and Shah, D. M. 1995. Disease resistance conferred by expression of a gene encoding H_2O_2 generating glucose oxidase in transgenic potato plants. Plant Cell 7:1357-1368.

Xiao, Y., Heu, S., Yi, J., Lu, Y. and Hutcheson, S. W. 1994. Identification of a putative alternate sigma factor and characterization of a multicomponent regulatory cascade controlling the expression of *Pseudomonas syringae* pv. syringae Pss61 *hrp* and *hrmA* genes. J. Bacteriol. 176:1025-1036.

Xiao, Y. and Hutcheson, S. W. 1994. A single promoter sequence recognized by a newly identified alternate sigma factor directs expression of pathogenicity and host range determinants in *Pseudomonas syringae*. J. Bacteriol. 176:3089-3091.

Yancey, P. H., Clark, M. E., Hand, S. C., Bowlus, R. D. and Somero, G. N. 1982. Living with water stress: evolution of osmolyte systems. Science 217:1214-1222.

Yu, J., Penaloza-Vazquez, A., Chakrabarty, A. M. and Bender, C. L. 1999. Involvement of the exopolysaccharide alginate in the virulence and epiphytic fitness of *Pseudomonas syringae* pv. syringae. Mol. Microbiol. 33:712-720.

Yuan, J. and He, S. Y. 1996. The *Pseudomonas syringae* Hrp regulation and secretion system controls the production and secretion of multiple extracellular proteins. J. Bacteriol. 178:6399-6402.

Chapter 2. Bacterial growth restriction during *Arabidopsis thaliana* resistance to *Pseudomonas syringae* is associated with leaf water loss and localized cessation of vascular activity

Brian C. Freeman and Gwyn A. Beattie
Department of Plant Pathology,
Iowa State University; Ames, IA, 50010, USA
(Accepted for publication in Molecular Plant-Microbe Interactions)

Abstract

The physiological mechanisms by which plants limit the growth of bacterial pathogens during gene-for-gene resistance are poorly understood. We characterized early events in the *Arabidopsis thaliana-Pseudomonas syringae* pathosystem to identify physiological changes for which the kinetics are consistent with bacterial growth restriction. Using a safranine-O dye solution to detect vascular activity, we demonstrated that *A. thaliana* Col-O resistance to *P. syringae* pv. tomato DC3000 cells expressing *avrRpm1* involved virtually complete cessation of vascular water movement into the infection site within only three hours post-inoculation (hpi) under the conditions tested. This vascular restriction preceded or was simultaneous with precipitous decreases in photosynthesis, stomatal conductance and leaf transpiration, with the latter two remaining at detectable levels. Microscopic plant cell death was detected as early as 2 hpi. Interestingly, suppression of bacterial growth during AvrRpm1-mediated resistance was eliminated by physically blocking leaf water loss through the stomata without altering plant cell death, and was nearly eliminated by incubating plants at high relative humidity. The majority of the population growth benefit from blocking leaf water loss occurred early after inoculation, i.e., between 4 and 8 hpi. Collectively, these results support a model in which *A. thaliana* suppresses *P. syringae* growth during gene-for-gene resistance, at least in part, by coupling restricted vascular flow to the infection site with water loss through partially open stomata; that is, the plants effectively starve the invading bacteria for water.

Introduction

Bacterial foliar pathogens have been a common subject of studies aimed at identifying the molecular and physiological basis of pathogen interactions with plants. One of the best-studied pathosystems is that of *Arabidopsis thaliana* and *Pseudomonas syringae* pv. tomato; this pathogen infects both tomato and *A. thaliana*. Like many other bacterial pathogens, *P. syringae* has developed the ability to suppress basal defenses and promote disease by injecting protein effectors directly into plant cells via the type III secretion system (T3SS) (DebRoy et al., 2004; Galan and Wolf-Watz, 2006; Hauck et al., 2003). Effectors promote disease and suppress resistance in part by interfering with defense-related molecular signaling pathways (Jamir et al., 2004; Kang et al., 2004; Mattoo et al., 2007). Plant resistance (*R*) genes facilitate recognition of specific intracellular effectors, triggering a disease resistance response. This gene-for-gene mediated resistance is often accompanied by a hypersensitive response, which is a rapid programmed plant cell death (PCD) that is localized to the site of infection (Dangl and Jones, 2001; Huang et al., 1988). Disease resistance may thus involve localized tissue necrosis as well as the production of antimicrobial compounds, the induction of defense-related genes, and the activation of systemic resistance which is effective against a broad range of pathogens (Heath, 2000; Mittler et al., 1997; Morel and Dangl, 1997; Mur et al., 2008).

Bacterial growth is limited during gene-for-gene mediated resistance. For example, *P. syringae* strains often attain populations as high as 10^8 to 10^9 cells per cm^2 in *A. thaliana* leaves of susceptible hosts but populations that are 10- to 200-fold smaller in resistant hosts (Jambunathan et al., 2001; Whalen et al., 1991). Identifying the physiological mechanisms that are directly responsible for limiting bacterial growth has been problematic because the effects of plant PCD are difficult to separate from other changes that occur during gene-for-gene mediated resistance. Interestingly, PCD is not necessarily required for bacterial inhibition as demonstrated by the ability of *A. thaliana* ecotype Col-O to inhibit the growth of *P. syringae* pv. tomato DC3000 expressing *avrRps4* (Hinsch and Staskawicz, 1996) or *hopPsyA* (Gassmann, 2005) in the absence of a visible hypersensitive response (HR). Similarly, *A. thaliana dnd1* mutants express effector-mediated resistance in response to some bacterial pathogens without inducing the HR (Clough et al., 2000; Yu et al., 1998). Consistent with this uncoupling of the HR and

restricted pathogen growth, *A. thaliana ndr1* mutants display exaggerated PCD in the presence of certain effector-expressing *P. syringae* strains without showing a proportional suppression of the bacterial populations (Century et al., 1995).

Leaf water status may play a key role in determining the outcome of plant-pathogen interactions. Maintaining water-soaked leaves in high humidity can suppress macroscopic HR necrosis and increase pathogen growth (Cook and Stall, 1977; Young, 1974) as well as promote the growth of saprophytic bacteria introduced into leaves (Stall and Cook, 1979). Furthermore, high humidity can suppress PCD in some *Arabidopsis* lesion-mimic defense gene mutants, including *cpr22*, *cpn1* and *lsd6* (Jambunathan et al., 2001; Weymann et al., 1995; Yoshioka et al., 2001), and can also suppress *Cf-4*/*Avr4*- and *Cf-9*/*Avr9*-dependent hypersensitivity and defense gene expression in transgenic tomato seedlings (Wang et al., 2005). These studies implicate leaf water status as a factor influencing plant defense.

Leaf water availability may have a direct impact on bacterial growth during gene-for-gene mediated disease resistance. Previously, we demonstrated that pathogen growth restriction was correlated with low water availability in the early stages of a gene-for-gene resistance response (Wright and Beattie, 2004). We used *P. syringae* strains containing transcriptional fusions responsive to low water potentials to monitor bacterial exposure to water stress following infection of *A. thaliana* leaves (Wright and Beattie, 2004). During gene-for-gene resistance triggered by a *P. syringae* effector, these cells were exposed to a rapid decrease in water potential to levels that were low enough to inhibit bacterial cell division when examined *in vitro*. The cells were exposed to much less severe levels of water stress during disease development than during the expression of resistance. Furthermore, the sizes of the *P. syringae* populations within leaves were strongly correlated with the water availability sensed by the bacterial cells. Collectively, these results suggest that low water availability is a major factor restricting bacterial growth during gene-for-gene mediated resistance. In this study, we test this hypothesis and explore the physiological mechanisms underlying changes in water availability to invading pathogens.

Leaf hydration represents a balance between water flowing into tissues through the xylem and water evaporating through stomata, and both of these activities can be altered during plant

defense. For example, some plants respond to some vascular pathogens by plugging the xylem via the formation of tyloses or gels within the vasculature, as occurs with *Xanthomonas campestris* pv. manihotis on cassava (Kpemoua et al., 1996). Alternately, water movement may be disrupted by the formation of ethylene-induced air bubbles (embolisms) in the xylem, as occurs with *Xylella fastidiosa* on grapes (Perez-Donoso et al., 2007). Defenses against non-vascular pathogens can also involve vascular disruption, although this has been reported primarily for non-bacterial pathogens and the mechanisms are unknown. For example, an HR in tomato cotyledons triggered by elicitors of the fungal pathogen *Cladosporium fulvum* involved early cell death of tissues lining the vascular system and loss of up to 80% of the initial leaf weight, suggestive of water loss, within 48 hours after inoculation (Hammond-Kosack et al., 1996). Similarly, tobacco leaves challenged with the tobacco mosaic virus (TMV) exhibited a reduction in transpiration preceding visible necrosis (Chaerle et al., 1999), and *Nicotiana edwardsonii* leaves infiltrated with TMV exhibited vascular restriction preceding visible necrosis (Wright et al., 2000). In contrast to gene-for-gene mediated resistance, basal resistance of *Nicotiana benthamiana* to *P. syringae* involved reduced vascular flow (Oh and Collmer, 2005). Interestingly, a variety of plants including tobacco and tomato express genes during a resistance response that share homology with genes induced in response to desiccation (Ciccarelli and Bork, 2005; Gopalan et al., 1996).

Stomatal apertures also change during plant defense. Stomata of tomato and *Commelina communis* close in response to exogenous application of fungal-derived elicitors and plant-derived elicitors, including oligogalacturonic acid and chitosan (Lee et al., 1999). Stomatal closure in *A. thaliana* in response to specific bacterial structures, designated microbial-associated molecular patterns (MAMPs), has been reported (Melotto et al., 2006) and has been interpreted as a deliberate plant defense reaction that prevents bacterial invasion (Lee et al., 1999; Melotto et al., 2006). Interestingly, the phytotoxin coronatine produced by some *P. syringae* strains, as well as a compound secreted by a *Xanthomonas campestris* pv. campestris strain, can reverse MAMP-mediated stomatal closure and thus increase bacterial access to the leaf interior (Gudesblat et al., 2009; Melotto et al., 2006).

The purpose of this study was to evaluate the fine-scale kinetics of water loss, vascular activity, and stomatal conductance during gene-for-gene mediated resistance using the *A. thaliana-P. syringae* pathosystem and identify the impact of leaf water loss on intercellular bacterial population sizes. Our results indicate that an effector-mediated resistance response in *A. thaliana* Col-O involves a rapid, near-complete cessation of vascular water flow into the infection site and a rapid reduction in stomatal conductance and leaf transpiration. Furthermore, preventing leaf drying completely reversed the inhibitory effect of this resistance response on bacterial growth without eliminating plant programmed cell death. Collectively, these results indicate that leaf water loss contributes to *A. thaliana* suppression of *P. syringae* growth during gene-for-gene mediated resistance.

Materials and Methods

Bacterial Strains

Derivatives of the rifampin (Rif)-resistant phytopathogen *P. syringae* pv. tomato strain DC3000 (Moore et al. 1989) were used in this study. DC3000(pPI*avrRpm1*) and DC3000(pPI*avrRpt2*) are derivatives that contain *avrRpm1* and *avrRpt2* cloned into the ClaI site of the kanamycin (Km)-resistant plasmid pPI, previously called pPProIce (Wright and Beattie, 2004); these genes were expressed from their native promoters. Two non-pathogenic strains were used: *Pseudomonas fluorescens* strain A506 (Wilson and Lindow, 1993), which is resistant to Rif, and DC3000 *hrcC* (Yuan and He, 1996), previously designated DC3000 *hrpH*, which is deficient in production of the type III secretion system and is resistant to chloramphenicol (Cm). The DC3000 mutant DC3118 (Ma et al., 1991) (Rif^R Km^R) is deficient in the production of coronatine. All strains were grown in King's B (KB) medium (King et al., 1954) at 28°C using antibiotics at the following levels (μg/ml): Rif, 50; Km, 50; and Cm, 30.

Plant Growth and Inoculation

Seeds of *A. thaliana* ecotype Columbia (Col-O) and *Solanum lycopersicum* cultivars Rio Grande PtoS and Rio Grande PtoR (obtained from A. Bogdanove, Iowa State University) were grown in a 10-h light/14-h dark cycle at 24°C and 50–60% relative humidity. Whole leaves of 5- to 6-week-old plants were used for all experiments. Bacterial cells grown overnight in liquid KB

medium were centrifuged and resuspended in 10 mM $MgSO_4$ to a final inoculum density of 10^8 cells/ml. For inoculation by vacuum-infiltration, plant leaves were immersed in buffer (10 mM $MgSO_4$) or bacterial suspensions containing 0.01% Silwet, exposed to a partial vacuum for 5 min, and allowed to air dry. For inoculation by syringe-infiltration, bacterial suspensions containing 0.01% Silwet were introduced into the abaxial side of leaves using a 5-ml syringe, and the region of infiltration was marked with a permanent marker. For inoculation by leaf immersion, plant leaves were dipped for 5 min into buffer (10 mM $MgSO_4$) or bacterial suspensions containing 0.02% Silwet and then were partially dried with a fan for 3 min.

Measurements of Stomatal Activity, Transpiration and Photosynthesis

Single-leaf measurements were performed using a LI-6400 photosynthesis system. This system was equipped with a light-emitting diode fixed on top of a 6-cm^2 standard chamber containing dual infrared gas analyzers. These gas analyzers were capable of measuring the difference in water vapor content (mmol H_2O/mol air) and CO_2 concentration (μmol CO_2/mol air) between the air streams entering and leaving the chamber. Gas flow was adjusted to a constant rate of 0.10 mmol/sec, and chamber temperature was maintained at 23°C with a constant light level of 150 μEinsteins. The LI-6400 system uses measurements of water vapor, CO_2, atmospheric pressure (kPa), and leaf temperature (°C) to estimate values for stomatal conductance (mol H_2O/m^2s), transpiration (mmol H_2O/m^2s), photosynthetic rate (μmol $CO_2/m^{-2}s$), and relative humidity (designated as RH). For each series of measurements, plants were used after exposure to their first two hours of light in the morning. The leaf chamber was clamped onto a single *A. thaliana* leaf, which was still attached to the plant, and measurements were taken every ten minutes for two hours. The leaf was uncoupled from the leaf chamber and inoculated using either vacuum-infiltration or immersion for 5 min, then dried by blotting with tissue or gentle air-drying with a fan for 3 min, respectively. The leaf chamber was again clamped onto the leaf for continued monitoring. The lights were turned off at 10 hpi, and monitoring was continued for one more hour.

Characterization of Vascular Activity and Plant Cell Death

Leaves of *A. thaliana* and *S. lycopersicum* were inoculated with bacterial suspensions by syringe-infiltration using a needle-less syringe applied to either side of the midrib of the abaxial

surface. The inoculation zone was marked with a permanent marker. Leaves were detached at the base of the petiole at various times, designated the sampling times, and the petiole was immediately placed in an aqueous 1% (w/v) safranine-O solution for two hours. Leaves were scanned using a flatbed scanner at 300 DPI and the quantity of safranine-O dye in target regions was measured using Adobe Photoshop (Adobe Systems Incorporated, San Jose, CA) by converting areas exhibiting the dye color to white and measuring the average number of white pixels against a black background of an area equal to the original leaf. To quantify dead or dying plant cells, excised whole leaves were immersed in a 1% (w/v) aqueous solution of Evans blue containing 0.05% Silwet. The submerged tissues were subjected to vacuum-infiltration 3 times for 5 min-intervals, followed by a 15-min incubation in the solution at atmospheric pressure. Leaves were rinsed 3 times for 5 min using a 10 mM $MgSO_4$ solution containing 0.05% Silwet followed by a 15-min incubation in the solution at atmospheric pressure. Leaves were scanned using a flatbed scanner and the Evans blue dye was quantified using Adobe Photoshop as described for safranine-O.

Quantification of Bacterial Population Sizes **in planta**

Leaves were inoculated by vacuum-infiltration, as described above, and were allowed to dry for 1 h. Leaves of selected plants were completely covered with a thin film of semi-molten (40°C) petroleum jelly; this was applied to both the adaxial and abaxial sides of each leaf using a sterile cotton swab. Other leaves were inoculated but were not treated with petroleum jelly. Alternatively, plants were inoculated and the canopy of leaves in each pot was immediately enclosed in a clear plastic bag, which was secured with a rubber band around the pot base, forming a humidity tent for the enclosed plants. Leaf disks collected with a 5-mm cork-borer, or entire leaves, were collected and homogenized in a 10 mM $MgSO_4$ solution. Dilutions were drop-plated onto KB medium containing appropriate antibiotics and grown for two days to quantify the colony-forming units (CFU).

Results

The kinetics of leaf mass loss indicate rapid water loss during an AvrRpm1-mediated resistance response

Tissue desiccation following necrosis is a hallmark of gene-for-gene mediated resistance; however, the kinetics of water loss for the period preceding visible necrosis have not been reported. Vacuum-infiltration of *P. syringae* pv. tomato DC3000(pPI*avrRpm1*) into *A. thaliana* ecotype Col-O resulted in a 54% reduction in leaf fresh weight within 9 hours post-inoculation (hpi) (Fig 1A). By comparison, inoculation with the disease-causing strain DC3000(pPI) resulted in only a 14% reduction over a similar period. These values increased to 80% and 34% by 24 hpi for DC3000(pPI*avrRpm1*) and DC3000(pPI), respectively (Fig 1A). In *A. thaliana* plants infected with DC3000(pPI*avrRpm1*), the largest decrease occurred between 6 and 9 hpi, and thus overlapped with the first detection of macroscopic lesions, which occurred at 6 hpi. A similar difference between a resistant and susceptible response in the kinetics of water loss was observed when DC3000(pI) was infiltrated into tomato cultivars Rio Grande PtoR (resistant) and Rio Grande PtoS (susceptible), although the reductions in leaf weight were proportionally smaller (Fig 1B).

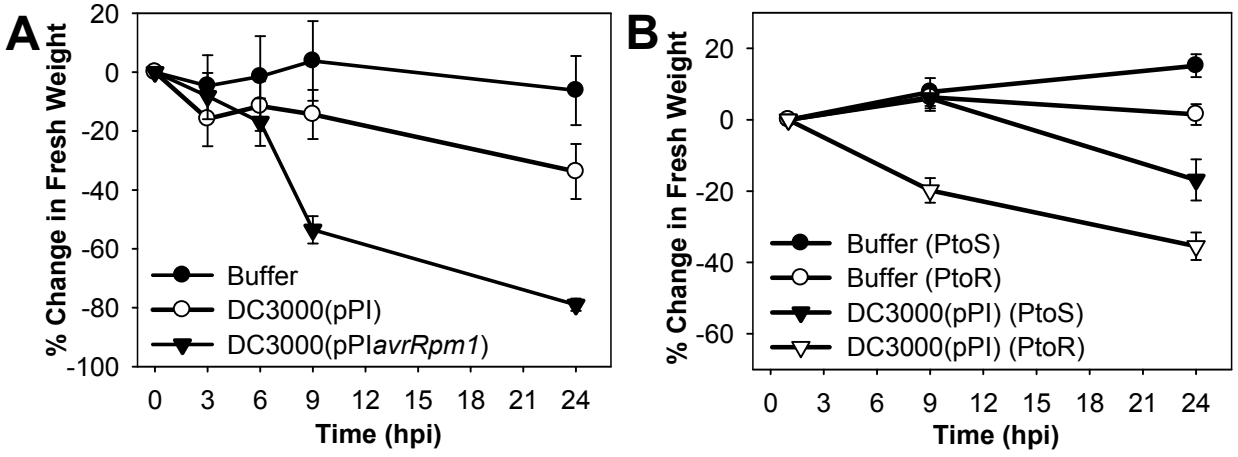

Figure 1. Kinetics of water loss in leaves following bacterial infection. (A) *A. thaliana* plants were vacuum-infiltrated with buffer, DC3000(pPI) or DC3000(pPI*avrRpm1*). (B) Tomato cultivars Rio Grande PtoS (susceptible) or Rio Grande PtoR (resistant) plants were vacuum-infiltrated with buffer or DC3000(pPI). Leaves were excised from plants at selected timepoints and individually weighed. Leaves weighed immediately following inoculation provided the 0 hours post-inoculation (hpi) values. Values shown are the mean percentage change in fresh weight from the mean fresh weight at 0 hpi ± SE (n = 15).

The LI-6400 photosynthesis system is effective for near-continuous monitoring of leaf physiology following bacterial inoculation

We investigated the possibility of using a LI-6400 photosynthesis system (LI-COR Biosciences, Lincoln, NE) to capture real-time measurements of whole-leaf physiology in inoculated *A. thaliana* leaves that were still attached to plants. The LI-6400 estimates stomatal conductance and rates of transpiration and photosynthesis based on gas exchange rates for CO_2 and water, leaf temperature, leaf area, and atmospheric pressure, and the instrument can collect measurements on a nearly continuous basis. In this study, leaf physiology measurements were taken at 10-min intervals from 2 h prior to inoculation until 10 hpi. Small amounts of residual water on the leaf surfaces obstructed accurate measurements in the 30 min following inoculation by influencing the estimates of water exchange rates (Fig 2). Although the physiological activities of individual leaves in the same treatment group showed leaf-to-leaf variability, as illustrated for stomatal conductance in leaves treated with buffer (Fig 2A) and DC3000(pPI*avrRpm1*) (Fig 2B), the kinetics of the physiological changes were generally consistent within a treatment. Some of the leaf-to-leaf variability was associated with the ambient relative humidity (RH), as illustrated in Fig 2A. To account for differences in the size and physiology of the leaves prior to treatment, estimates of stomatal conductance and rates of transpiration and photosynthesis were expressed as a percentage of the values that were measured just prior to inoculation. Expressing these values as "percent change" reduced the apparent leaf-to-leaf variation and better reflected the kinetic similarity among the replicate leaves within each treatment (Fig 2).

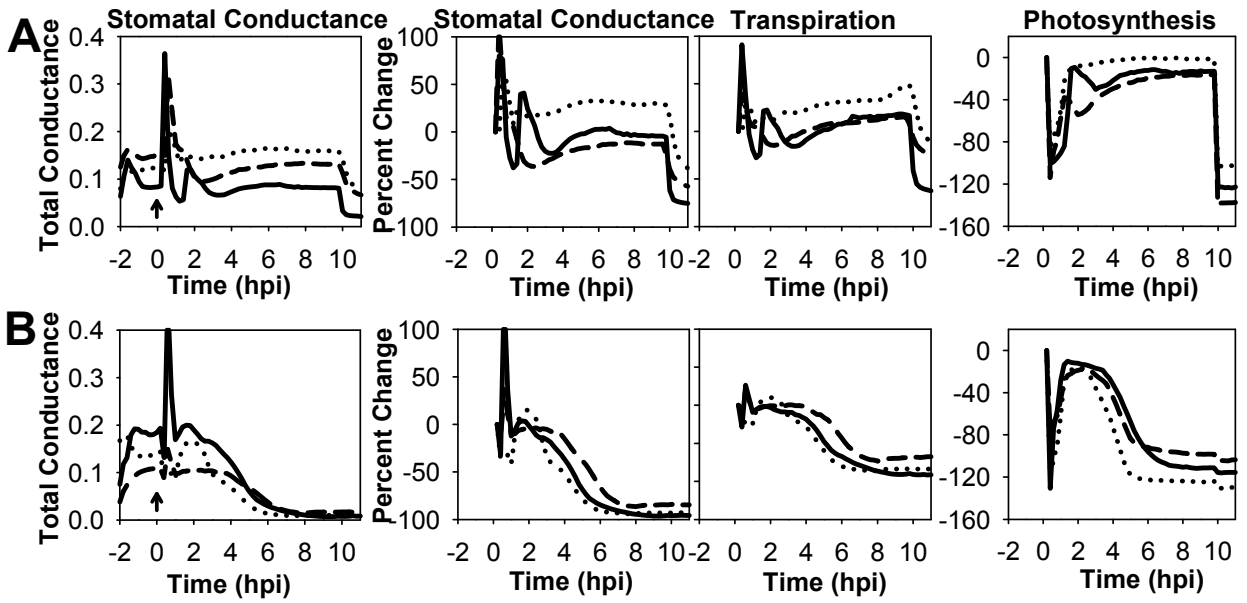

Figure 2. Reproducibility of real-time changes in *A. thaliana* leaves vacuum-infiltrated with (A) buffer or (B) DC3000(pPI*avrRpm1*) cells. Single leaf measurements were taken every 10 min using an LI-6400 photosynthesis system. Three replicate leaves, each indicated by a separate line, were vacuum-infiltrated with buffer or DC3000(pPI*avrRpm1*) two hours after measurements began (arrows indicate time of inoculation). Lights were turned off at 10 hpi. The replicate leaves indicated by the solid, dashed and dotted lines were examined at ambient relative humidity levels of (A) 53, 61 and 75%, and (B) 45,70 and 75%, respectively. For each (A) and (B), the first figure shows the conductance of the stomata to water vapor (mol H_2O/m^2s), whereas the latter three show the percentage change in stomatal conductance, transpiration and photosynthesis, respectively, relative to the values at 0 hpi.

The kinetics of the physiological changes in leaves following pathogen infiltration are complex

Following vacuum-infiltration with the disease-inducing strain DC3000(pPI), the stomatal conductance increased between 2.5 and 5 hpi (Fig 3A). This large increase was likely the result of coronatine, a phytotoxin that can open stomata during bacterial challenge (Melotto et al., 2006). This was confirmed by the absence of an increase in leaves infiltrated with the coronatine-deficient mutant DC3118 (Fig 3B) (Mittal and Davis, 1995; Moore et al., 1989). Interestingly, continuous monitoring of stomatal activity indicated that this coronatine-mediated

increase is only transient, as a large and rapid decrease occurred between 5 and 7 hpi in the DC3000(pPI)-inoculated leaves (Fig 3A). To evaluate whether factors secreted by the type III secretion system influence the kinetics of stomatal conductance, we infiltrated plants with a DC3000 mutant defective in HrcC, an outer membrane protein required for type III-mediated secretion (Yuan and He, 1996). This mutant caused a large sustained increase in stomatal conductance, consistent with its ability to produce coronatine, but did not induce a subsequent decrease as observed with the wild-type strain (Fig 3B). This observation suggests that effectors secreted through the T3SS are responsible for the eventual decrease in conductance, although the sustained increase could be due to the previously reported overproduction of coronatine by the *hrcC* mutant (Penaloza-Vazquez et al., 2000).

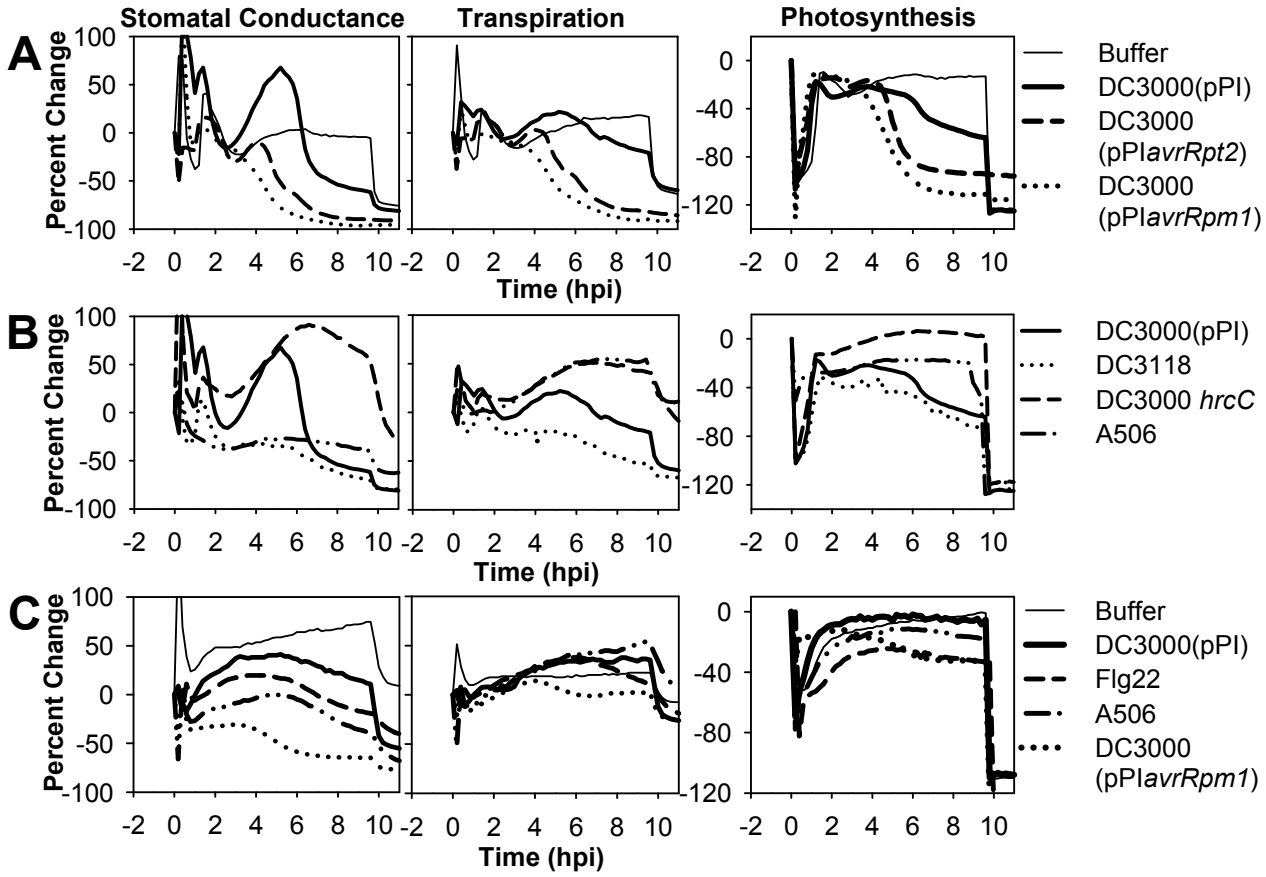

Figure 3. Physiological changes in *A. thaliana* leaves following treatment with buffer or bacteria. (A) Leaves were vacuum infiltrated with buffer, DC3000(pPI), DC3000(pPI*avrRpt2*) and DC3000(pPI*avrRpm1*); lines are representative of at least 3 replicate treated leaves. (B) Leaves were vacuum infiltrated with DC3000(pPI), a DC3000 *hrcC* mutant, the coronatine-

deficient DC3118 mutant and *P. fluorescens* strain A506; lines are representative of at least 2 replicate treated leaves. (C) Leaves were inoculated by immersion in buffer, DC3000(pPI), 20 µM Flg22, *P. fluorescens* A506 and DC3000(pPI*avrRpm1*). Lines are representative of at least 3 replicate leaves. All values reflect the percentage change from the values at 0 hpi.

The stomatal conductance of leaves infiltrated with the effector-expressing strains DC3000(pPI*avrRpm1*) and DC3000(pPI*avrRpt2*) decreased rapidly starting as early as 1 hpi (Fig 3A). Although both strains are capable of producing coronatine, stomatal conductance did not increase after 1 hpi with either strain suggesting that coronatine-mediated stomatal changes are suppressed during the effector-mediated resistance. The stomatal conductance of these leaves clearly diverged from that of leaves infiltrated with DC3000(pPI) by as early as 3 hpi, with DC3000(pPI) inducing an increase and the incompatible pathogens inducing a large and sustained decrease (Fig 3A).

Stomatal conductance is influenced by stomatal aperture, stomatal density, guard cell size, and environmental conditions (Farquhar and Sharkey, 1982). Microscopic examination of leaf surfaces confirmed that stomatal density and average guard cell sizes were similar among the leaves in distinct treatments, and the environmental conditions were controlled by the LI-6400 photosynthesis system. Therefore, the relative stomatal conductance was likely proportional to the relative stomatal aperture for the leaves in these experiments. The increased conductance induced by coronatine-producing strains therefore suggests stomatal opening, as shown in a previous study (Melotto et al., 2006), whereas the decreased conductance induced by incompatible strains suggests stomatal closure. Microscopic examination indicated that stomatal widths on DC3000(pPI*avrRpm1*)-treated leaves were reduced nearly 70% compared to the pre-inoculation values in 6 h but they did not completely close (Fig 4), despite that the stomatal conductance decreased by as much as 90% within 8 hpi (Fig 3).

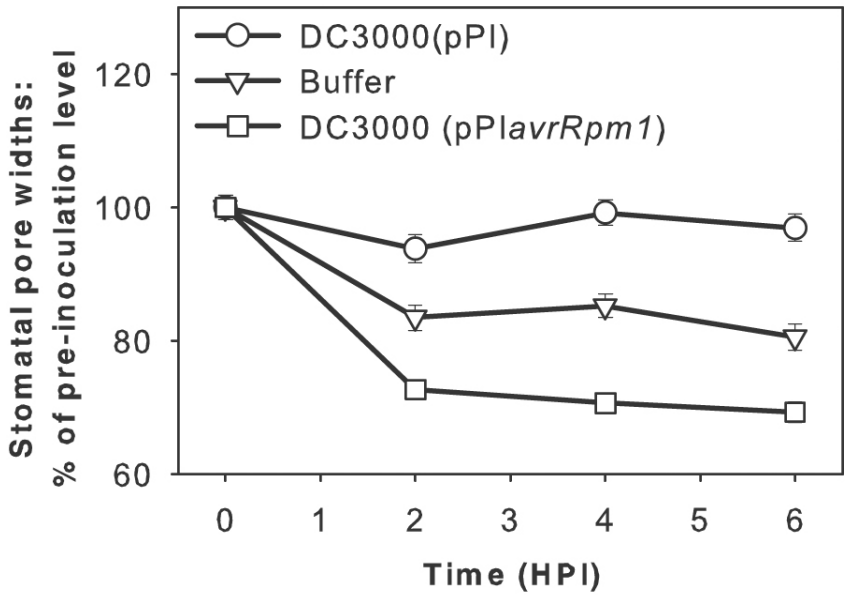

Figure 4. Stomatal changes in syringae-infiltrated *A. thaliana* leaves. Leaves were syringe-infiltrated with 10mM $MgSO_4$ containing 0.01% Silwet (triangles) with DC3000(pPI) (circles) or DC3000 (pPI*avrRpm1*) (squares) at 10^8 CFU/ml and the stomatal pore widths measured over time using light microscopy. Values indicated are mean percent change from pre-inoculation mean stomatal pore sizes. n=350 stomata from 6 total leaves per strain per timepoint.

Transpiration rates were correlated with stomatal conductance in all vacuum-infiltrated leaves, although changes in transpiration rate were attenuated relative to changes in stomatal conductance (Figs 3A and 3B). Similarly, photosynthetic rates were correlated with transpiration rates. For all physiological properties examined, the kinetic events following infiltration of DC3000(pPI*avrRpt2*) were delayed approximately 2 h relative to those following infiltration with DC3000(pPI*avrRpm1*).

The kinetics of physiological changes following leaf infiltration with the non-pathogenic strain *P. fluorescens* A506 were complex and depended on RH. At a RH of 62%, the stomatal conductance of A506-treated leaves decreased within 2 hpi and then remained steady (Fig 3B), as expected for an organism inducing only a basal defense response. Surprisingly, A506 was similar to the *hrcC* mutant in its effect on transpiration (Fig 3B), despite that A506 does not

produce coronatine, and coronatine produced by the *hrcC* mutant likely increased transpiration by inducing stomatal opening. At 12% RH, however, A506 increased stomatal conductance and did not increase transpiration (Fig 5A), an observation that we cannot presently explain.

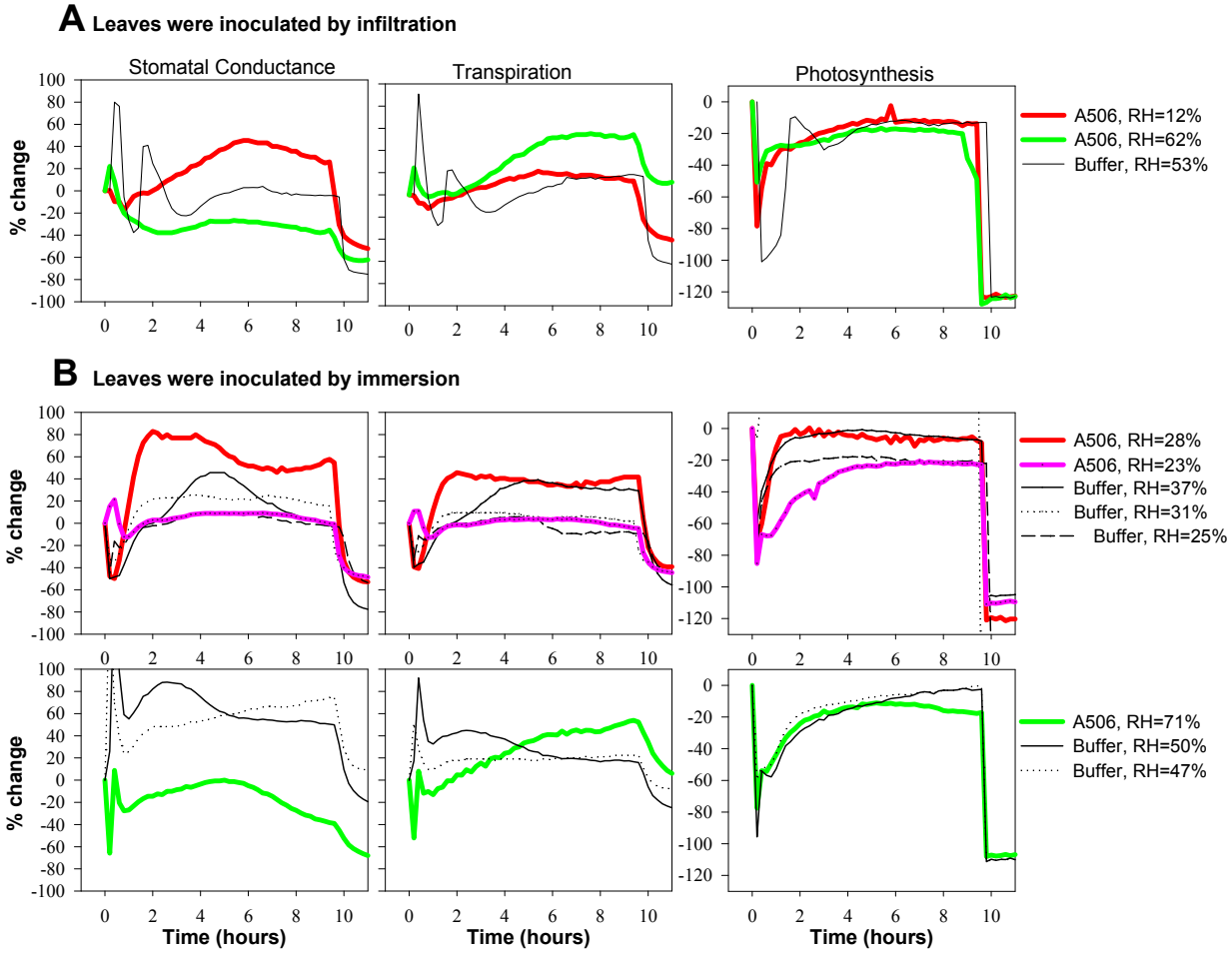

Figure 5. Physiological changes in *A. thaliana* leaves at various levels of relative humidity following infiltration (A) or immersion (B). Leaves were vacuum infiltrated or immersed in buffer or *P. fluorescens* strain A506; lines are representative of single leaf measurements. All values reflect the percentage change from the values at 0 hpi.

Inoculation by leaf immersion shows physiological changes that occur within 1 h after inoculation

We also measured physiological changes in leaves after inoculation by immersion, a method that mimics natural leaf invasion better than vacuum-infiltration. Stomatal conductance following immersion in buffer was particularly dependent on RH; it increased within 1 hpi when the ambient RH was 45 to 50% (Fig 3C), but decreased within 1 hpi when the ambient RH was 25 to 40% (Fig 5B). When comparing treatments at RH levels >45% (Fig 3C), the stomatal conductance in DC3000(pPI)-immersed leaves was significantly lower than in the buffer-immersed leaves at 1 hpi (Fig 3C), consistent with reports of rapid MAMP-mediated stomatal closure. Similarly, plants immersed in MAMP-rich suspensions of the bacterial peptide elicitor flg22 exhibited lower stomatal conductance within 1 hpi than those immersed in buffer, confirming a role for flg22 in stomatal closure. These observations also support the possibility that flg22 and other DC3000(pPI)-associated MAMPs prevented an increase in stomatal opening, as occurred in the buffer treatment, rather than inducing stomatal closure. Interestingly, the stomatal conductance in the DC3000(pPI*avrRpm1*)-immersed leaves was significantly lower than in the DC3000(pPI)-treated leaves at 1 hpi (Fig 3C), suggesting that the AvrRpm1 effector affects stomatal activity, directly or indirectly, as early as 1 hpi. DC3000(pPI)-immersed leaves exhibited an increase in stomatal conductance between 30 min and 3 hpi that was induced by coronatine, as evidenced by its absence in leaves immersed in DC3118 (Fig 6). Similar to the results following infiltration of the strains, the absence of an increase in stomatal conductance in the DC3000(pPI*avrRpm1*)-immersed leaves between 1 and 2 hpi indicates that coronatine-mediated stomatal opening is suppressed during the plant response to DC3000(pPI*avrRpm1*). Similar to the results following infiltration of A506, the stomatal conductance of A506-immersed leaves was lower than the buffer-treated leaves at 1 hpi at RH levels >45% (Fig 3C), suggestive of MAMP activity in these leaves, but was not lower in leaves at lower RH levels (25 to 30%) (Fig 5B).

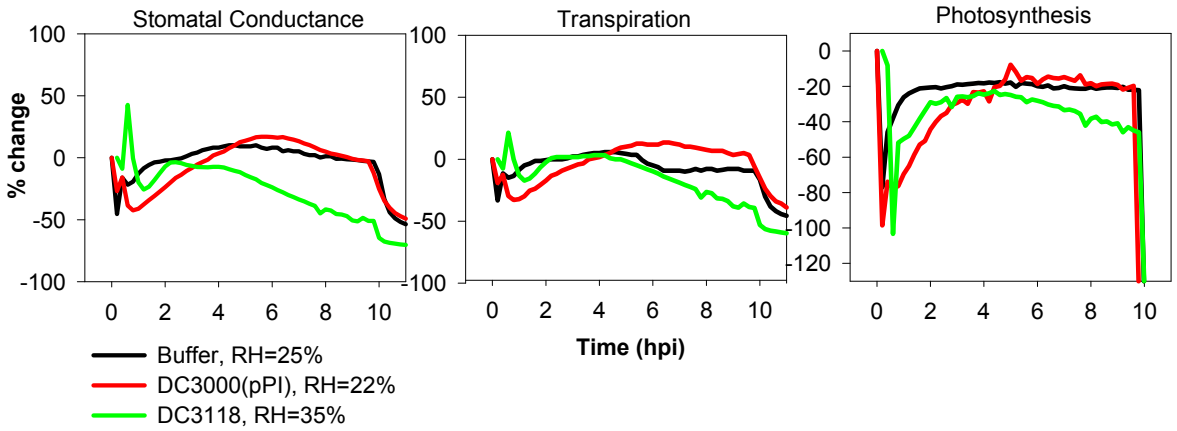

Figure 6. Physiological changes in *A. thaliana* leaves at various levels of relative humidity following immersion. Leaves were immersed in buffer, DC3000(pPI), or the coronatine-deficient DC3118 mutant; lines are representative of single leaf measurements. All values reflect the percentage change from the values at 0 hpi.

The changes in transpiration and photosynthetic activity in the leaves subjected to leaf immersion were not as closely correlated with stomatal conductance as in the leaves subjected to infiltration (Fig 3). This may be due to the presence of more bacteria in the leaf intercellular spaces following infiltration, and a greater opportunity for intercellular bacteria than surface bacteria to introduce effectors into guard cells and other leaf cells due to the absence of a cuticle on internal plant cell surfaces. Despite the attenuated effects of the immersion treatments, DC3000(pPI*avrRpm1*)-immersed leaves showed decreased transpiration and photosynthetic activity after 4 hpi, consistent with the infiltration results. The flg22-immersed leaves showed a particularly large decrease in photosynthetic activity; this decrease was not observed in leaves immersed in only 10 µM flg22 and thus was likely a function of the high flg22 concentration used.

The kinetics of vascular activity changes indicate rapid and extreme vascular restriction during an avrRpm1-mediated resistance response

The decreased water availability sensed by intercellular bacteria during gene-for-gene mediated resistance in a previous study (Wright and Beattie, 2004) could have resulted from increased water evaporation through stomata with increased stomatal apertures; however, the

stomatal conductance decreased rather than increased during an effector-mediated resistance response (Fig 3). Alternatively, decreased water availability could have resulted from a reduction in the vascular water flow to the infected region. To evaluate this, we syringe-infiltrated bacteria into *A. thaliana* leaves and then placed the petioles of detached leaves at various times into a safranine-O dye solution for two hours. The movement of the dye through the xylem provided an excellent visual indication of vascular water flow (Fig 7A), and indicated that vascular flow into regions infiltrated with DC3000(pPI*avrRpm1*) was almost totally halted by 3 hpi (Fig 7A). When quantified using Adobe Photoshop, dye levels in these regions averaged only 10% of the dye levels in buffer- and DC3000(pPI)-infiltrated regions (Fig 7B). Dye levels in DC3000(pPI)-treated regions also decreased, but at a slower rate than in DC3000(pPI*avrRpm1*)-treated regions (Figs 7A and 7B). Reduced vascular flow was localized to the site of bacterial infiltration (Fig 7C), with dye levels in adjacent areas remaining virtually unchanged for at least 24 h. Infiltration with *P. fluorescens* strain A506, which induces basal resistance, resulted in a slight reduction of vascular water flow by 48 hpi (Fig 7D). Strong vascular restriction was also observed during gene-for-gene mediated resistance in the tomato cultivar Rio Grande PtoR when infiltrated with DC3000(pI) (Fig 7E). Hence, reduced vascular flow occurs during a variety of microbe interactions with *A. thaliana* and tomato, with rapid and virtually complete vascular restriction occurring during gene-for-gene resistance.

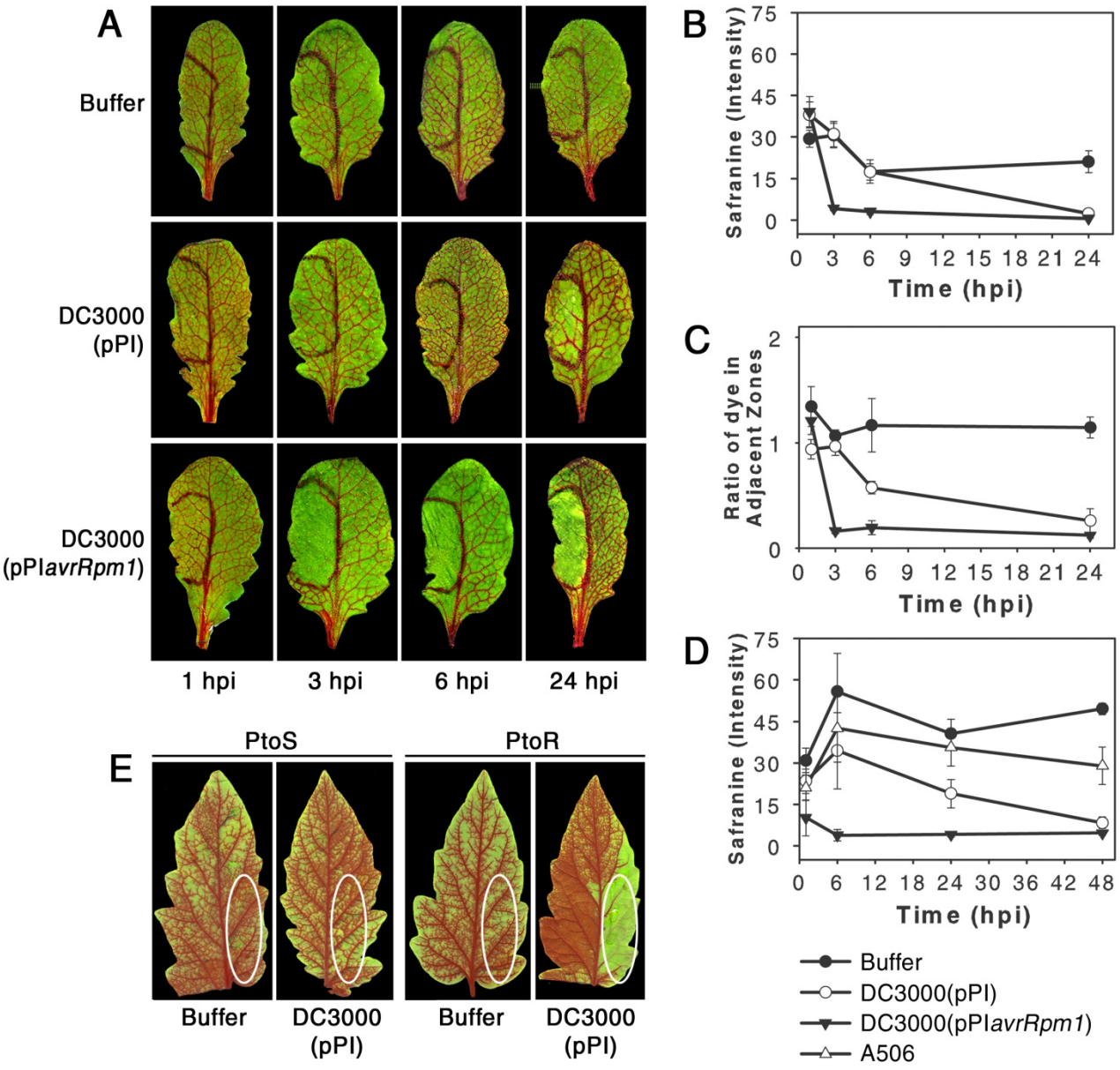

Figure 7. Vascular activity in the infiltrated regions of (A-D) *A. thaliana* and (E) tomato leaves. Leaves were inoculated with buffer or bacteria, as indicated. Syringe-infiltrated leaves were excised at (A-C) 1, 3, 6, and 24 h after infiltration, as well as at (D) 48 hpi, or at (E) 3 hpi. The petioles were immersed in a 1% aqueous safranine-O dye solution for two hours. The infiltrated zones on each leaf were indicated (A) with a black marker on the leaf or (E) as demarcated with a white line. (B, D) The total amount of dye in the infiltrated zones was assessed in digital scans and was expressed as intensity, which reflects mean Photoshop luminosity units ± SE. (C) The

mean ratio of dye in the infiltrated leaf zone to that in the adjacent uninoculated region ± SE is shown.Values are based on (B,C) 5 to 23 replicate leaves and (D) 3 to 5 replicate leaves.

Microscopic plant cell death is evident as early as 2 h after inoculation

Although programmed cell death is a well-established hallmark of *R* gene-mediated resistance, we evaluated the kinetics with which dead plant cells arose during the initial 24 hpi. Plant cell death increased dramatically over the first 3 h after inoculation with DC3000(pPI*avrRpm1*) (Fig 8) and was detected as early as 2 hpi using microscopy. Plant cell death did not increase until 9 to 24 hpi in the DC3000(pPI)-treated plants (Fig 8B). Levels of plant cell death remained relatively unchanged following infiltration with buffer or the non-pathogen *P. fluorescens* A506 (Fig 8B). Using microscopy, we observed that confluent regions of dead plant cells often occurred along leaf veins (Fig 9), implying a possible causal relationship between plant cell death and vascular restriction.

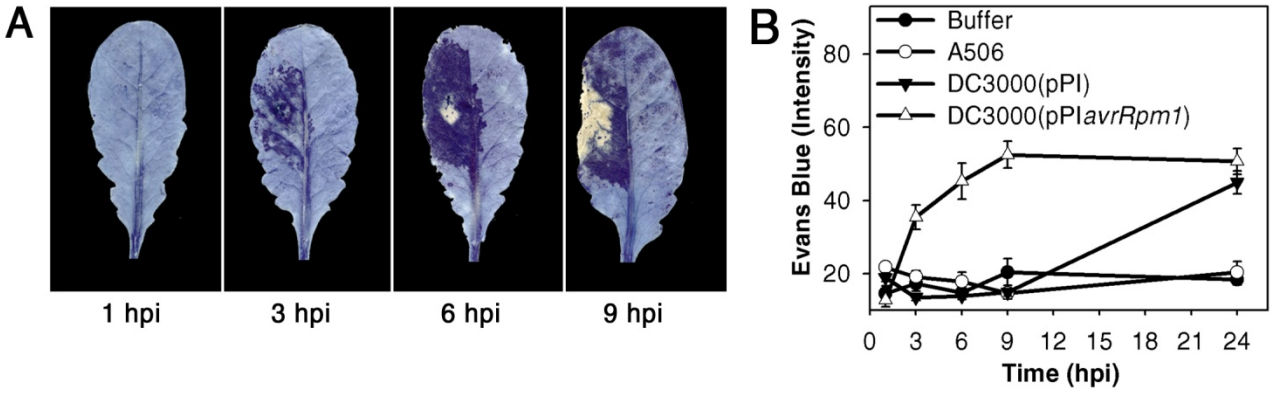

Figure 8. Plant cell death in the infiltrated region of *A. thaliana* leaves inoculated with (A) DC3000(pPI*avrRpm1*) or (B) buffer, DC3000(pPI), DC3000(pPI*avrRpm1*) or *P. fluorescens* A506. After syringe-infiltration and excision, as in Figure 7, leaves were stained with Evan's blue solution and digitally scanned. The total amount of dye in the infiltrated zones reflected the amount of plant cell death and is expressed as mean Photoshop luminosity units ± SE (n = 7 to 11).

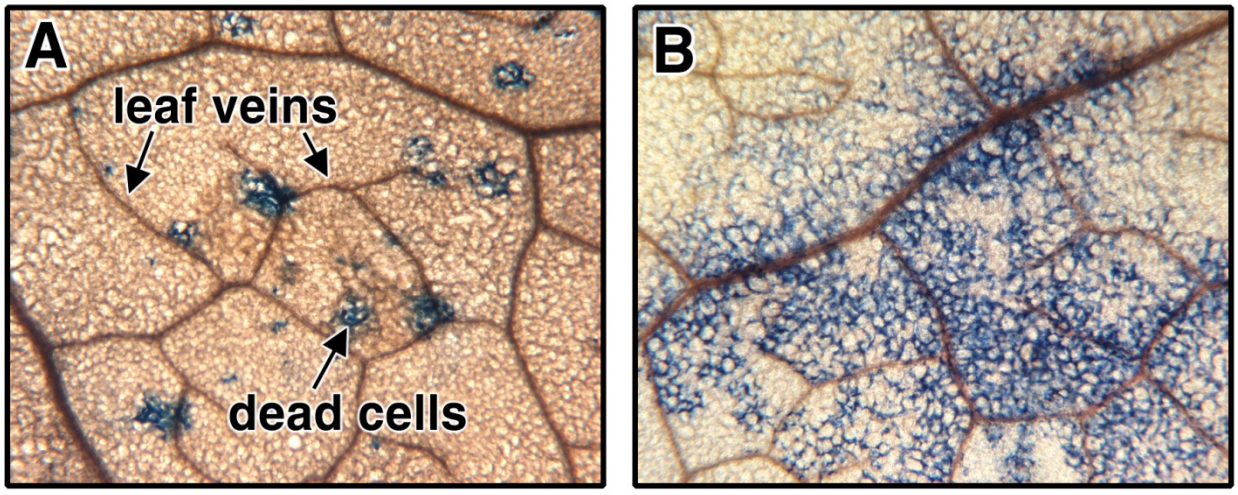

Figure 9. Dead cell-stained *A. thaliana* leaves following the HR. Leaves were vacuum-infiltrated with DC3000(pPI*avrRpm1*) at 10^8 CFU/ml suspended in 10mM $MgSO_4$ containing 0.01% Silwet. After two (A) or three (B) hours, leaves were excised and stained with Evan's blue dye to indicate dead plant cells. Leaves were fixed and cleared using formaldehyde, acetic acid and ethanol and the leaves were photographed using a light microscope at 10x magnification.

Preventing water loss from infected leaves prevents bacterial growth suppression during gene-for-gene mediated resistance

To evaluate the impact of leaf water loss on intercellular bacterial populations, we vacuum-infiltrated *A. thaliana* with bacterial suspensions and then halted leaf drying by covering both the upper and lower leaf surfaces with a thin layer of petroleum jelly. The presence of a water-impermeable barrier prevented water loss through epidermal openings as evidenced by the lack of significant mass loss with subsequent incubation. The petroleum jelly treatment increased the population sizes of DC3000(pPI) by an average of 0.2 log units per cm^2 by 24 hpi (Fig 10A) ($P = 0.03$, Student's *t*-test), and increased the population sizes of DC3000(pPI*avrRpm1*) and DC3000(pPI*avrRpt2*) by an average of 1.0 and 0.7 log units per cm^2, respectively, by 24 hpi (Figs 10B and 10C) ($P < 0.001$). In fact, the *avrRpm1*- and *avrRpt2*-expressing strains grew to levels nearly identical to those of the disease-inducing strain DC3000(pPI) in petroleum jelly-covered leaves. Interestingly, the majority of the population growth benefit in the petroleum jelly-covered leaves occurred early after inoculation, i.e., between 4 and 8 hpi, with little significant growth benefit detected in the 8-24 hpi period after inoculation (Fig 10D). Significant plant cell death had occurred by 8 hpi in DC3000(pPI*avrRpm1*)-inoculated leaves regardless of

the petroleum jelly treatment (Fig 10E), demonstrating that this treatment did not inhibit the HR. Furthermore, the observation that DC3000(pPI*avrRpm1*) grew to unrestricted levels in the petroleum jelly-treated leaves despite a high level of plant cell death supports prior evidence that plant programmed cell death can be uncoupled from pathogen growth suppression (Clough et al., 2000; Gassmann, 2005; Hinsch and Staskawicz, 1996; Yu et al., 1998). We also evaluated the impact of leaf water loss on intercellular bacterial populations by enclosing the plants in humidity tents to minimize water loss through evaporation. Plants in the humidity tents maintained visible leaf water-soaking for at least 24 h and supported the establishment of significantly larger populations of both DC3000(pPI) and DC3000(pPI*avrRpm1*) by 24 hpi than plants that were outside the humidity tents (Fig 11) ($P < 0.001$, Student's *t* test), although DC3000(pPI*avrRpm1*) did not establish populations quite as large as those of DC3000(pPI). Collectively, these results provide strong evidence that leaf water loss contributes to the restriction of *P. syringae* growth during gene-for-gene mediated resistance in *A. thaliana.*

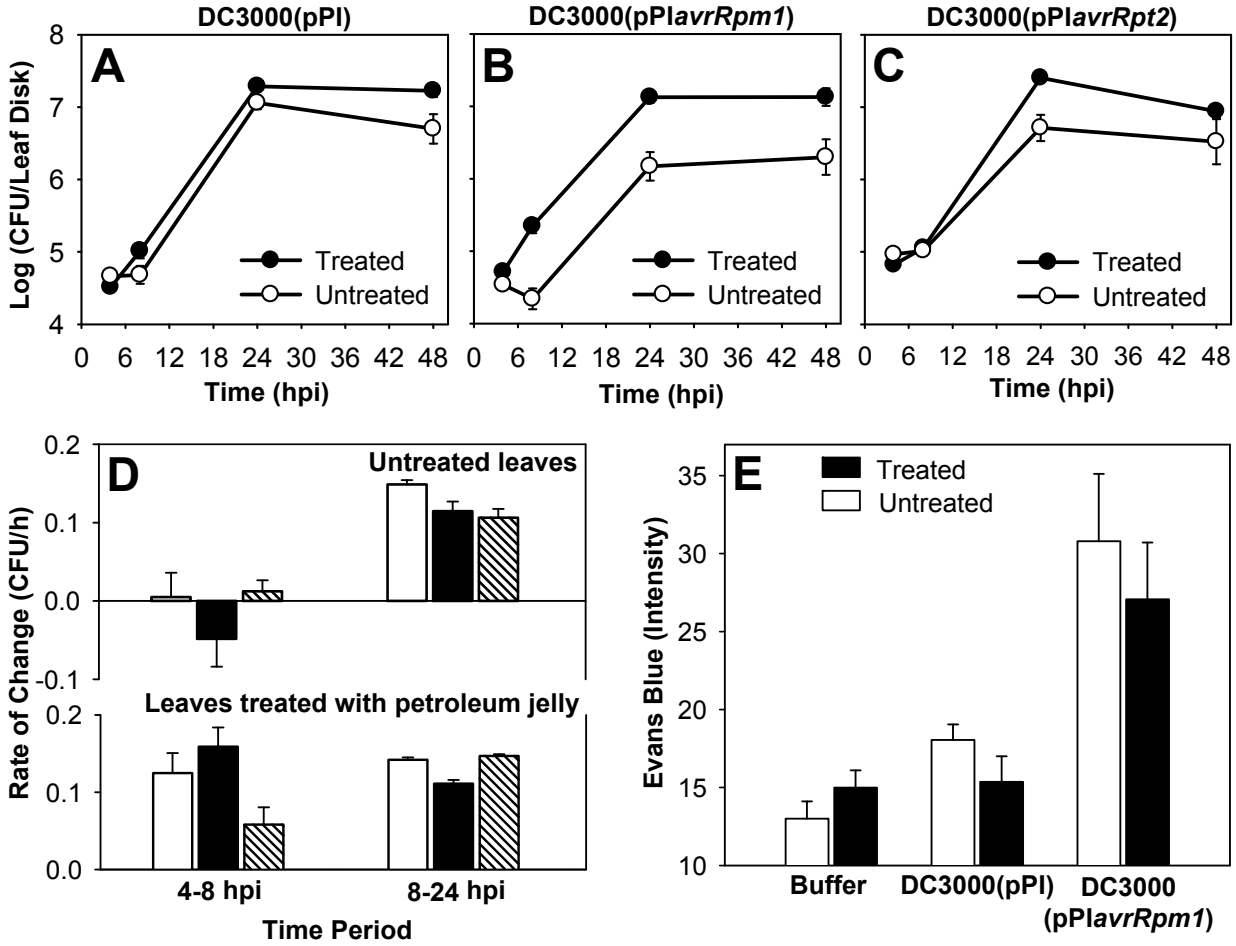

Figure 10. Effect of stomatal blockage on the growth of bacterial populations and plant cell death in inoculated *A. thaliana* leaves. Plants were inoculated by vacuum-infiltration and the surfaces were allowed to dry for 1 hour. A thin layer of petroleum jelly was applied uniformly to both the upper and lower surfaces of leaves to block stomata and thus leaf drying. The population sizes were determined by plate counts for petroleum jelly treated (●) and untreated (○) leaves inoculated with (A) DC3000, (B) DC3000(pPI*avrRpm1*) or (C) DC3000(pPI*avrRpt2*). In (D), the rate of change in the bacterial populations between 4 and 8 h is contrasted with the rate of change between 8 and 24 h for the data shown in A-C, with DC3000(pPI) (white bars), DC3000(pPI*avrRpm1*) (black bars), and DC3000(pPI*avrRpt2*) (hatched bars). (E) The extent of plant cell death is shown for the untreated (black bars) and petroleum jelly treated (white bars) leaves sampled at 8 hpi as determined using Evans blue staining. Data are represented as mean ± SE (n = 24 to 29 for A-D and 10 to 23 for E).

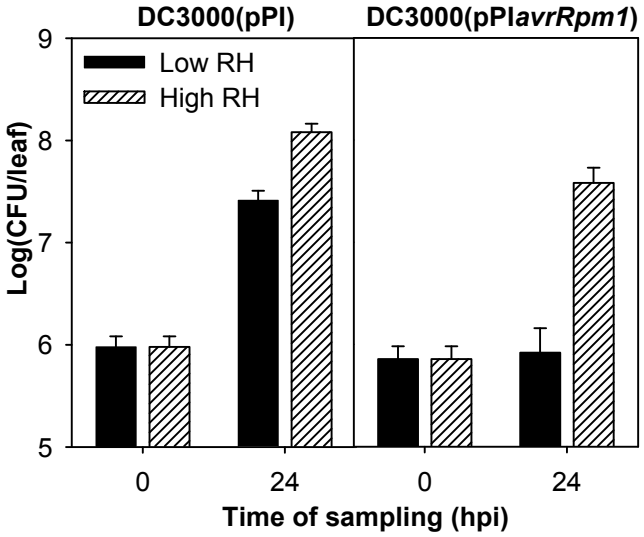

Figure 11. Effect of continuous incubation under high relative humidity (RH) on the growth of bacterial populations in *A. thaliana* leaves. Plants were inoculated with DC3000(pPI) or DC3000(pPI*avrRpm1*) by vacuum-infiltration and were placed on a laboratory bench with (high RH) or without (low RH) being enclosed in a humidity tents. The population sizes were determined at 0 and 24 hpi. Data are represented as mean ± SE (n = 14).

Discussion

A major functional outcome of gene-for-gene resistance is the limited growth and spread of a pathogens within plants. Identifying the physiological and biochemical mechanisms by which this resistance suppresses bacterial growth has been problematic due to the co-occurrence of many changes in the plant. Although this suppression occurs within the first 24 hpi in the *A. thaliana-P. syringae* pathosystem (Figs 10B and 10C), the majority of physiological research on resistance in this pathosystem has characterized events only after 24 hpi. This study characterized early events in gene-for-gene mediated resistance with the intention of identifying physiological changes for which the kinetics are consistent with a causal role in limiting bacterial growth. The combination of these kinetic studies (Figs 1-9) and the studies blocking leaf water loss (Figs 10-11) provide strong evidence that plant-mediated drying at the infection site is an important physiological mechanism by which bacterial growth is limited during gene-for-gene mediated resistance.

These studies demonstrate that vascular restriction occurs during *avrRpm1*-induced resistance to *P. syringae,* a non-vascular bacterial pathogen, and that this restriction is virtually complete within 3 hpi. The timeline presented in Fig 12 illustrates the sequence of physiological changes that occurred within 9 hours after *P. syringae* infiltration leading to resistance or disease. The vascular restriction preceded or was simultaneous with reductions in stomatal conductance, leaf transpiration, and photosynthesis, with microscopic cell death detected at 2 hpi, and significant cell death observed at 3 hpi. Macroscopic lesions were first visible at 6 hpi and coincided with the onset of maximum leaf drying. In contrast to resistance, the induction of disease symptoms by DC3000(pPI) involved a dramatic increase in stomatal conductance and leaf transpiration preceding a rapid decline in these values starting at approximately 5 hpi. Visible necrosis was not observed until at least 24 hours post-inoculation.

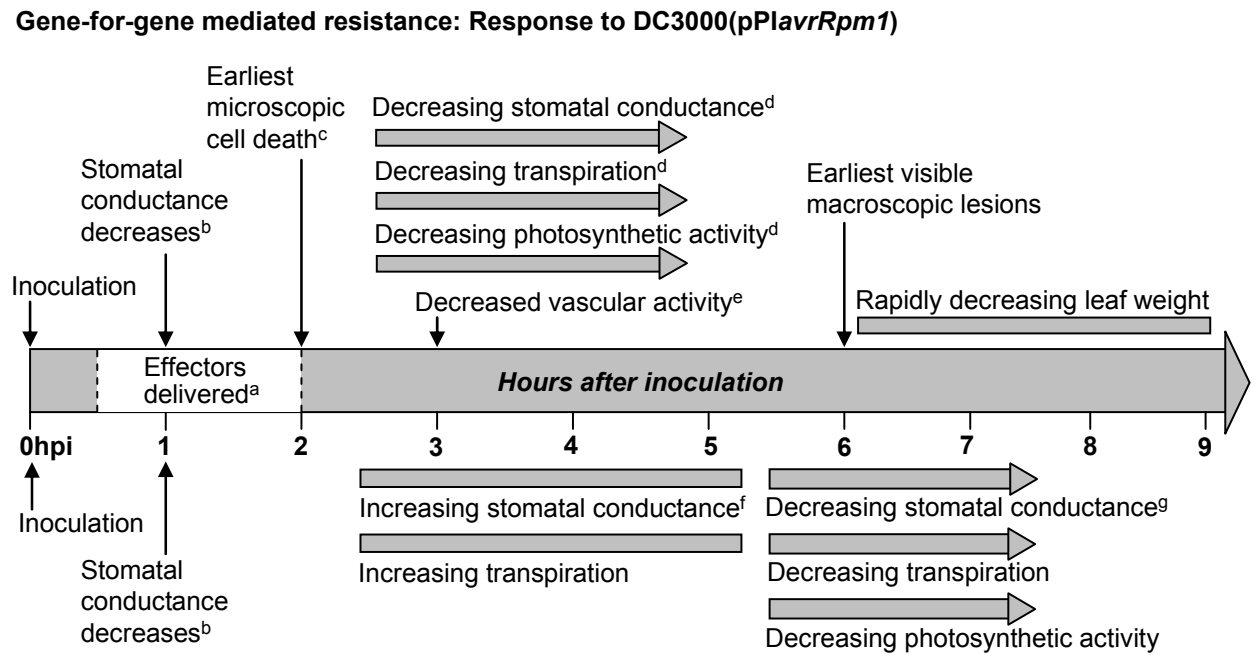

Figure 12. Timeline of physiological changes in *A. thaliana* in response to *P. syringae* pv. tomato. All events occurred following vacuum-infiltration, except as indicated. The inocula contained 10^8 cells/ml. [a] The time of effector delivery is based on the work of de Torres et al. (2003). [b] Reduced stomatal conductance within 1 hpi was observed only following immersion inoculation and likely reflects MAMP-mediated stomatal closure. A greater decrease in stomatal conductance with DC3000(pPI*avrRpm1*) than by DC3000(pPI) within 1 hpi suggests effector-related stomatal closure. [c] In the leaves inoculated with DC3000(pPI*avrRpm1*), Evans blue cell staining showed substantial plant cell death by 3 hpi. [d] The kinetics of the events following vacuum-infiltration with DC3000(pPI*avrRpt2*) were delayed approximately 2 h relative to those with DC3000(pPI*avrRpm1*). [e] Near complete loss of vascular activity, based on the exclusion of the vascular dye Safranine-O from the infiltrated region, had occurred by 3 hpi. [f] Increased conductance reflected coronatine-mediated stomatal opening, as reported by Melotto et al. (2006). [g] Decreased conductance appeared to reflect type III secretion system-dependent effector-mediated stomatal closure based its absence following inoculation with DC3000 *hrcC*.

The kinetics described here are for events following infiltration with an inoculum density of 10^8 cells/ml. This density is commonly used in studies focused on the HR. Although delivery of this high density of cells into the apoplast induces macroscopic levels of plant cell death, delivery of lower densities have been verified to similarly induce PCD but on a microscopic level (Turner and Novacky, 1974). The techniques for assessing vascular activity used in this study were not amenable to detecting potentially localized changes in vascular activity resulting from the infiltration of low cell densities. However, measurements of changes in leaf transpiration showed clear differences between treatments with DC3000(pPI) and DC3000(pPI*avrRpm1*) after inoculation by immersion (Fig 3C), a process that introduces far fewer cells into the apoplast than vacuum infiltration.

We do not yet know the mechanism of vascular restriction. We observed that confluent regions of plant cell death often overlapped one or more vascular bundles at 3 hpi. In fact, vascular tissue may be selectively targeted for programmed cell death during *R* gene-mediated resistance based on the observation that a lesion mimic mutant of *A. thaliana* called *vad1* (for *vascular associated death*) exhibits HR-like PCD preferentially in mesophyll cells lining the vascular tissue (Lorrain et al., 2004). The Vad1 protein is constitutively expressed at very low levels in healthy plants but is highly induced in vascular tissues upon syringe-inoculation with DC3000 expressing *avrRpm1*, as well as with an HR-inducing strain of *Xanthomonas campestris* pv. campestris. This induction was rapid, peaking at 3 hpi, and thus was consistent with the kinetics of vascular restriction in the present study. The death of the vascular-associated cells, such as the bundle sheath cells, could conceivably allow air to enter the xylem and form a block, or embolism, in the water column. Such embolisms would form more easily if water flowed primarily through xylem vessels rather than the network of tracheids that are commonly present at the ends of the minor veins in leaves (Chatelet et al., 2006); these networks provide multiple pathways for water flow. Because the water movement into the areoles bound by the minor veins appeared to be stopped in response to DC3000(pPI*avrRpm1*) (Fig 7), embolism formation is unlikely to be the mechanism of vascular restriction. The formation of tyloses or gels is also unlikely to be the mechanism because of the speed with which vascular movement into the infection site was halted, which was within 3 hpi, relative to the speed of tylosis formation, which typically is days rather than hours. In *A. thaliana*, the minor veins function as the primary

sites for photoassimilate collection with this collection mediated primarily by apoplastic phloem loading (Turgeon, 2006). Because phloem loading involves sucrose-proton co-transporters, it is conceivable that the function of these co-transporters could be disrupted, such as via cell death or rapid changes in apoplastic ions, and that this could reduce xylem flow because of the coupled phloem loading and xylem movement inherent to the osmotically generated pressure-flow mechanism for movement of photoassimilates (Evert, 2006).

A major finding of this work is that bacterial growth suppression in plant tissues during gene-for-gene mediated resistance could be completely reversed by halting leaf water loss; water loss was halted by blocking transpiration using either petroleum jelly or continuous incubation at high RH. This finding, in conjunction with our previous observation that *P. syringae* cells sensed inhibitory levels of water stress in resistant *A. thaliana* plants (Wright and Beattie, 2004), supports the possibility that the gene-for-gene mediated resistance response suppresses the growth and spread of bacterial populations by limiting water availability to the bacteria and thus effectively starving them of water. The petroleum jelly treatment enhanced bacterial growth in the first 8 hpi, a period during which the bacteria generally exhibited little to no growth in untreated leaves. A lag preceding a period of exponential growth is characteristic of bacterial adaptation to a new environment or to environmental stress. The finding that the petroleum jelly eliminated this putative adaptation period by eliminating leaf water loss is consistent with an adaptation period necessitated by low water availability and a period of exponential growth after resumption of cellular homeostasis. Halting leaf water loss could have impacted other aspects of the resistance response that are critical to bacterial growth suppression; however, the petroleum jelly treatment did not prevent plant PCD, indicating that the signaling pathways culminating in PCD were not inhibited. Furthermore, limiting leaf water loss by incubation at high RH also reversed the bacterial growth suppression associated with resistance. Functionally, limiting water in the early hours of gene-for-gene mediated resistance may provide time for the plant to deploy other mechanisms to limit pathogen growth, spread and damage. These other mechanisms may be causal to the smaller populations of bacteria that are ultimately established in plants exhibiting this resistance as compared to disease.

The *P. syringae*-derived phytotoxin coronatine promotes stomatal opening as reported previously (Melotto et al., 2006) and confirmed here, but this opening appears to be only transient during disease induction and is suppressed during the effector-mediated resistance. Coronatine-induced stomatal opening was demonstrated by Melotto et al. (2006) using microscopy to directly measure stomatal aperture. Here, measurements of stomatal conductance independently verified this phenomenon. Interestingly, the increase in stomatal conductance that occurred between 2.5 and 5 hpi in DC3000(pPI)-inoculated plants was followed by a large and rapid decrease between 5 and 7 hpi (Fig 3A). This stomatal closure may function to reduce the rate of water loss through the stomata and thus improve the intercellular environment as a habitat for pathogenic cells following their entry into the leaves. This function was proposed by Goel et al. (2008) to explain the increased growth of *P. syringae* in water-stressed plants in the presence of high levels of the effector HopAM1, which enhances abscisic acid-mediated stomatal closure. Our results also indicate that stomatal closure may be mediated by one or more T3SS effectors based on the absence of a dramatic closure in plants inoculated with a T3SS-deficient *hrcC* mutant. Whether HopAM1 is involved in promoting stomatal closure under the test conditions here is unclear. During gene-for-gene resistance, the coronatine-mediated stomatal opening was greatly attenuated or did not occur. This could be due to suppression of coronatine production in *P. syringae*, or to the suppression of the coronatine-mediated effects on stomatal activity. The dramatic decrease in stomatal conductance that accompanies this resistance response suggests the latter.

Leaves exposed to the MAMP flg22 exhibited reduced stomatal conductance. This is consistent with previous reports of MAMP-mediated stomatal closing (Lee et al., 1999; Melotto et al., 2006). However, based on our observation that leaf immersion in buffer promotes sustained stomatal opening, at least under conditions of ambient RH >45%, our results are also consistent with the possibility that flg22 inhibits stomatal opening rather than promotes stomatal closure. Such inhibition of stomatal opening by flg22 was recently reported by Zhang et al. (2008). When inoculated by immersion, leaves exposed to DC3000(pPI*avrRpm1*) consistently exhibited a lower stomatal conductance within 1 hpi than those exposed to DC3000(pPI). This result is consistent with a previous report of AvrRpt2-mediated stomatal closing (Lee et al., 1999; Melotto et al., 2006) and suggests that the AvrRpm1 effector, like flg22, promotes

stomatal closure or inhibits stomatal opening. This rapid effect following inoculation may reflect effector entry into the guard cells themselves.

This study demonstrates the power of a real-time analysis of living leaves for characterizing leaf physiology during bacterial challenge. In particular, the stomatal conductance, leaf transpiration and photosynthesis, as monitored using a LI-6400 photosynthesis system, were shown to be highly dynamic following *P. syringae* inoculation. Static measurements of physiological properties such as vascular activity and plant cell death were needed during the early hours of a gene-for-gene mediated resistance response to begin to relate these properties to pathogen dynamics. Such physiological data are critical to complement the accumulating wealth of knowledge on the signal transduction cascades and transcriptional changes associated with resistance and pathogenesis (e.g., Kim et al., 2008; Livaja et al., 2008; Pieterse and Dicke, 2007; Thilmony et al., 2006). In particular, our demonstration that vascular activity can be strongly and rapidly altered following infection, and can be altered in a highly localized manner, indicates the need to examine cellular targets influencing vascular activity and water relations within leaves for a role in plant defense against pathogens.

Acknowledgements

We thank Kelly Peterson for the construction of the bacterial strains DC3000(pPI*avrRpm1*) and DC3000(pPI*avrRpt2*), the department of Genetics, Developmental and Cellular Biology at Iowa State University for the use of the LI-6400 photosynthesis system, LI-COR Biosciences for training and assistance, Sheng Yang He for the coronatine mutant DC3118, Adam Bogdanove for providing tomato seeds, Larry Halverson and Ed Braun for the use of their microscopes, Michael Deal and Jordan Sherbondy for laboratory assistance, and Ashley Middle for assistance with *A. thaliana* propagation. This project was supported by the National Research Initiative of the USDA-CSREES, grant No. 2005-35319-15300.

References

Century, K.S., Holub, E.B., and Staskawicz, B.J. 1995. *ndr1*, a Locus of *Arabidopsis thaliana* that is required for disease resistance to both a bacterial and a fungal pathogen. Proc. Natl. Acad. Sci. U.S.A. 92:6597-6601.

Chaerle, L., Van Caeneghem, W., Messens, E., Lambers, H., Van Montagu, M., and Van Der Straeten, D. 1999. Presymptomatic visualization of plant-virus interactions by thermography. Nat. Biotechnol. 17:813-816.

Chatelet, D.S., Matthews, M.A., and Rost, T.L. 2006. Xylem structure and connectivity in grapevine (*Vitis vinifera*) shoots provides a passive mechanism for the spread of bacteria in grape plants. Ann. Bot. 98:483-494.

Ciccarelli, F.D., and Bork, P. 2005. The WHy domain mediates the response to desiccation in plants and bacteria. Bioinformatics 21:1304-1307.

Clough, S.J., Fengler, K.A., Yu, I.C., Lippok, B., Smith, R.K., Jr., and Bent, A.F. 2000. The *Arabidopsis dnd1* "defense, no death" gene encodes a mutated cyclic nucleotide-gated ion channel. Proc. Natl. Acad. Sci. U.S.A. 97:9323-9328.

Cook, A.A., and Stall, R.E. 1977. Effects of watersoaking on response to *Xanthomonas vesicatoria* in pepper leaves. Phytopathology 67:1101-1103.

Dangl, J.L., and Jones, J.D. 2001. Plant pathogens and integrated defense responses to infection. Nature 411:826-833.

DebRoy, S., Thilmony, R., Kwack, Y.B., Nomura, K., and He, S.Y. 2004. A family of conserved bacterial effectors inhibits salicylic acid-mediated basal immunity and promotes disease necrosis in plants. Proc. Natl. Acad. Sci. U.S.A. 101:9927-9932.

Evert, R.F. 2006. Esau's Plant Anatomy. 3rd edition. John Wiley & Sons, Inc., Hoboken, NJ.

Farquhar, G.D., and Sharkey, T.D. 1982. Stomatal conductance and photosynthesis. Ann. Rev. Plant Physiol. Plant Mol. Biol. 33:317-345.

Galan, J.E., and Wolf-Watz, H. 2006. Protein delivery into eukaryotic cells by type III secretion machines. Nature 444:567-573.

Gassmann, W. 2005. Natural variation in the *Arabidopsis* response to the avirulence gene *hopPsyA* uncouples the hypersensitive response from disease resistance. Mol. Plant-Microbe Interact. 18:1054-1060.

Goel, A.K., Lundberg, D., Torres, M.A., Matthews, R., Akimoto-Tomiyama, C., Farmer, L., Dangl, J.L., and Grant, S.R. 2008. The Pseudomonas syringae type III effector HopAM1 enhances virulence on water-stressed plants. Mol. Plant-Microbe Interact. 21:361-370.

Gopalan, S., Wei, W., and He, S.Y. 1996. *hrp* gene-dependent induction of *hin1*: a plant gene activated rapidly by both harpins and the *avrPto* gene-mediated signal. Plant J. 10:591-600.

Gudesblat, G.E., Torres, P.S., and Vojnov, A.A. 2009. *Xanthomonas campestris* overcomes *Arabidopsis* stomatal innate immunity through a DSF cell-to-cell signal-regulated virulence factor. Plant Physiol. 149:1017-1027.

Hammond-Kosack, K.E., Silverman, P., Raskin, I., and Jones, J. 1996. Race-specific elicitors of *Cladosporium fulvum* induce changes in cell morphology and the synthesis of ethylene and salicylic acid in tomato plants carrying the corresponding *cf* disease resistance gene. Plant Physiol. 110:1381-1394.

Hauck, P., Thilmony, R., and He, S.Y. 2003. A *Pseudomonas syringae* type III effector suppresses cell wall-based extracellular defense in susceptible *Arabidopsis* plants. Proc. Natl. Acad. Sc.i U.S.A. 100:8577-8582.

Heath, M.C. 2000. Hypersensitive response-related death. Plant Mol. Biol. 44:321-334.

Hinsch, M., and Staskawicz, B. 1996. Identification of a new *Arabidopsis* disease resistance locus, *RPS4*, and cloning of the corresponding avirulence gene, *avrRps4*, from *Pseudomonas syringae* pv. pisi. Mol. Plant-Microbe Interact. 9:55-61.

Huang, H.C., Schuurink, R., Denny, T.P., Atkinson, M.M., Baker, C.J., Yucel, I., Hutcheson, S.W., and Collmer, A. 1988. Molecular cloning of a *Pseudomonas syringae* pv. syringae gene-cluster that enables *Pseudomonas fluorescens* to elicit the hypersensitive response in tobacco plants. J. Bacteriol. 170:4748-4756.

Jambunathan, N., Siani, J.M., and McNellis, T.W. 2001. A humidity-sensitive *Arabidopsis* copine mutant exhibits precocious cell death and increased disease resistance. Plant Cell 13:2225-2240.

Jamir, Y., Guo, M., Oh, H.S., Petnicki-Ocwieja, T., Chen, S., Tang, X., Dickman, M.B., Collmer, A., and Alfano, J.R. 2004. Identification of *Pseudomonas syringae* type III effectors that can suppress programmed cell death in plants and yeast. Plant J. 37:554-565.

Kang, L., Tang, X., and Mysore, K.S. 2004. *Pseudomonas* type III effector AvrPto suppresses the programmed cell death induced by two nonhost pathogens in *Nicotiana benthamiana* and tomato. Mol. Plant-Microbe Interact. 17:1328-1336.

Kim, M.G., Kim, S.Y., Kim, W.Y., Mackey, D., and Lee, S.Y. 2008. Responses of *Arabidopsis thaliana* to challenge by *Pseudomonas syringae*. Molecules and Cells 25:323-331.

King, E.O., Ward, M.K., and Raney, D.E. 1954. Two simple media for the demonstration of pyocyanin and fluorescin. J. Lab. Clin. Med. 44:301-307.

Kpemoua, K., Boher, B., Nicole, M., Calatayud, P., and Geiger, J.P. 1996. Cytochemistry of defense responses in cassava infected by *Xanthomonas campestris* pv. manihotis. Can. J. Microbiol. 42:1131-1143.

Lee, S., Choi, H., Suh, S., Doo, I.S., Oh, K.Y., Choi, E.J., Schroeder Taylor, A.T., Low, P.S., and Lee, Y. 1999. Oligogalacturonic acid and chitosan reduce stomatal aperture by inducing the evolution of reactive oxygen species from guard cells of tomato and *Commelina communis*. Plant Physiol. 121:147-152.

Livaja, M., Zeidler, D., von Rad, U., and Durner, J. 2008. Transcriptional responses of Arabidopsis thaliana to the bacteria-derived PAMPs harpin and lipopolysaccharide. Immunobiology 213:161-171.

Lorrain, S., Lina, B.Q., Auriac, M.C., Kroj, T., Saindrenan, P., Nicole, M., Balague, C., and Roby, D. 2004. Vascular associated death1, a novel gram domain-containing protein, is a regulator of cell death and defense responses in vascular tissues. Plant Cell 16:2217-2232.

Ma, S.W., Morris, V.L., and Cuppels, D.A. 1991. Characterization of a DNA region required for production of the phytotoxin coronatine by *Pseudomonas syringae* pv. tomato. Mol. Plant-Microbe Interact. 4:69-74.

Mattoo, S., Lee, Y.M., and Dixon, J.E. 2007. Interactions of bacterial effector proteins with host proteins. Curr. Opin. Immunol. 19:392-401.

Melotto, M., Underwood, W., Koczan, J., Nomura, K., and He, S.Y. 2006. Plant stomata function in innate immunity against bacterial invasion. Cell 126:969-980.

Mittal, S., and Davis, K.R. 1995. Role of the phytotoxin coronatine in the infection of *Arabidopsis thaliana* by *Pseudomonas syringae* pv. tomato. Mol. Plant-Microbe Interact. 8:165-171.

Mittler, R., Simon, L., and Lam, E. 1997. Pathogen-induced programmed cell death in tobacco. J. Cell Sci. 110:1333-1344.

Moore, R.A., Starratt, A.N., Ma, S.W., Morris, V.L., and Cuppels, D.A. 1989. Identification of a chromosomal region required for biosynthesis of the phytotoxin coronatine by *Pseudomonas syringae* pv. tomato. Can. J. Microbiol. 35:910-917.

Morel, J.B., and Dangl, J.L. 1997. The hypersensitive response and the induction of cell death in plants. Cell Death Differ. 4:671-683.

Mur, L.A.J., Kenton, P., Lloyd, A.J., Ougham, H., and Prats, E. 2008. The hypersensitive response; the centenary is upon us but how much do we know? J. Exp. Bot. 59:501-520.

Oh, H.S., and Collmer, A. 2005. Basal resistance against bacteria in *Nicotiana benthamiana* leaves is accompanied by reduced vascular staining and suppressed by multiple *Pseudomonas syringae* type III secretion system effector proteins. Plant J. 44:348-359.

Penaloza-Vazquez, A., Preston, G.M., Collmer, A., and Bender, C.L. 2000. Regulatory interactions between the Hrp type III protein secretion system and coronatine biosynthesis in *Pseudomonas syringae* pv. tomato DC3000. Microbiology 146:2447-2456.

Perez-Donoso, A.G., Greve, L.C., Walton, J.H., Shackel, K.A., and Labavitch, J.M. 2007. *Xylella fastidiosa* infection and ethylene exposure result in xylem and water movement disruption in grapevine shoots. Plant Physiol. 143:1024-1036.

Pieterse, C.M.J., and Dicke, M. 2007. Plant interactions with microbes and insects: from molecular mechanisms to ecology. Trends Plant Sci. 12:564-569.

Stall, R.E., and Cook, A.A. 1979. Evidence that bacterial contact with the plant-cell is necessary for the hypersensitive reaction but not the susceptible reaction. Physiol. Plant Pathol. 14:77-84.

Thilmony, R., Underwood, W., and He, S.Y. 2006. Genome-wide transcriptional analysis of the *Arabidopsis thaliana* interaction with the plant pathogen *Pseudomonas syringae* pv. tomato DC3000 and the human pathogen *Escherichia coli* O157:H7. Plant J 46:34-53.

Turgeon, R. 2006. Phloem loading: how leaves gain their independence. Bioscience 56:15-24.

Turner, J.G., and Novacky, A. 1974. The quantitative relation between plant and bacterial cells involved in the hypersensitive reaction. Phytopathology 64:885-890.

Wang, C., Cai, X., and Zheng, Z. 2005. High humidity represses *Cf-4/Avr4*- and *Cf-9/Avr9*-dependent hypersensitive cell death and defense gene expression. Planta 222:947-956.

Weymann, K., Hunt, M., Uknes, S., Neuenschwander, U., Lawton, K., Steiner, H.Y., and Ryals, J. 1995. Suppression and restoration of lesion formation in *Arabidopsis lsd* mutants. Plant Cell 7:2013-2022.

Whalen, M.C., Innes, R.W., Bent, A.F., and Staskawicz, B.J. 1991. Identification of *Pseudomonas syringae* pathogens of *Arabidopsis* and a bacterial locus determining avirulence on both *Arabidopsis* and soybean. Plant Cell 3:49-59.

Wilson, M., and Lindow, S.E. 1993. Interactions between the biological control agent *Pseudomonas fluorescens* A506 and *Erwinia amylovora* in pear blossoms. Phytopathology 83:117-123.

Wright, C.A., and Beattie, G.A. 2004. *Pseudomonas syringae* pv. *tomato* cells encounter inhibitory levels of water stress during the hypersensitive response of *Arabidopsis thaliana*. Proc. Natl. Acad. Sc.i U.S.A. 101:3269-3274.

Wright, K.M., Duncan, G.H., Pradel, K.S., Carr, F., Wood, S., Oparka, K.J., and Cruz, S.S. 2000. Analysis of the *N* gene hypersensitive response induced by a fluorescently tagged tobacco mosaic virus. Plant Physiol. 123:1375-1386.

Yoshioka, K., Kachroo, P., Tsui, F., Sharma, S.B., Shah, J., and Klessig, D.F. 2001. Environmentally sensitive, SA-dependent defense responses in the *cpr22* mutant of *Arabidopsis*. Plant J. 26:447-459.

Young, J.M. 1974. Effect of water on bacterial multiplication in plant-tissue. NZ J. Agric. Res. 17:115-119.

Yu, I.C., Parker, J., and Bent, A.F. 1998. Gene-for-gene disease resistance without the hypersensitive response in *Arabidopsis dnd1* mutant. Proc. Natl. Acad. Sci. U.S.A. 95:7819-7824.

Yuan, J., and He, S.Y. 1996. The *Pseudomonas syringae* Hrp regulation and secretion system controls the production and secretion of multiple extracellular proteins. J. Bacteriol. 178:6399-6402.

Zhang, W., He, S.Y., and Assmann, S.M. 2008. The plant innate immunity response in stomatal guard cells invokes G-protein-dependent ion channel regulation. Plant J. 56:984-996.

Chapter 3. Whole-genome transcript responses of *Pseudomonas syringae* pv. syringae B728a and pv. tomato DC3000 to osmotic stress

Brian C. Freeman, Chiliang Chen, Kelly Peterson, Nicole O'Toole, Gwyn A. Beattie
Department of Plant Pathology,
Iowa State University; Ames, IA, 50010, USA

(Chiliang Chen and Kelly Peterson performed the initial cell treatments and RNA isolations for the microarray experiment, and Nicole O'Toole assisted with organizing the genes into functional categories).

Abstract

Whole-genome transcriptome analysis was performed to characterize the response of *P. syringae* to osmotic stress and to elucidate differences between two closely related pathovars of *P. syringae* in this response. *P. syringae* pv. syringae B728a is an epiphyte with high abiotic stress tolerance that is able to colonize leaf surfaces and achieve high population sizes. In contrast, *P. syringae* pv. tomato DC3000 has a more pronounced endophytic stage and only poorly colonizes leaf surfaces. The transcript profiles of the two pathovars were examined after exposure to moderate osmotic shock in a solution of NaCl for 15 minutes. The two strains shared a number of responses, including the suppression of a large number of genes involved with general metabolism, iron storage, chemotaxis, motility and attachment. Both strains also shared induction of a number of osmoadaptation genes involved in alginate biosynthesis, osmoprotectant transporter, and compatible solute synthesis, although the magnitude of induction of many of these genes was higher in B728a compared with DC3000. Comparison of the transcriptional responses also revealed clear differences between the two strains. Many genes involved with pathogenicity and virulence, including the HrpL regulon, were suppressed in DC3000 but not altered or even induced in B728a. Other genes that were differentially regulated included some involved in carbohydrate metabolism, heat shock tolerance, aromatic carbon degradation, and sulfate transport.

Introduction

Low water availability may be the most significant obstacle faced by resident microbes on leaf surfaces. Bacteria able to colonize these habitats have developed numerous traits that enable them to withstand desiccation and osmotic stress brought about as surface water evaporates and remaining dissolved solutes become concentrated. *Pseudomonas syringae* is a gram-negative bacterial plant pathogen that is ubiquitous on leaves and serves as a model organism for the study of plant-pathogen interactions (Hirano and Upper 1990). *P. syringae* is subdivided into over 50 pathovars that differ considerably with respect to host range, ecology, and stress tolerance (Sawada et al. 1999; Feil et al. 2005). *P. syringae* pv. syringae strain B728a is a pathogen of bean (*Phaseolus vulgaris*) that exhibits a very pronounced epiphytic phase on plants, often reaching surface populations as high as 10^7 cells per gram (Hirano and Upper 2000; Boureau et al. 2002). In contrast, the tomato (*Solanum lycopersicum*) pathogen *P. syringae* pathovar tomato strain DC3000 is a relatively poor colonist of leaf surfaces, seldom reaching populations $>10^5$ cells per gram (Chen, Freeman & Beattie, unpublished data). These two strains differ greatly in their ability to tolerate osmotic stress, with B728a tolerating NaCl concentrations as high as 0.6M and DC3000 tolerating NaCl as high as 0.4M NaCl (Chen & Beattie, unpublished data). Osmotolerance may also be an important component of epiphytic survival in *P. syringae* based on the reduced fitness of osmosensitive mutants, albeit pleiotropic mutants, of *P. syringae* B728a on drying leaf surfaces (Lindow et al. 1993; Beattie and Lindow 1994; Beattie and Lindow 1994).

Bacteria often respond to changes in external osmolarity by accumulating compatible solutes, which are compounds that can accumulate to high concentrations without disrupting cellular metabolism. Pseudomonads accumulate a variety of compatible solutes, including potassium glutamate, trehalose, ectoine, N-acetylglutaminylglutamine amide (NAGGN), mannitol, and glucosylglycerol (Yancey et al. 1982; Dinnibier et al. 1988; Cayley et al. 1992; D'Souza-Ault et al. 1993; Kets et al. 1996). These compounds may be synthesized *de novo*; alternatively, compounds that can function as, or be converted to, compatible solutes such as betaine, choline or carnatine can be transported into the cell from the external environment. Pseudomonads also produce exopolymeric substances (EPS) that encapsulate the bacterial cells and may help to protect them from desiccation (Yu et al. 1999; Chang et al. 2007).

Pseudomonads have the potential to produce many different types of EPS constituents, including alginate, levan, marginalan, and cellulose, in addition to several uncharacterized polymers (Fialho et al. 1990; Fett et al. 1995; Kachlany et al. 2001; Jackson et al. 2004).

A recent genomic analysis of DC3000 and B728a revealed a very high genetic similarity between them; of the 5,090 protein-encoding genes on the B728a chromosome, 4,273 (84%) are shared with DC3000 (Feil et al. 2005). Not surprisingly, both strains share a large number of genes involved with osmoadaptation. Both DC3000 and B728a make betaine from choline due to the presence of choline dehydrogenase and betaine-aldehyde dehydrogenase, and both strains share a large number of choline and glycine betaine transporter genes. Both strains also possess genes for the production of NAGGN, as well as genes for the biosynthesis of the EPS constituent alginate. Hence, the differential expression of genes in response to osmotic stress may contribute to differences in the osmotolerance of B728a versus DC3000. In this study, we used whole-genome microarrays to investigate the early transcriptional response of *P. syringae* to osmotic shock and evaluate the variability in gene expression profiles between two closely related *P. syringae* strains, DC3000 and B728a.

Materials and Methods

Bacterial strains, growth conditions and treatments

Pseudomonas syringae pv. tomato strain DC3000 (Moore et al. 1989) and pv. syringae strain B728a (Loper and Lindow 1987) were grown on King's B (KB) medium (King et al. 1954) for two days at 28°C using 50 μg/ml rifampin (Rif) for selection. 5-ml volumes of ½ 21C medium containing 0.3% glucose and 5mM succinate (½ 21C-GS) were inoculated with single colonies and grown until dense (approximately 10^9 cells/ml). 10ul of cells were then subcultured into 5-ml of ½ 21C-GS and again grown until dense. A 30-ml volume of ½ 21C-GS was inoculated and grown until mid-log phase (approximately 10^8 cells/ml). Cell cultures were centrifuged at 5,000xg for 10 min and the pellets resuspended in 3.6ml pre-warmed ½ 21C-GS to a final OD of 0.4 (approx. $8x10^8$ cells/ml). 300ul aliquots were transferred to 10-ml tubes and incubated at 28°C with shaking at 200rpm for 15 min. 0.8 ml of pre-warmed ½ 21C-GS with or without NaCl was added to yield a final concentration of 219 mM NaCl (-1 MPa) or 0 mM NaCl (-0.2 MPa),

respectively. The tubes were incubated at 28°C with shaking, and cells were harvested after 15 min by mixing with 2 ml of Qiagen RNA Protect Bacteria reagent.

RNA extraction, hybridization, and microarray design

RNA was purified using a Qiagen RNeasy mini kit and DNA was removed using the on-column DNase I digestion described by the manufacturer (Qiagen Inc., Valencia, CA). DNase I was removed by using RNeasy column purification. RNA integrity was evaluated using an Agilent 2100 bioanalyzer. Two biological replicates each consisting of pooled RNA from 4 replicate cultures collected from 4 separate days were used for each treatment. RNA samples were sent to NimbleGen Inc. (Madison, WI) for conversion into cDNA, labeling with U-CYA-3 fluorophore, and hybridization to the arrays. ORF-based microarrays were designed using complete genome sequence information for DC3000, including both plasmids (accession numbers NC_004578, NC_004632, and NC_004633), and a draft-phase sequence for B728a (accession numbers NZ_AABP02000001- NZ_AABP02000026). Two complete microarrays were present on each slide and these technical replicates were designated as blocks. Each gene was represented by a minimum of 17 (DC3000) or 19 (B728a) 24-mer nucleotide probes, with each block containing a complete set of perfect match and mismatch probes.

Microarray data analysis

Fluorescence intensity for each probe was measured and the fluorescent intensities subjected to robust multiarray averaging (RMA), which included adjustment for the background intensity, quantile normalization and median polishing. A robust estimated mean value for each gene on the array was determined for each technical replicate and the two values for each gene were averaged. Analysis of variance (ANOVA) was used to determine *p*- and *q*-values for each gene. In B728a, this included four values: two biological replicates representing cells with and without NaCl exposure. For DC3000 this included the two biological replicates representing cells with and without NaCl exposure as well as two replicates for each of three additional treatments which were part of another study and included cells exposed to polyethylene glycol, H_2O_2, or phenol. Results from the latter three treatments will not be discussed in this chapter. Genes with *p*-values ≤ 0.05 were considered significant.

Quantitative RT-PCR

To validate the results of the microarray, quantitative RT-PCR analysis was performed on select open reading frame targets in DC3000. Bacterial cells were grown as described above. Two concentrations of NaCl were used: 219 mM (-1 MPa) and 438 mM (-1.9 MPa). Cells were harvested after 15 min and after 60 min, and RNA extraction and purification was performed as described above. One-step RT conversion of RNA to cDNA and amplification of select targets was performed using a SYBR Green I-based Stratagene Full Velocity master mix (Stratagene, Cedar Creek, TX) in an Opticon thermocycler (Opticon Inc, Orangeburg, NY). The housekeeping gene *hemD* (PSPTO_0129) was used as an internal control to normalize induction values for all ORFs. The fold-change for each ORF was calculated using $2^{(-\Delta\Delta Ct)}$, where $\Delta\Delta Ct = (Ct(target) - Ct(\textit{hemD}))_{treatment} - (Ct(target) - Ct(\textit{hemD}))_{control}$. The mean fold-change was calculated from two replicate samples for each treatment per timepoint. Primer sequences are shown in Table 1.

Table 1. Primers used in quantitative RT-PCR analysis.

Target	Primer	
hemD	F	5'-TCAGCAGCAGTCTGCCTTTA-3'
	R	5'-GTTGCTGAACCCACACTGAA-3'
glnA	F	5'-TCACGGACACTAAAGGTACGC-3'
	R	5'-TGATGTCGCACACCAGAATC-3'
cspC	F	5'- AATGGCTGAACGTCAGAGCG-3'
	R	5'-CCTTCGGCGTGTACTTCG-3'
hfnA	F	5'-AGTGGGCAACGTCAAGCAAG-3'
	R	5'-CGTCTTTCACTTCGCCTTTAGC-3'
asnB	F	5'-CGCTCAATCATTACCTCAACTTC-3'
	R	5'-TGCTGTCCAGTACACGGTCG-3'
glgA	F	5'-TCGTGACCTCCGAACTGG-3'
	R	5'-TCCATACGCCCAACCTTG-3'
treY	F	5'-CTGTTCAATGAATCAACCGTC-3'
	R	5'-TAGTTGCTGGTCATGCTC-3'
opuCD	F	5'-AACACCGTTCCGCCACTC-3'
	R	5'-GACACGCACGCCACCAATA-3'
bfr	F	5'-GGCAACACGCTCAAAGAAATG-3'
	R	5'-GCCGATGTACTGAATGATCTCGC-3'

Results

Overview of transcriptional responses to water stress

We determined the global transcriptome of *Pseudomonas syringae* pathovars tomato strain DC3000 and syringae strain B728a exposed to a water potential of -1MPa imposed by NaCl for 15 minutes. In DC3000, 5,607 genes were analyzed; 2,113 genes, or 38% of the genome, exhibited differential expression among five treatments (see Materials and Methods) (p<0.05, q<0.02). In B728a, 4,900 genes were analyzed; 1,257 genes, or 12% of the genome, exhibited differential expression between two treatments: the basal medium with and without NaCl (p<0.05, q<0.13). This difference in the percentage of genes responding to osmotic stress in DC3000 and B728a was likely due, at least in part, to differences in the statistical power for detecting differences rather than in a biological difference between the strains.

In DC3000, more genes were repressed than induced by NaCl. The number of genes that were repressed more than 1.3-fold was 582 and more than 1.8-fold was 169, whereas the number of genes that were induced by NaCl more than 1.3-fold was 337 and more than 1.8-fold was 131. In contrast, B728a exhibited similar numbers of genes that were induced and repressed by osmotic stress. 143 genes were induced by NaCl more than 1.3-fold, and 76 genes were induced by NaCl more than 1.8-fold. 161 genes were repressed by NaCl more than 1.3-fold, and 67 genes were repressed by NaCl more than 1.8-fold.

Induced genes

Alginate biosynthetic genes were strongly induced by osmotic stress in both strains (Table 2). In DC3000, the alternative sigma factor *algU* (*rpoE,* σ^{24}) as well as the negative regulators of *algU*, *mucA* and *mucB*, were strongly induced by water stress in DC3000. *mucA* and *mucB* are likely in the same operon as *algU*, based on their downstream arrangement and short intergenic regions (<35bp). The increased expression of *mucB* suggests it may have an additional promoter or increased stability under water stress. DC3000 genes that are known to be induced by AlgU in other pseudomonads were also increased in expression under water stress; these include *algR* (PSPTO_0127), a transcriptional regulator of the phosphomannomutase gene *algC* (PSPTO_0083), and *algD* (PSPTO_1243), the first gene in the alginate biosynthetic cluster

(PSPTO_1243-1232). In B728a, induction of genes in the alginate biosynthetic cluster (Psyr_1052-1063) was considerably stronger than in DC3000. Surprisingly, the induction levels for the alginate regulators *algC* (Psyr_0219) and *algR* (Psyr_0063) were not similarly stronger in B728a than DC3000. Although an *algU* homolog was not represented on the B728a microarray, which was designed based on contigs rather than a complete genome sequence, *mucA* (Psyr_3957) and *mucB* (Psyr_3956) were present and strongly induced.

Table 2. *P. syringae* genes induced at least 1.8-fold in response to osmotic stress. Values in parentheses indicate that gene expression did not differ significantly between treatments with and without NaCl (p>0.05); dashes indicate the ORF was not present on the microarray*; NH* (no homolog) = a gene identified in B728a that exhibited a high sequence similarity to the target DC3000 ORF was not identified in B728a.

Predicted Function	Gene Name	DC3000		B728a	
		Gene (PSPTO#)	Fold change	Gene (Psyr #)	Fold change
Alginate biosynthesis					
Alginate response regulator	*algC*	0083	**2.66**	0219	**1.56**
Alginate transcriptional activator	*algR*	0127	**2.18**	0063	**1.59**
Alginate biosynthetic protein	*algG*	1238	**1.73**	1058	**17.02**
Alginate biosynthetic protein	*algE*	1239	**1.33**	1059	**8.14**
Alginate biosynthetic protein	*algK*	1240	**1.37**	1060	**5.26**
Alginate biosynthetic protein		1241	**2.15**	1061	**7.78**
Alginate biosynthetic protein		1242	**1.42**	1062	**7.66**
Alginate biosynthetic protein	*algD*	1243	**3.40**	1063	**16.38**
AlgU negative regulatory protein	*mucB*	4222	**6.58**	3956	**4.15**
AlgU negative regulatory protein	*mucA*	4223	**4.41**	3957	**4.23**
RNA polymerase sigma factor	*rpoE* / a*lgU*	4224	**5.53**	3958	**--**
Osmoprotectant transport					
Betaine/choline	*bccV*	0462	**1.85**	4711	**--**
Betaine/choline	*bccW*	0463	**3.15**	4710	**--**
Betaine/choline	*bccX*	0464	**10.41**	4709	**--**
Betaine/choline	*opuCA*	4575	**4.86**	4249	**9.57**
Betaine /carnitine/choline	*opuCB*	4576	**5.64**	4250	**13.63**
Betaine /carnitine/choline	*opuCC*	4577	**8.12**	4251	**26.28**
Betaine /carnitine/choline	*opuCD*	4578	**9.26**	4252	**19.90**
Choline	*betT*	5269	**1.91**	4827	**1.15**
Compatible solute synthesis					
NAGGN biosynthesis		1630	**4.56**	3750	**2.11**
NAGGN biosynthesis		1631	**5.58**	3749	**6.75**
NAGGN biosynthesis		1632	**9.76**	3748	**14.17**
NAGGN biosynthesis	*asnB*	1633	**10.90**	3747	**3.88**
Trehalose biosynthesis		2760	**3.02**	2489	**1.59**

Trehalose biosynthesis	*amyA*	2761	**1.75**	2490	**1.65**
Trehalose biosynthesis	*glgA*	3125	**3.04**	2992	**1.46**
Trehalose biosynthesis	*glgB*	3126	**2.38**	2993	**(1.75)**
Trehalose biosynthesis	*malQ*	3127	**2.19**	2994	**(2.25)**
Trehalose biosynthesis	*treY*	3128	**1.42**	2995	**1.70**
Trehalose biosynthesis		3129	**2.42**	2996	**5.04**
Trehalose biosynthesis	*glgX*	3130	**1.94**	2997	**2.28**
Cell envelope and periplasm					
Outer membrane lipoprotein	*osmE*	4903	**2.41**	4446	**5.07**
Outer membrane lipoprotein	*ompA*	1506	**7.33**	1316	**4.71**
Outer membrane lipoprotein	*ompA*	1164	**3.16**	1005	**2.03**
Periplasmic osmotic shock protein	*osmC*	0152	**5.99**	0040	**4.09**
Periplasmic osmotic shock protein	*osmY*	4484	**24.89**	4175	**12.65**
Periplasmic glucan biosynthesis	*mdoH*	5161	**1.80**	0378	**--**
Periplasmic glucan biosynthesis	*mdoG*	5162	**1.83**	0377	**--**
Miscellaneous					
Aconitate hydratase	*acnA*	2016	**1.92**	3404	**1.54**
Catalase	*katE*	5263	**1.45**	0280	**2.26**
Carbohydrate metabolism		3119	**1.27**	2986	**(1.21)**
Carbohydrate metabolism		3120	**1.71**	2987	**1.60**
Carbohydrate metabolism	*zwf-2*	3121	**2.43**	2988	**1.43**
Carbohydrate metabolism		3122	**1.74**	2989	**1.78**
Nutrient transport: C4-dicarboxylate/malate		4613	**1.03**	1479	**4.34**
Resolvase (putative)	*pinR*	2319	**6.34**	2668	**--**
Iron metabolism					
Bacterioferritin-associated ferredoxin	*bfd*	4159	**(1.51)**	3099	**2.30**
Hemerythrin (putative)		2773	**1.95**	2501	**4.20**
Iron transport	*tonB*	0067	**1.27**	0203	**2.16**
Iron utilization (putative)		4193	**1.60**	3927	**1.26**
Non-heme Dps ferritin (putative)		4906	**9.11**	4448	**4.30**
DC3000 plasmid genes					
DNA transfer protein	*traT*	A0059	**2.04**	NH	
DNA transfer protein	*traU*	A0060	**2.04**	NH	
DNA transfer protein	*traW*	A0062	**2.11**	NH	
DNA transfer protein	*traX*	A0063	**2.11**	NH	
DNA transfer protein	*traY*	A0064	**2.19**	NH	
DNA transfer protein	*trbB*	A0067	**2.58**	NH	
Conjugal transfer protein	*traG/traD*	A0068	**2.63**	NH	
Transcriptional regulator		A0071	**3.50**	NH	

The *bccVWX* operon encodes a binding protein-dependent active transport system for glycine betaine and choline in DC3000 (PSPTO_0462-0464). This operon was strongly induced by NaCl (Table 2). The B728a *bcc* operon (Psyr_4709-4711) was not present on the microarray.

The genes encoding the high-affinity osmoprotectant transporter OpuC (Chen and Beattie 2007), (PSPTO_ 4575-4578) and (Psyr_4749-4753), were highly induced by osmotic stress in both strains. NaCl induction of these genes was also considerably stronger in B728a (avg. 17-fold) than in DC3000 (avg. 7-fold). The gene encoding the low-affinity-high-capacity choline transporter BetT was mildly induced by osmotic stress in DC3000 and B728a and is known to be osmoregulated primarily at the post-transcriptional level (Chen and Beattie 2008).

The putative NAGGN biosynthetic clusters in DC3000 (PSPTO_1633-1630) and B728a (Psyr_3747-3750) were strongly induced by exposure to osmotic stress. Interestingly, in B728a, the second gene of the putative operon (Psyr_3749) showed much stronger induction than the first gene, whereas in DC3000, the first gene (PSPTO_1633) was induced more strongly (Table 2). The two genes are separated by only four nucleotides in both strains.

The trehalose biosynthetic pathway has not been characterized in *P. syringae*. DC3000 has two sets of genes showing sequence similarity to the trehalose biosynthetic loci in *Corynebacterium glutamicum, treZ* (PSPTO_3126) and *treY* (PSPTO_3128), which encode a malto-oligosyltrehalose synthase and a malto-oligosyltrehalose trehalohydrolase, respectively, and *treS* (PSPTO_2761), a trehalose synthase (maltose alpha-*D*-glucosyltransferase) that synthesizes trehalose via a pathway distinct from TreZ and TreY. The pathway catalyzed by TreS is the only putative trehalose synthetic pathway in *P. aeruginosa*. These genes appear to be in two clusters in each strain, PSPTO_2760-2762 and PSPTO_3125-3134, and Psyr_ 2489-2491 and Psyr_2992-3001. Genes in all of these clusters were induced by NaCl, but the levels of induction of individual genes were poorly correlated between the strains (Table 2). Overall, gene induction for trehalose synthesis was lower than for NAGGN synthesis in both strains, consistent with reports in *P. aeruginosa* (D'Souza-Ault et al. 1993) and *E. coli* (Dinnibier et al. 1988) that NAGGN and glutamate are the predominant early-accumulated osmolytes at low to moderate osmotic stress levels, whereas trehalose accumulates primarily in the later stages of growth in culture and at high osmotic stress levels.

Genes encoding outer membrane-associated and periplasmic proteins were highly induced by NaCl; these include *osmE*, two *ompA* homologs, *osmC*, and *osmY* (Table 2).

Hypothetical proteins encoded upstream of the *ompA* homologs in DC3000 (PSPTO_1507) and B728a (Psyr_1317) were highly induced by NaCl (12.84- and 21.99-fold, respectively). These genes may lie within the same operon as *ompA* (60 nt gap in each strain) suggesting that these hypothetical proteins may be related to the osmotic stress response. PSPTO_1507 and Psyr_1317 are highly conserved among pseudomonads. Surprisingly, two periplasmic glucan biosynthesis genes, *mdoG* (PSPTO_5162) and *mdoH* (PSPTO_5161) were induced by NaCl in DC3000. Periplasmic glucans are a group of oligosaccharides that are synthesized by some bacteria in response to low osmolarity (Bohin 2000; Page et al. 2001).

A gene cluster putatively involved in carbohydrate metabolism (PSPTO_3119-3122, Psyr_2986-2989) was induced in both strains (Table 1). One gene in particular, PSPTO_3120/Psyr_2987, putatively encodes a HAD superfamily domain, which is a domain present in sucrose and trehalose phosphatases and phosphomannomutases that is involved in catalyzing the production of sugars. The glucose-6-phosphate dehydrogenase gene *zwf-2* (PSPTO_3121, Psyr_2988) in this cluster was also induced. Its homolog *zwf-1* (PSPTO_1300, Psyr_1120) is the primary enzyme responsible for glucose metabolism in the Entner-Doudoroff (ED) pathway in *P. putida* (Kim et al. 2008): *zwf-1* and other enzymes of the ED pathway were repressed by water stress (Table 4), consistent with a general repression of glucose metabolism.

A small number of genes involved in general metabolism were induced by NaCl, including an aconitase, a catalase, several genes involved with carbohydrate metabolism, a nutrient transporter and a putative resolvase. Several genes involved in iron accumulation and storage were also induced by water stress in both strains, including a putative hemerythrin, a putative siderophore-interacting protein, and *tonB*, a periplasmic protein that facilitates uptake of iron-bound siderophores (Zhao and Poole 2002). In addition, water stress induced the expression of several genes in DC3000 involved with plasmid replication and transfer.

Repressed Genes

DC3000 and B728a exhibited repression of a large number of genes involved in general metabolism following exposure to NaCl; these included genes involved in amino acid transport and metabolism, carbohydrate metabolism, glycolysis, the pentose phosphate pathway, the citric

acid cycle, fatty acid synthesis, cell wall biogenesis, levan synthesis, biodegradation of aromatic carbon compounds, and nutrient storage (Table 3). A particularly large number of amino acid transporters were repressed, including the amino acid transporters PSPTO_1255 (Psyr_1072) and PSPTO_4108 (Psyr_3845), and the amino acid porin *oprD* (PSPTO_3987, Psyr_1400).

Table 3. *P. syringae* genes repressed at least 1.8-fold in response to osmotic stress. Values in parentheses indicate that gene expression did not differ significantly between treatments with and without NaCl (p>0.05); dashes indicate the ORF was not present on the microarray*; NH* (no homolog) = a gene identified in B728a that exhibited a high sequence similarity to the target DC3000 ORF was not identified in B728a.

Predicted Function	Gene Name	DC3000		B728a	
		Gene (PSPTO#)	Fold change	Gene (Psyr#)	Fold change
Cell envelope and periplasm					
Outer membrane lipoprotein	*omlA*	4509	**-1.97**	4199	**-1.48**
Outer membrane lipoprotein	*oprL*	2272	**-1.88**	2071	**(-1.77)**
Outer membrane lipoprotein (putative)	*vacJ*	2115	**-2.17**	1910	**-1.83**
Outer membrane transporter	*tolQ*	3975	**-1.55**	1412	**-2.07**
Iron metabolism and transport					
Bacterioferritin (heme-associated)	*bfr*	4160	**-2.00**	3897	**-1.35**
Bacterioferritin (heme-associated)		0653	**-1.36**	4521	**-1.92**
Ferredoxin		0416	**-1.44**	4759	**-1.08**
Heme synthesis	*cyoE*	1329	**-1.70**	1145	**-2.21**
Nutrient transport and metabolism					
Amino acid transport		1255	**-3.21**	1072	**-4.00**
Amino acid transport		1256	**-1.85**	1073	**-2.93**
Amino acid transport		1257	**-1.53**	1074	**-2.43**
Amino acid transport		1258	**-1.82**	1075	**-3.25**
Amino acid transport		4108	**-2.41**	3845	**-3.05**
Amino acid transport		4109	**-1.45**	3846	**-1.90**
Amino acid transport		4136	**-1.50**	3874	**-2.36**
Amino acid transport		4171	**-1.69**	3908	**--**
Amino acid metabolism	*putA*	0728	**-2.40**	0629	**-2.12**
Amino acid metabolism	*aspC*	2163	**-2.23**	1973	**-1.86**
Amino acid metabolism	*maiA*	3554	**-1.94**	1842	**-1.48**
Amino acid metabolism		1843	**-2.03**	3555	**-1.77**
Amino acid metabolism	*argJ*	4399	**-1.27**	4093	**-2.58**
Amino acid metabolism	*glnA*	0359	**-4.74**	4817	**-5.66**
Amino acid metabolism	*gltB*	5123	**(-1.29)**	0411	**-2.16**
Amino acid porin	*oprD*	3987	**-3.79**	1400	**-2.95**
Amino acid porin	*oprD*	5318	**-1.65**	4878	**-7.41**

Aromatic ring degradation		3919	**-1.25**	1566	**-2.27**
Carbohydrate metabolism	*gntV*	3564	**-2.04**	3337	**--**
Carbohydrate metabolism	*pckA*	0239	**-1.68**	0168	**--**
Carbohydrate metabolism	*glpK*	4168	**-1.01**	3905	**-1.99**
Carbon metabolism	*acs*	1825	**-2.34**	3572	**-2.53**
Carbon metabolism	*lsc*	1453	**-1.55**	0754	**-2.30**
Cell membrane biosynthesis	*psd*	4955	**-1.72**	0559	**(-1.06)**
Cell wall biosynthesis	*pal*	3971	**-2.50**	1416	**-2.48**
Cell wall biosynthesis	*ddl*	4182	**-1.46**	3919	**-1.99**
Citric acid cycle	*sucD*	2203	**-1.75**	2013	**-1.56**
Citric acid cycle	*gltA*	2194	**-1.88**	2004	**(-1.39)**
Citric acid cycle	*acnB*	3752	**-1.72**	1726	**-1.68**
Coenzyme biosynthesis	*thiC*	4976	**-3.10**	0544	**--**
Fatty acid synthesis	*accA*	1550	**-1.93**	1359	**-2.07**
Fatty acid synthesis	*fabL*	3721	**-1.83**	1754	**-1.92**
Fatty acid synthesis	*fabB*	2210	**-1.81**	2019	**-1.87**
Fatty acid synthesis		4100	**-1.95**	3838	**-2.39**
Glucose transport		1292	**-2.99**	1113	**-2.13**
Glucose transport	*gltK*	1295	**-2.50**	1116	**(-1.72)**
Glucose transport (putative)		1294	**-1.44**	1115	**-1.85**
Glucose porin	*oprB*	1296	**-2.43**	1117	**-2.81**
Glycolysis	*gap*	1287	**-1.81**	1108	**-1.75**
Glycolysis	*zwf-1*	1300	**-2.37**	1120	**-2.46**
Glycolysis	*pyk*	4337	**-1.82**	4029	**-1.81**
Nitrogen regulatory protein	*glnK*	0217	**-2.67**	0190	**-5.17**
Nitrogen transport	*amt*	0218	**(-1.17)**	0189	**-1.97**
Nucleotide metabolism	*pcaB*	2341	**-2.08**	2125	**1.19**
Nutrient storage	*phaI*	5148	**-1.63**	0391	**(-1.42)**
Nutrient transport	*dctA*	1682	**-1.80**	3707	**-1.40**
Pentose phosphate pathway	*pgl*	1301	**-1.83**	1121	**-1.90**
Peptide ABC transporter		4557	**-1.60**	4234	**-2.57**
Peptide ABC transporter (putative)		4558	**-1.98**	4235	**-1.34**
Protein turnover	*pepA*	1271	**-2.14**	1091	**-1.89**
Protein turnover	*smpB*	4515	**-1.59**	4203	**(1.02)**
Purine metabolism	*purU*	4314	**-2.45**	4018	**(-1.18)**
Purine metabolism	*purC*	3950	**-1.54**	1551	**-1.38**
Putrescine transport	*potD*	5307	**-1.69**	4865	**-1.67**
Stress proteins					
Alkyl hydroperoxide reductase	*ahpC*	3108	**-1.54**	2975	**(-1.59)**
ATP-dependent Clp protease	*clpX*	3725	**-1.85**	1748	**-2.25**
ATP-dependent Clp protease	*clpP*	3726	**-2.04**	1747	**(-1.52)**
Catalase/peroxidase	*katG*	4530	**-1.90**	4208	**-1.74**
Chaperone	*tig*	3727	**-1.57**	1746	**--**
Cold shock protein	*capA*	2376	**-3.37**	2160	**-2.54**
Cold shock protein	*cspC*	1274	**-5.58**	1094	**-3.48**
Heat shock protein	HSP20	2170	**-1.42**	1751	**-1.68**
Heat shock protein	*dnaJ*	4504	**-1.43**	4194	**-3.51**
Heat shock protein	*cbpA*	4897	**-1.05**	4440	**-1.97**
DNA replication and repair		5472	**-3.15**	2668	**--**
DNA replication and repair	*hupB*	3723	**-2.58**	1750	**-2.27**
Methionine sulfoxide reductase	*msrA*	0405	**-1.36**	4771	**-2.08**
Nucleotide metabolism	*nrdA*	1671	**-1.75**	3717	**(-1.34)**
Thiol peroxidase	*tpx*	2752	**-2.10**	2481	**-1.96**

Motility and attachment					
Motility sigma factor	*fliA*	1979	**-2.07**	3437	**-2.14**
Flagella biosynthesis		1924	**-1.59**	3489	**(-1.28)**
Flagella biosynthesis (putative)	*flgM*	1925	**-2.27**	3488	**-1.77**
Flagella biosynthesis	*flgB*	1933	**-3.73**	3481	**-2.51**
Flagella biosynthesis	*flgC*	1934	**-4.30**	3480	**-3.02**
Flagella biosynthesis	*flgD*	1935	**-3.15**	3479	**-1.78**
Flagella biosynthesis	*flgG*	1940	**-2.13**	3475	**-1.64**
Flagella biosynthesis	f*liC*	1949	**-4.43**	3466	**--**
Flagella biosynthesis (putative)	*flaG*	1950	**-3.82**	3465	**-2.37**
Flagella biosynthesis	*fliD*	1951	**-1.91**	3464	**-2.13**
Flagella biosynthesis	*fliS*	1952	**-2.36**	3463	**-2.26**
Flagella biosynthesis	*fliF*	1958	**-1.06**	3457	**-1.13**
Chemotaxis (putative)	*cheV*	1927	**-1.87**	3486	**-1.70**
Chemotaxis	*cheY*	1980	**-2.74**	3436	**-2.92**
Chemotaxis	*cheZ*	1981	**-2.41**	3435	**-1.95**
Chemotaxis	*cheW*	1988	**-2.00**	3428	**-1.56**
Type IV pilus biogenesis		0927	**-4.19**	0799	**--**
Miscellaneous					
RpoS sigma-38	*rpoS*	1565	**-1.04**	1374	**(-1.19)**
Transcriptional regulator	*tetR*	1758	**-2.42**	3634	**--**
Plant hormone modification	*iaaL*	0371	**-1.96**	2577	**--**
Coronatine		4681	**-1.23**	NH	
Coronatine		4710	**-1.26**	NH	

Genes coding for enzymes involved in glutamate synthesis, including glutamate synthase (PSPTO_5121, PSPTO_5123) and glutamate dehydrogenase (GltB), were unchanged by water stress or were repressed; the latter included the aldehyde dehydrogenase PutA. In contrast, the glutamate-depleting enzymes glutamine synthetase GlnA and glutathione synthetase GshB were among the genes that were the most strongly repressed by water stress in both strains, Oxidative stress-responsive genes were also generally unchanged or mildly repressed by NaCl. Expression of the global oxidative stress regulator OxyR (PSPTO_0066, Psyr_0202) was unchanged by water stress in both strains, as were the genes regulated by OxyR including the catalase *katB* (PSPTO_3582, Psyr_3353) and the alkyl hydroperoxide reductase *aphF* (PSPTO_3107, Psyr_2974). Several ROS scavenging genes were repressed by water stress, including the alkyl hydroperoxide reductase *ahpC*, the bifunctional catalase/peroxidase *katG*, the methionine sulfoxide reductase *msrA*, and the thiol peroxidase *tpx*. Interestingly, the heme-dependent catalase gene *katE* was mildly induced by water stress (Table 2).

The cold shock proteins (Csps) CapA and CspC were strongly repressed during water stress in both strains. Csps are expressed in response to cold shock and appear to be involved in various cellular functions including transcription, translation, and DNA recombination (Jones et al. 1987). The DC3000 and B728a CspC proteins have 68% and 67% amino acid similarity, respectively, to a *P. aeruginosa* protein that is also repressed during osmotic up-shock. Many genes involved in motility and attachment were also repressed by NaCl in both strains, including the motility sigma factor FliA and a putative anti-sigma factor FlgM. Genes encoding the major flagellin subunits FliC, FliD and FlaG, and basal body proteins FlgBCDFG were also repressed. Chemotaxis genes *cheVWYZ* were similarily repressed.

Differentially expressed genes

B728a and DC3000 differ considerably with respect to host range and virulence determinants. For example, the genome of DC3000 encodes 55 type III secretion system (T3SS) effectors while B728a encodes 27, and only 20 effectors are shared between them (Feil et al. 2005). The HrpL alternative sigma factor activates the expression of many genes that are essential to plant pathogenicity in *P. syringae*, including the genes for the type III secretion system and its effectors (Ferreira et al. 2006). Interestingly, water stress suppressed *hrpL* expression in DC3000 but had no effect on *hrpL* expression in B728a (Table 4). The expression of 109 genes in the HrpL regulon in DC3000 was significantly affected by at least one of the five treatments in the microarray analysis ($p<0.05$, see Materials and Methods for treatments). With regard to water stress, 12 of these genes were induced by NaCl (11%), 56 were repressed (51%), and 39 were unchanged (36%). DC3000 and B728a both contain a large pathogenicity island that codes for the structural components of the T3SS, and these genes exhibit a high level of sequence similarity between the two strains. Many of these genes were repressed by water stress in DC3000 but not altered in B728a. For example, in DC3000, 48% of the T3SS structural genes were repressed, 4% were induced, and 44% were not altered. In contrast in B728a, only 4% of the T3SS structural genes present on the microarray were repressed, 8% were induced, and 88% were not altered. DC3000 and B728a also share 20 effectors, and probes for ten of these genes were present on the microarray for both strains. 60% were repressed in DC3000 (Table 4) and 40% were unchanged, while 100% of these effectors were not altered in expression in B728a. In addition to type III secretion, DC3000 and B728a contain gene clusters with homology to loci in

P. aeruginosa that encode a type VI secretion system (T6SS) (Mougous et al. 2006; Pukatzki et al. 2006). Surprisingly, these genes were strongly induced in B728a yet were repressed or unchanged in DC3000.

Table 4. *P. syringae* genes differentially-expressed in response to osmotic stress. Values in parentheses indicate that gene expression did not differ significantly between treatments with and without NaCl (p>0.05); dashes indicate the ORF was not present on the microarray*; NH* (no homolog) = a gene identified in B728a that exhibited a high sequence similarity to the target DC3000 ORF was not identified in B728a.

		DC3000		B728a	
Predicted Function	**Gene Name**	**Gene (PSPTO#)**	**Fold change**	**Gene (Psyr#)**	**Fold change**
RNA polymerase sigma factor	*hrpL*	1404	**-2.59**	1217	**(1.00)**
Type III secretion system					
T3SS protein	*hrpW*	1373	**-2.70**	1184	**(-1.06)**
T3SS protein	*hrpA1*	1381	**-3.04**	1192	**(-1.01)**
T3SS protein	*hrpZ1*	1382	**-3.23**	1193	**(1.05)**
T3SS protein	*hrpB*	1383	**-2.21**	1194	**(1.00)**
T3SS protein	*hrcJ*	1384	**-1.70**	1195	**1.12**
T3SS protein	*hrpD*	1385	**-1.20**	1196	**(-1.04)**
T3SS protein	*hrpE*	1386	**(-1.11)**	1197	**-1.24**
T3SS protein	*hrpF*	1387	**-2.04**	1198	**(1.01)**
T3SS protein	*hrpG*	1388	**-1.61**	1199	**(-1.12)**
T3SS protein	*hrcC*	1389	**-1.29**	1200	**(-1.06)**
T3SS protein	*hrpV*	1391	**1.55**	1202	**(1.03)**
T3SS protein	*hrcS*	1394	**-1.04**	1207	**(-1.04)**
T3SS protein	*hrcR*	1395	**-1.02**	1208	**(-1.06)**
T3SS protein	*hrcQb*	1396	**-1.05**	1209	**(1.10)**
T3SS protein	*hrpK1*	1405	**-1.45**	1218	**(-1.03)**
T3SS effectors					
T3SS effector	*hopAK1*	4101	**-1.55**	3839	**(-1.04)**
T3SS effector	*hopI1*	4776	**-1.67**	4326	**(-1.01)**
T3SS effector	*hrpK1*	1405	**-1.45**	1218	**(-1.03)**
T3SS effector	*hrpW1*	1373	**-2.70**	1184	**(-1.06)**
T3SS effector	*HopAM1*	1179	**-1.24**	1017	**(-1.38)**
T3SS effector	*hopA1*	5354	**-1.37**	0780	**(-1.02)**
T3SS effector	*avrPto1*	4001	**-3.36**	4919	**--**
T3SS effector	*hopAH2-1*	3292	**-1.59**	3123	**--**
T3SS effector	*hopAH2-2*	3293	**-1.19**	3123	**--**
T3SS effector	*hopH1*	0588	**-6.22**	1889	**--**
T3SS effector	*hopZ1*	1382	**-3.23**	1193	**--**
T3SS chaperone	*shcN*	1369	**-2.64**	NH	
T3SS effector	*hopC*	0589	**-2.46**	NH	
T3SS effector	*HopAM1*	1022	**-5.81**	NH	

T3SS effector	*hopE1*	4331	**-3.36**	NH	
T3SS effector	*hopAO1*	4722	**-2.13**	NH	
T3SS effector (putative)	*hopAQ1*	4703	**-2.13**	NH	
Type VI secretion system					
T6SS protein		2546	**(-1.03)**	4956	**6.25**
T6SS protein		5420	**-1.09**	4960	**4.54**
T6SS protein		5421	**-1.22**	4959	**3.89**
T6SS protein		5425	**(-1.03)**	4958	**4.37**
T6SS protein		5426	**-1.09**	4957	**3.60**
T6SS protein		5431	**-1.43**	4955	**8.15**
T6SS protein		5432	**(-1.53)**	4954	**5.57**
T6SS protein	*hcp-2*	5435	**-1.87**	0101	**-3.57**
Metabolism and nutrient transporters					
Alginate lyase (putative)		5015	**-2.10**	0508	**(1.11)**
Amino acid metabolism		3954	**-2.10**	1547	**(1.08)**
Amino acid metabolism	*cysK*	3902	**-1.43**	1090	**2.29**
Aromatic ring degradation	*pcaH*	2338	**-8.25**	2122	**(1.03)**
Aromatic ring degradation	*pcaB*	2341	**-2.08**	2125	**1.19**
Aromatic ring degradation	*pcaC-1*	2342	**-2.53**	2126	**(1.16)**
Carbon storage regulator	*csrA*	1844	**-3.31**	3554	**(-1.93)**
Heat shock protein	*hslV / clpQ*	5140	**(1.13)**	0395	**-3.68**
Heat shock protein	*hslU / clpP*	5141	**(1.13)**	0394	**-3.01**
Mechanosensitive ion channel		2297	**-1.35**	2095	**1.20**
Sulfate transport	*sbp*	0308	**-1.35**	0084	**3.56**
Sulfate transport	*cysT*	0309	**1.05**	0083	**2.14**
Sulfate transport	*cysW*	0310	**(1.03)**	0082	**1.41**
Sulfate transport	*cysA*	0311	**(-1.08)**	0081	**(1.31)**
Sulphonate transport (putative)		5316	**1.29**	4876	**1.18**
Sulfate binding protein	*sbp*	0308	**-1.35**	0084	**3.56**

Water stress also repressed expression of the global carbon storage regulator CsrA in DC3000 but did not significantly affect CsrA expression in B728a (Table 4). CsrA is a negative regulator of stationary phase genes including those responsible for gluconeogenesis, glycogen metabolism, and biofilm formation (Romeo et al. 1993; Sabnis et al. 1995; Jackson et al. 2002). CsrA acts post-transcriptionally by binding to mRNA and repressing expression of essential enzymes in carbohydrate metabolism, including glycogen synthase (*glgA*) and glycogen branching enzyme (*glgB*), which are both components of trehalose biosynthetic operons in *P. syringae*. Repression of *csrA* could be important for promoting trehalose synthesis in response to NaCl; however, since both B728a and DC3000 synthesize trehalose, at least in response to growth at high osmolarity (Chen and Beattie, unpublished), it is not clear why *csrA* would be differentially regulated by NaCl in the two strains.

Other differentially regulated genes include those of the *hslVU* complex that were repressed in B728a but unchanged in DC3000 (Table 4). HslUV forms a serine threonine protease complex that controls levels of key regulatory proteins in bacterial cells including RcsA, a positive transcriptional regulator of *cps* (capsule synthesis) genes, and SulA, a cell division inhibitor (Gille et al. 2003; Kuo et al. 2004). Suppression of HslVU in B728a could result in decreased capsule formation and increased cell division compared to DC3000. Also, a small-conductance mechanosensitive ion channel, PSPTO_2297/Psyr_2095, was repressed in DC3000 and slightly induced in B728a. Mechanosensitive ion channels open during osmotic shock in order to help bacterial cells survive sudden increases in external osmolarity (Martinac et al. 1987; Martinac 2001; Perozo 2006), and although regulated primarily post-translationally, even a slight induction in B728a could positively impact survival. Lastly, genes coding for enzymes associated with aromatic carbon ring degradation were strongly repressed in DC3000 but unchanged in B728a.

Identification of putative hydrophilins in DC3000 and B728a

Hydrophilins are a class of relatively small, highly hydrophilic proteins found in a broad range of organisms including bacteria, yeast, and plants where their production confers tolerance to water stress (Imai et al. 1996; Xu et al. 1996; Swire-Clark and Marcotte 1999; Zhang et al. 2000). Their defining characteristics are high glycine content (>6%) and a hydrophilicity index >1 (Anchordoquy and Carpenter 1996). We analyzed several hundred uncharacterized ORFs from the complete genome of DC3000 and the B728a contigs that were selected based on size (generally $\leq$300 nt), glycine content (>6%) and predicted hydrophilicity value >1 (hydrophilicity calculated using ExPASy's ProtScale, http://www.expasy.ch/tools/protscale.html). As a result, we identified nine putative hydrophilins in each strain, which we designated as *hfn* genes, for hydrophilin function (Table 5). Of these nine, five were induced in response to water stress, one was slightly repressed and three were not significantly altered in their expression. The gene PSPTO_1596 and its B728a homolog Psyr_3782 were highly induced and exhibit 49% amino acid similarity to an *E. coli* hydrophilin (*yjbJ*). The YjbJ hydrophilin has been demonstrated to rescue enzymatic activity from the negative effects of osmotic stress *in vitro* (Reyes et al. 2005)

and is controlled in an RpoS-dependent manner, similar to other water stress-responsive genes (Vijayakumar et al. 2004; Weber et al. 2005).

Table 5. Responsiveness to osmotic upshock of *P. syringae* genes that putatively encode hydrophilins based on gene size, glycine content, and estimated hydrophilicity of the encoded products.

Predicted Function	Gene Name	DC3000		B728a	
		Gene (PSPTO#)	Fold Change	Gene (Psyr#)	Fold Change
Hydrophilin	*hfnA*	1596	**4.52**	3782	**9.61**
Hydrophilin	*hfnB*	0281	**1.92**	0128	**1.97**
Hydrophilin	*hfnC*	0993	**3.79**	0858	**1.86**
Hydrophilin	*hfnD*	4237	**3.76**	3971	**1.38**
Hydrophilin	*hfnE*	0891	**2.25**	0768	**2.21**
Hydrophilin	*hfnF*	4315	**(-1.29)**	4019	**--**
Hydrophilin	*hfnG*	1931	**(-1.13)**	3482	**--**
Hydrophilin	*hfnH*	3346	**(1.11)**	3176	**(1.07)**
Hydrophilin	*hfnJ*	4637	**-1.63**	4272	**-1.55**

Quantitative RT-PCR analysis of select genes

To validate and expand upon the results of the microarray experiment, we used a quantitative RT-PCR analysis to measure the osmoresponsiveness of several genes in DC3000 (Table 6). Similar to the microarray experiment, exponential-phase cells were exposed to a moderate osmotic stress (219 mM NaCl; -1 MPa) for 15 min. In addition, cells were exposed to a high osmotic stress (438 mM NaCl; -2 MPa) for 15 min. Cells were also exposed to a moderate and high osmotic stress for 60 min. Qualitatively, the results of the qRT-PCR were consistent with the findings from the microarray: genes that exhibited induction (or repression) on the microarray also exhibited induction (or repression) after 15 min using qRT-PCR (Table 6). However, the extent of induction or repression as estimated by qRT-PCR was not correlated with that estimated by the microarray. Temporal analysis revealed distinct trends in gene expression. Repression of the glutamine synthetase gene *glnA* and putative cold shock protein *cscP* decreased between 15 and 60 min under moderate osmotic stress, consistent with a role in generating glutamate as a compatible solute needed only in the initial stage of the response. In contrast, gene induction of *glnA*, trehalose synthesis (*treY*) and NAGGN production (*asnB*) increased between 15 and 60 min when cells were exposed to high osmotic stress, suggesting

gene induction in proportion to stress and duration of stress. The putative hydrophilin *hfnA* was selected for analysis based on its homology to a characterized *E. coli* hydrophilin that was able to rescue enzymatic activity from the negative effects of osmotic stress *in vitro* (Reyes et al. 2005). *hfnA* showed stronger induction at 15 min for both stresses, possibly indicating a role for this protein immediately following osmotic up-shock and irrespective of the level of stress. In contrast, the trehalose synthesis gene *glgA*, glycine betaine transporter *opuCD*, and the putative Dps ferritin gene PSPTO_4906 showed stronger induction at 60 min under both stresses, indicating a role for these genes that extends beyond the initial exposure to water stress.

Table 6. Quantitative RT-PCR analysis of select DC3000 genes. DC3000 gene expression at 15 minutes and 60 minutes following immersion of cells in low (219mM: -1 MPa) or high (438mM: -1.9 MPa) concentrations of NaCl in ½ 21C containing 0.3% glucose and 5mM succinate. Fold change = $2^{(-\Delta\Delta Ct)}$, where $\Delta\Delta Ct = (Ct(target) - Ct(\textit{hemD}))_{treatment} - (Ct(target) - Ct(\textit{hemD}))_{control}$. *Value rejected due to poor melt curve.

	15 min	15 min		60 min	
Gene	**Microarray**	**Low NaCl**	**High NaCl**	**Low NaCl**	**High NaCl**
PSPTO_0359 (*glnA)*	**-4.74**	**-9.51**	**-3.39**	**-1.78**	**-26.91**
		-7.07	**-2.36**	**-3.03**	**-23.75**
PSPTO_1274 (*cspC)*	**-5.58**	**-3.36**	**-1.60**	**-1.68**	**-7.26**
		-1.69	**-1.08**	**-2.27**	**-7.89**
PSPTO_1596 (*hfnA)*	**4.52**	**8.51**	**3.84**	**3.16**	**2.35**
		10.13	**4.47**	**8.34**	**1.96**
PSPTO_1633 (*asnB)*	**10.90**	**2.62**	**4.03**	**2.33**	**3.18**
		3.68	**3.48**	**2.20**	**6.50**
PSPTO_3125 (*glgA)*	**3.04**	**1.61**	**2.06**	**2.38**	**4.23**
		1.62	**3.81**	**3.07**	**10.78**
PSPTO_3128 (*treY)*	**1.42**	**4.92**	**1.19**	**2.97**	**3.53**
		2.55	*	**2.01**	**5.39**
PSPTO_4578 (*opuCD)*	**9.26**	**3.01**	**1.54**	**4.14**	**5.17**
		3.27	**1.42**	**5.17**	**8.88**
PSPTO_4906	**9.11**	**8.40**	**3.68**	**8.94**	**2.93**
		3.16	**1.29**	**8.00**	**5.39**

Discussion

The global transcriptome analysis performed in this study demonstrates that the general responses of *P. syringae* to osmotic stress are similar to those reported previously for *P. aeruginosa* (Aspedon et al. 2006), including an induction of genes involved in compatible solute synthesis, transport, and EPS production, and a repression in general metabolic activities, but

vary in many specific responses with some occurring in a strain-specific manner. The two strains, B728a and DC3000 share a large number of homologous genes but differ in their osmotic stress tolerance. We found considerable differences between the strains in the expression of many pathogenesis-related genes, including the Hrp type III secretion system, type III effectors, and the type VI secretion system. The nature of the changes in gene expression suggest that osmotic stress may attenuate the virulence or growth of DC3000 while having little influence, or even a positive influence, on the virulence or growth of B728a.

Many genes were co-induced or co-repressed in the strains, although some genes exhibited quantitative differences. Alginate is an important component of bacterial EPS that is widespread among pseudomonads (Fialho et al. 1990) and provides a hygroscopic matrix that helps protect bacterial cells from desiccation (Chang and Halverson 2003). Alginate can hold several times its weight in water (Sutherland 2001) and may slow water loss in order to allow cellular mechanisms to activate and prevent further desiccation. Many alginate promoters in both *P. syringae* and *P. aeruginosa* are triggered by elevated osmolarity from NaCl or sorbitol (Penaloza-Vazquez and Bender 1998; Keith and Bender 1999; Laue et al. 2006) via the global regulator AlgU, also known as RpoE (σ^{22}) (Schenk et al. 2008). In this study, *algU* was strongly upregulated in response to NaCl in DC3000, but alginate biosynthetic genes were more strongly induced in B728a. This may translate into more robust alginate production in B728a and possibly greater survival in response to an equivalent level of water stress compared with DC3000, especially over the long-term. Another constituent of pseudomonad EPS is levan, a high-molecular-mass polyfructan synthesized from sucrose by the extracellular enzyme levansucrase. Levan production typically occurs early in exponential growth and is thought to be a nutrient-storage component of EPS and not an osmoadaptive strategy (Laue et al. 2006). The levansucrase (*lsc*) genes PSPTO_1453 and Psyr_0754 were highly expressed in the absence of stress but were suppressed by NaCl, suggesting that levan was not accumulated during water stress; this is consistent with its primary role as a nutrient storage molecule accumulated during exponential growth.

The sigma factor RpoS (σ^{38}) is a general stress response regulator that controls the expression of many genes that collectively confer increased resistance to various stresses in some

gram-negative bacteria, including starvation, osmotic stress, and oxidative stress (Kolter et al. 1993; Loewen and Hengge-Aronis 1994; Hengge-Aronis 1996). In *E. coli*, over 100 genes constitute the RpoS regulon (Ishihama 2000), and RpoS is required for optimal survival of *P. aeruginosa* stationary-phase cells exposed to osmotic stress (Suh et al. 1999). The RpoS regulon has not been fully characterized in *P. syringae*, but many genes altered in expression during water stress may belong to this regulon. Although log-phase cells were used in this study and RpoS activity was likely relatively low in the basal medium, *rpoS* expression was sufficiently high to detect repression by water stress. This response may be tied to the predicted influx of potassium glutamate (Gralla and Vargas 2006),which can promote a re-programming of the cellular transcription apparatus, especially genes responsive to RNA polymerases containing RpoS (σ^{38}) in *E. coli* (Weber and Jung 2002; Cheung et al. 2003; Polen et al. 2003; Gralla and Vargas 2006). Specifically, potassium glutamate can act directly on certain σ^{38} promoters to activate them without the participation of macromolecular repressors or activators, thus reducing the need for RpoS activity (Lee and Gralla 2004). Potassium glutamate can also affect the activity of other transcription factors, as illustrated by its promotion of transcription by AlgU (RpoE)-regulated genes by promoting the release of the σ^{22} factor from the RNA polymerase and transcription following transcription initiation (Lee and Gralla 2004). Such poise-and-release mechanisms may be common in bacteria: A chromatin immunoprecipitation (ChIP)–chip study found that nearly a quarter of all *E. coli* σ^{70} promoter transcription complexes consisted of poised RNA polymerases (Reppas et al. 2006). The induction of genes belonging to the RpoS regulon in this study may have therefore resulted from the triggering of transcription of genes that were pre-primed for expression by the rapid accumulation of potassium glutamate.

Genes for glutamate synthesis were unchanged or moderately repressed by water stress, indicating that glutamate did not accumulate via *de novo* synthesis through these pathways. The accumulation of glutamate likely occurred via the suppression of glutamate-depleting enzymes including glutamine synthetase and glutathione synthetase. The *P. syringae* genome contains four glutamine synthetase loci; one of these genes was strongly repressed by water stress and three were not altered. The glutathione synthetase genes *gluAB* were also mildly repressed by water stress. Interestingly, qRT-PCR analysis demonstrated that the *glnA* gene was strongly repressed at 15 minutes under moderate NaCl stress but repression eased at 1 hour, suggesting

that cells were re-establishing osmotic balance. In response to high osmotic stress, however, *glnA* was only mildly repressed at 15 min but repression increased almost 25-fold by 1 hour, suggesting that these cells had not yet regained osmotic balance and were continuing to rapidly accumulate glutamate.

qRT-PCR analysis also showed that NAGGN gene expression peaked early but declined by 1 hour, in contrast to trehalose gene expression which tended to gradually increase over time. In *P. aeruginosa*, trehalose appears to be accumulated at high osmotic stress levels, with NAGGN and glutamate accumulating at low to moderate osmotic stress levels in this species (D'Souza-Ault et al. 1993). Recent evidence suggests that NAGGN is the major organic osmoprotectant in *P. aeruginosa*, especially in low to moderate levels of osmotic stress (D'Souza-Ault et al. 1993). In this study, NAGGN-related genes exhibited much stronger induction compared to trehalose genes after 15 minutes of water stress, suggesting that NAGGN is more critical than trehalose early in the osmotic stress response of *P. syringae* just as it is in *P. aeruginosa*.

Several genes involved with iron storage and metabolism were induced by NaCl. In general, genes associated with iron-scavenging were not expressed in the unstressed medium, suggesting that iron was not limited during growth in ½ 21C medium. Water stress did not induce siderophore-related genes including pyoverdine synthetases or transporters, and it did not induce expression of most TonB receptors. A putative non-heme-associated Dps (DNA-binding protein during starvation) ferritin was highly induced by water stress in both DC3000 (PSPTO_4906) and B728a (Psyr_4448). Dps is found throughout the bacterial kingdom and has been shown to protect DNA under a variety of stresses including starvation and oxidative damage (Nair and Finkel 2004). Dps proteins have ferroxidase activity and can bind and sequester iron (Ceci et al. 2005) thereby preventing oxidative damage due to the production of hydroxyl radicals via Fenton chemistry (Zhao et al. 2002). Some Dps homologs can also bind nonspecifically to double-stranded DNA and presumably provide physical protection against these stresses (Ceci et al. 2005). The cells in this study likely did not perceive oxidative stress because oxidative stress-responsive genes were either not altered or were repressed (Table 3). A recent transcriptome analysis of the soil actinomycete *Rhodococcus jostii* RHA1 revealed that

the *dps1* gene was highly upregulated when the cells were exposed to extreme desiccation (LeBlanc et al. 2008). The strong induction of Dps ferritin in this study suggests that this protein may play an important role in protecting *Pseudomonas syringae* cells from water stress.The heme-dependent catalase gene *katE* was mildly induced by water stress in both strains. Heme-dependent catalases in other bacteria have been shown to protect cells from osmotic stress, including CatB in *Streptomyces coelicolor* (Cho et al. 2000) and KatA in *P. aeruginosa* PA14 (Lee et al. 2005); therefore, KatE may play a similar osmoadaptive role in *P. syringae*.

Repression of a large number of metabolic and nutrient transporter genes suggests that the cells were shifting metabolic resources away from rapid growth and toward water stress adaptation. In addition, flagellar motility and chemotaxis may have been actively turned off in response to osmotic water stress. Interestingly, DC3000 and B728a both contain aconitases that were differentially regulated by water stress, AcnA (PSPTO_2016, Psyr_3404), which was induced, and AcnB (PSPTO_3752, Psyr_1726), which was repressed. Physiological studies have shown that AcnB is the major citric acid cycle enzyme in *E. coli* that is synthesized during exponential growth, whereas AcnA is a stable stress-induced stationary phase enzyme that participates in response to iron deficiency or oxidative stress (Bradbury et al. 1996; Cunningham et al. 1997). During iron sufficiency, both enzymes assemble iron-sulfur (4Fe-4S) clusters that subsequently associate with enzymes, but during iron starvation or exposure to oxidative stress, these iron-sulfur clusters are disassembled, catalytic activity is lost, and the resulting proteins bind to specific mRNAs (Beinert et al. 1996). The mRNA sequences recognized by the Acn proteins are called iron-responsive elements, and binding can result in either enhanced transcript stability or inhibition of translation (Beinert et al. 1996; Alen and Sonenshein 1999; Tang and Guest 1999; Tang et al. 2002). Induction of *acnA* and genes involved in iron-accumulation in this study suggests that iron-scavenging may be important during a response to water stress even though iron is not limited in the growth medium.

The *sbp-cysTWA* gene cluster encodes a sulfate ABC transport system that was induced by water stress in B728a (Psyr_0084-0081) but was not influenced by water stress in DC3000 (PSPTO_0308-0311). Little is known about the availability of sulfur-containing compounds on leaf surfaces. A recent study found that a gene in the sulfate-starvation regulon, *ssuE*, was highly

induced in B728a during bean leaf colonization, indicating that sulfate was not abundant on the bean leaf surfaces (Marco et al. 2005). In another study, *sbp* and *cysTWA* gene clusters were highly induced in *P. aeruginosa* on *Nicotiana tabacum* leaves during an incompatible reaction (Weir et al. 2008). If sulfur is limiting in the phyllosphere, the induction of sulfur transporters by a phyllosphere-triggered signal, such as water stress, may impart a selective advantage on B728a.

The global transcriptome analysis performed in this study demonstrates that *P. syringae* responds to osmotic up-shock by repressing a large number of genes involved with general metabolism, including genes for catabolism, nutrient storage and acquisition, iron storage, chemotaxis, motility, and attachment. On the other hand, *P. syringae* upregulates many genes involved with adaptation to the osmotic stress, including alginate biosynthesis, osmoprotectant transport, and compatible solute synthesis. These results suggest that *P. syringae* responds to osmotic stress by switching nutrient and energy resources away from growth and towards osmoadaptation. Differences exist, however, between closely related strains of *P. syringae* in their genomic responses to water stress, as B728a exhibited stronger induction of certain osmoadaptive genes compared with DC3000, suggesting that B728a may be able to better adapt to water stress than DC3000. Further studies may help shed light on whether these transcriptional differences result in increased survival of B728a compared with DC3000 in natural settings such as on leaves or in pathogenic associations with susceptible hosts.

Acknowledgements

Thank you to Dan Nettleton for help with the statistical analysis, and the Plant Sciences Institute for my graduate fellowship. This project was supported by the National Research Initiative of the USDA-CSREES, grant No. 2005-35319-15300.

References

Alen, C. and Sonenshein, A. L. 1999. *Bacillus subtilis* aconitase is an RNA-binding protein. Proc. Natl. Acad. Sci. U.S.A. 96:10412-10417.

Anchordoquy, T. J. and Carpenter, J. F. 1996. Polymers protect lactate dehydrogenase during freeze-drying by inhibiting dissociation in the frozen state. Arch. Biochem. Biophys. 332:231-238.

Aspedon, A., Palmer, K. and Whiteley, M. 2006. Microarray analysis of the osmotic stress response in *Pseudomonas aeruginosa*. J. Bacteriol. 188:2721-2725.

Beattie, G. A. and Lindow, S. E. 1994. Comparison of the behavior of epiphytic fitness mutants of *Pseudomonas syringae* under controlled and field conditions. Appl. Environ. Microbiol. 60:3799-3808.

Beattie, G. A. and Lindow, S. E. 1994. Survival, growth, and localization of epiphytic fitness mutants of *Pseudomonas syringae* on leaves. Appl. Environ. Microbiol. 60:3790-3798.

Beinert, H., Kennedy, M. C. and Stout, C. D. 1996. Aconitase as iron-sulfur protein, enzyme, and iron-regulatory protein. Chem. Rev. 96:2335-2373.

Bohin, J. P. 2000. Osmoregulated periplasmic glucans in Proteobacteria. FEMS Microbiol. Lett. 186:11-19.

Boureau, T., Routtu, J., Roine, E., Taira, S. and Romantschuk, M. 2002. Localization of hrpA-induced *Pseudomonas syringae* pv. tomato DC3000 in infected tomato leaves. Mol. Plant Pathol. 3:451-460.

Bradbury, A. J., Gruer, M. J., Rudd, K. E. and Guest, J. R. 1996. The second aconitase (AcnB) of *Escherichia coli*. Microbiology 142:389-400.

Cayley, S., Lewis, B. A., Guttman, H. J. and Record, M. T. 1991. Characterization of the cytoplasm of *Escherichia coli* K-12 as a function of external osmolarity - Implications for protein DNA interactions *in vivo*. J. Mol. Biol. 222:281-300.

Cayley, S., Lewis, B. A. and Record, M. T., Jr. 1992. Origins of the osmoprotective properties of betaine and proline in *Escherichia coli* K-12. J. Bacteriol. 174:1586-1595.

Ceci, P., Ilari, A., Falvo, E., Giangiacomo, L. and Chiancone, E. 2005. Reassessment of protein stability, DNA binding, and protection of *Mycobacterium smegmatis* Dps. J. Biol. Chem. 280:34776-34785.

Chang, W. S. and Halverson, L. J. 2003. Reduced water availability influences the dynamics, development, and ultrastructural properties of *Pseudomonas putida* biofilms. J. Bacteriol. 185:6199-6204.

Chang, W. S., van de Mortel, M., Nielsen, L., Nino de Guzman, G., Li, X. and Halverson, L. J. 2007. Alginate production by *Pseudomonas putida* creates a hydrated microenvironment and contributes to biofilm architecture and stress tolerance under water-limiting conditions. J. Bacteriol. 189:8290-8299.

Chen, C. and Beattie, G. A. 2008. *Pseudomonas syringae* BetT is a low-affinity choline transporter that is responsible for superior osmoprotection by choline over glycine betaine. J. Bacteriol. 190:2717-2725.

Chen, C. L. and Beattie, G. A. 2007. Characterization of the osmoprotectant transporter OpuC from *Pseudomonas syringae* and demonstration that cystathionine-beta-synthase domains are required for its osmoregulatory function. J. Bacteriol. 189:6901-6912.

Cheung, K. J., Badarinarayana, V., Selinger, D. W., Janse, D. and Church, G. M. 2003. A microarray-based antibiotic screen identifies a regulatory role for supercoiling in the osmotic stress response of *Escherichia coli*. Genome Res. 13:206-215.

Cho, Y. H., Lee, E. J. and Roe, J. H. 2000. A developmentally regulated catalase required for proper differentiation and osmoprotection of *Streptomyces coelicolor*. Mol. Microbiol. 35:150-160.

Cunningham, L., Gruer, M. J. and Guest, J. R. 1997. Transcriptional regulation of the aconitase genes (*acnA* and *acnB*) of *Escherichia coli*. Microbiology 143:3795-3805.

D'Souza-Ault, M. R., Smith, L. T. and Smith, G. M. 1993. Roles of N-acetylglutaminylglutamine amide and glycine betaine in adaptation of *Pseudomonas aeruginosa* to osmotic stress. Appl. Environ. Microbiol. 59:473-478.

Dinnibier, U., Limpinsel, E., Schmid, R. and Bakker, E. P. 1988. Transient accumulation of potassium glutamate and its replacement by trehalose during adaptation of growing-cells of *Escherichia coli* K-12 to elevated sodium chloride concentrations. Arch. Microbiol. 150:348-357.

Feil, H., Feil, W. S., Chain, P., Larimer, F., DiBartolo, G., Copeland, A., Lykidis, A., Trong, S., Nolan, M., Goltsman, E., Thiel, J., Malfatti, S., Loper, J. E., Lapidus, A., Detter, J. C., Land, M., Richardson, P. M., Kyrpides, N. C., Ivanova, N. and Lindow, S. E. 2005. Comparison of the complete genome sequences of *Pseudomonas syringae* pv. syringae B728a and pv. tomato DC3000. Proc. Natl. Acad. Sci. U.S.A. 102:11064-11069.

Ferreira, A. O., Myers, C. R., Gordon, J. S., Martin, G. B., Vencato, M., Collmer, A., Wehling, M. D., Alfano, J. R., Moreno-Hagelsieb, G., Lamboy, W. F., DeClerck, G., Schneider, D. J. and Cartinhour, S. W. 2006. Whole-genome expression profiling defines the HrpL regulon of *Pseudomonas syringae* pv. tomato DC3000, allows *de novo* reconstruction of the Hrp cis clement, and identifies novel coregulated genes. Mol. Plant-Microbe Interact. 19:1167-1179.

Fett, W. F., Wells, J. M., Cescutti, P. and Wijey, C. 1995. Identification of exopolysaccharides produced by fluorescent pseudomonads associated with commercial mushroom (*Agaricus bisporus*) production. Appl. Environ. Microbiol. 61:513-517.

Fialho, A. M., Zielinski, N. A., Fett, W. F., Chakrabarty, A. M. and Berry, A. 1990. Distribution of alginate gene sequences in the *Pseudomonas* rRNA homology group I-*Azomonas-Azotobacter* lineage of superfamily B prokaryotes. Appl. Environ. Microbiol. 56:436-443.

Gille, C., Goede, A., Schloetelburg, C., Preissner, R., Kloetzel, P. M., Gobel, U. B. and Frommel, C. 2003. A comprehensive view on proteasomal sequences: implications for the evolution of the proteasome. J. Mol. Biol. 326:1437-1448.

Gralla, J. D. and Vargas, D. R. 2006. Potassium glutamate as a transcriptional inhibitor during bacterial osmoregulation. EMBO J. 25:1515-1521.

Hengge-Aronis, R. 1996. Back to log phase: sigma-S as a global regulator in the osmotic control of gene expression in *Escherichia coli*. Mol. Microbiol. 21:887-893.

Hirano, S. S. and Upper, C. D. 1990. Population biology and epidemiology of *Pseudomonas syringae*. Ann. Rev. Phytopathol. 28:155-177.

Hirano, S. S. and Upper, C. D. 2000. Bacteria in the leaf ecosystem with emphasis on *Pseudomonas syringae*-a pathogen, ice nucleus, and epiphyte. Microbiol. Mol. Biol. Rev. 64:624-653.

Imai, R., Chang, L., Ohta, A., Bray, E. A. and Takagi, M. 1996. A lea-class gene of tomato confers salt and freezing tolerance when expressed in *Saccharomyces cerevisiae*. Gene 170:243-248.

Ishihama, A. 2000. Functional modulation of *Escherichia coli* RNA polymerase. Annu. Rev. Microbiol. 54:499-518.

Jackson, D. W., Suzuki, K., Oakford, L., Simecka, J. W., Hart, M. E. and Romeo, T. 2002. Biofilm formation and dispersal under the influence of the global regulator CsrA of *Escherichia coli*. J. Bacteriol. 184:290-301.

Jackson, K. D., Starkey, M., Kremer, S., Parsek, M. R. and Wozniak, D. J. 2004. Identification of *psl*, a locus encoding a potential exopolysaccharide that is essential for *Pseudomonas aeruginosa* PAO1 biofilm formation. J. Bacteriol. 186:4466-4475.

Jones, P. G., VanBogelen, R. A. and Neidhardt, F. C. 1987. Induction of proteins in response to low temperature in *Escherichia coli*. J. Bacteriol. 169:2092-2095.

Kachlany, S. C., Levery, S. B., Kim, J. S., Reuhs, B. L., Lion, L. W. and Ghiorse, W. C. 2001. Structure and carbohydrate analysis of the exopolysaccharide capsule of *Pseudomonas putida* G7. Environ. Microbiol. 3:774-784.

Keith, L. M. and Bender, C. L. 1999. AlgT (sigma22) controls alginate production and tolerance to environmental stress in *Pseudomonas syringae*. J. Bacteriol. 181:7176-7184.

Kets, E. P., Galinski, E. A., de Wit, M., de Bont, J. A. and Heipieper, H. J. 1996. Mannitol, a novel bacterial compatible solute in *Pseudomonas putida* S12. J. Bacteriol. 178:6665-6670.

Kim, J., Jeon, C. O. and Park, W. 2008. Dual regulation of *zwf-1* by both 2-keto-3-deoxy-6-phosphogluconate and oxidative stress in *Pseudomonas putida*. Microbiology 154:3905-3916.

King, E. O., Ward, M. K. and Raney, D. E. 1954. Two simple media for the demonstration of pyocyanin and fluorescin. J. Lab Clin. Med. 44:301-307.

Kolter, R., Siegele, D. A. and Tormo, A. 1993. The stationary phase of the bacterial life cycle. Annu. Rev. Microbiol. 47:855-874.

Kuo, M. S., Chen, K. P. and Wu, W. F. 2004. Regulation of RcsA by the ClpYQ (HslUV) protease in *Escherichia coli*. Microbiol. 150:437-446.

Laue, H., Schenk, A., Li, H., Lambertsen, L., Neu, T. R., Molin, S. and Ullrich, M. S. 2006. Contribution of alginate and levan production to biofilm formation by *Pseudomonas syringae*. Microbiology 152:2909-2918.

LeBlanc, J. C., Goncalves, E. R. and Mohn, W. W. 2008. Global response to desiccation stress in the soil actinomycete *Rhodococcus jostii* RHA1. Appl. Environ. Microbiol. 74:2627-2636.

Lee, J. S., Heo, Y. J., Lee, J. K. and Cho, Y. H. 2005. KatA, the major catalase, is critical for osmoprotection and virulence in *Pseudomonas aeruginosa* PA14. Infect.Immun. 73:4399-4403.

Lee, S. J. and Gralla, J. D. 2004. Osmo-regulation of bacterial transcription via poised RNA polymerase. Mol. Cell 14:153-162.

Lindow, S. E., Andersen, G. and Beattie, G. A. 1993. Characteristics of insertional mutants of *Pseudomonas syringae* with reduced epiphytic fitness. Appl. Environ. Microbiol. 59:1593-1601.

Loewen, P. C. and Hengge-Aronis, R. 1994. The role of the sigma factor sigma S (KatF) in bacterial global regulation. Annu. Rev. Microbiol. 48:53-80.

Loper, J. E. and Lindow, S. E. 1987. Lack of evidence for *in situ* fluorescent pigment production by *Pseudomonas syringae* pv. syringae on bean leaf surfaces. Phytopathology 77:1449-1454.

Marco, M. L., Legac, J. and Lindow, S. E. 2005. *Pseudomonas syringae* genes induced during colonization of leaf surfaces. Environ. Microbiol. 7:1379-1391.

Martinac, B. 2001. Mechanosensitive channels in prokaryotes. Cell Physiol. Biochem. 11:61-76.

Martinac, B., Buechner, M., Delcour, A. H., Adler, J. and Kung, C. 1987. Pressure-sensitive ion channel in *Escherichia coli*. Proc. Nat. Acad. Sci. U.S.A. 84:2297-2301.

Moore, R. A., Starratt, A. N., Ma, S. W., Morris, V. L. and Cuppels, D. A. 1989. Identification of a chromosomal region required for biosynthesis of the phytotoxin coronatine by *Pseudomonas syringae* pv. tomato. Can. J. Microbiol. 35:910-917.

Mougous, J. D., Cuff, M. E., Raunser, S., Shen, A., Zhou, M., Gifford, C. A., Goodman, A. L., Joachimiak, G., Ordonez, C. L., Lory, S., Walz, T., Joachimiak, A. and Mekalanos, J. J. 2006. A virulence locus of *Pseudomonas aeruginosa* encodes a protein secretion apparatus. Science 312:1526-1530.

Nair, S. and Finkel, S. E. 2004. Dps protects cells against multiple stresses during stationary phase. J. Bacteriol. 186:4192-4198.

Page, F., Altabe, S., Hugouvieux-Cotte-Pattat, N., Lacroix, J. M., Robert-Baudouy, J. and Bohin, J. P. 2001. Osmoregulated periplasmic glucan synthesis is required for *Erwinia chrysanthemi* pathogenicity. J. Bacteriol. 183:3134-3141.

Penaloza-Vazquez, A. and Bender, C. L. 1998. Characterization of CorR, a transcriptional activator which is required for biosynthesis of the phytotoxin coronatine. J. Bacteriol. 180:6252-6259.

Perozo, E. 2006. Gating prokaryotic mechanosensitive channels. Nature Rev. Mol. Cell Biol. 7:109-119.

Polen, T., Rittmann, D., Wendisch, V. F. and Sahm, H. 2003. DNA microarray analyses of the long-term adaptive response of *Escherichia coli* to acetate and propionate. App. Environ. Microbiol. 69:1759-1774.

Pukatzki, S., Ma, A. T., Sturtevant, D., Krastins, B., Sarracino, D., Nelson, W. C., Heidelberg, J. F. and Mekalanos, J. J. 2006. Identification of a conserved bacterial protein secretion system in *Vibrio cholerae* using the *Dictyostelium* host model system. Proc. Nat. Acad. Sci. U.S.A. 103:1528-1533.

Reppas, N. B., Wade, J. T., Church, G. M. and Struhl, K. 2006. The transition between transcriptional initiation and elongation in *E. coli* is highly variable and often rate limiting. Mol. Cell 24:747-757.

Reyes, J. L., Rodrigo, M. J., Colmenero-Flores, J. M., Gil, J. V., Garay-Arroyo, A., Campos, F., Salamini, F., Bartels, D. and Covarrubias, A. A. 2005. Hydrophilins from distant organisms can protect enzymatic activities from water limitation effects in vitro. Plant Cell Environ. 28:709-718.

Romeo, T., Gong, M., Liu, M. Y. and Brunzinkernagel, A. M. 1993. Identification and molecular characterization of *csrA*, a pleiotropic gene from *Escherichia coli* that affects glycogen biosynthesis, gluconeogenesis, cell size, and surface properties. J. Bacteriol. 175:4744-4755.

Sabnis, N. A., Yang, H. H. and Romeo, T. 1995. Pleiotropic regulation of central carbohydrate metabolism in *Escherichia coli* via the gene *csrA*. J. Biol. Chem. 270:29096-29104.

Sawada, H., Suzuki, F., Matsuda, I. and Saitou, N. 1999. Phylogenetic analysis of *Pseudomonas syringae* pathovars suggests the horizontal gene transfer of *argK* and the evolutionary stability of *hrp* gene cluster. J. Mol. Evol. 49:627-644.

Schenk, A., Weingart, H. and Ullrich, M. S. 2008. The alternative sigma factor AlgT, but not alginate synthesis, promotes in planta multiplication of *Pseudomonas syringae* pv. glycinea. Microbiology 154:413-214.

Suh, S. J., Silo-Suh, L., Woods, D. E., Hassett, D. J., West, S. E. and Ohman, D. E. 1999. Effect of *rpoS* mutation on the stress response and expression of virulence factors in *Pseudomonas aeruginosa*. J. Bacteriol. 181:3890-3897.

Sutherland, I. 2001. Biofilm exopolysaccharides: a strong and sticky framework. Microbiology 147:3-9.

Swire-Clark, G. A. and Marcotte, W. R. 1999. The wheat LEA protein Em functions as an osmoprotective molecule in *Saccharomyces cerevisiae*. Plant Mol. Biol. 39:117-128.

Tang, Y. and Guest, J. R. 1999. Direct evidence for mRNA binding and post-transcriptional regulation by *Escherichia coli* aconitases. Microbiology 145:3069-3079.

Tang, Y., Quail, M. A., Artymiuk, P. J., Guest, J. R. and Green, J. 2002. *Escherichia coli* aconitases and oxidative stress: post-transcriptional regulation of *sodA* expression. Microbiology 148:1027-1037.

Vijayakumar, S. R., Kirchhof, M. G., Patten, C. L. and Schellhorn, H. E. 2004. RpoS-regulated genes of *Escherichia coli* identified by random *lacZ* fusion mutagenesis. J. Bacteriol. 186:8499-8507.

Weber, A. and Jung, K. 2002. Profiling early osmostress-dependent gene expression in *Escherichia coli* using DNA microarrays. J. Bacteriol. 184:5502-5507.

Weber, H., Polen, T., Heuveling, J., Wendisch, V. F. and Hengge, R. 2005. Genome-wide analysis of the general stress response network in *Escherichia coli*: sigmaS-dependent genes, promoters, and sigma factor selectivity. J. Bacteriol. 187:1591-1603.

Weir, T. L., Stull, V. J., Badri, D., Trunck, L. A., Schweizer, H. P. and Vivanco, J. 2008. Global gene expression profiles suggest an important role for nutrient acquisition in early pathogenesis in a plant model of *Pseudomonas aeruginosa* infection. Appl. Environ. Microbiol. 74:5784-5791.

Xu, D., Duan, X., Wang, B., Hong, B., Ho, T. and Wu, R. 1996. Expression of a late embryogenesis abundant protein gene, HVA1, from barley confers tolerance to water deficit and salt stress in transgenic rice. Plant Physiol. 110:249-257.

Yancey, P. H., Clark, M. E., Hand, S. C., Bowlus, R. D. and Somero, G. N. 1982. Living with water stress: evolution of osmolyte systems. Science 217:1214-1222.

Yu, J., Penaloza-Vazquez, A., Chakrabarty, A. M. and Bender, C. L. 1999. Involvement of the exopolysaccharide alginate in the virulence and epiphytic fitness of *Pseudomonas syringae* pv. syringae. Mol. Microbiol. 33:712-720.

Zhang, L., Ohta, A., Takagi, M. and Imai, R. 2000. Expression of plant group 2 and group 3 *lea* genes in *Saccharomyces cerevisiae* revealed functional divergence among LEA proteins. J. Biochem. 127:611-616.

Zhao, G., Ceci, P., Ilari, A., Giangiacomo, L., Laue, T. M., Chiancone, E. and Chasteen, N. D. 2002. Iron and hydrogen peroxide detoxification properties of DNA-binding protein from starved cells. A ferritin-like DNA-binding protein of *Escherichia coli*. J. Biol. Chem. 277:27689-27696.

Zhao, Q. X. and Poole, K. 2002. Mutational analysis of the TonB1 energy coupler of *Pseudomonas aeruginosa*. J. Bacteriol. 184:1503-1513.

Chapter 4. Identification of the trehalose biosynthetic loci in *Pseudomonas syringae* pv. tomato and their contribution to osmotolerance and phyllosphere fitness

Brian C. Freeman and Gwyn A. Beattie
Department of Plant Pathology,
Iowa State University; Ames, IA, 50010, USA

Abstract

Low water availability is a significant obstacle faced by bacteria in the phyllosphere. Many bacteria respond to water stress by accumulating compatible solutes such as trehalose, a disaccharide that protects cells from desiccation and osmotic stress. The impact of trehalose accumulation on survival of leaf-associated bacteria is poorly understood. In addition, trehalose biosynthetic pathways have not been characterized for many foliar plant pathogens including *Pseudomonas syringae*. In this study, we identified three putative trehalose biosynthesis operons in *P. syringae* pv. tomato DC3000 based on homology to known trehalose biosynthetic genes in other bacteria. These operons suggest that DC3000 utilizes a TreYZ-based two-step pathway in which maltodextrins, including glycogen, are converted into trehalose, as well as a TreS-based pathway in which maltose is converted directly into trehalose. DC3000 also appears to possess genes for an alternate pathway (TreS) that converts maltose directly into trehalose. Single and pyramided marked deletions of these putative biosynthetic operons were generated. All of the mutants exhibited decreased tolerance to hyperosmolarity in culture. Moreover, a mutant lacking all of the biosynthetic operons lacked trehalose, based on NMR data, and exhibited slightly decreased survival relative to the wild type on leaves of host plants (susceptible and resistant tomato) and non-host plants (soybean) under field conditions. These results indicate that trehalose biosynthesis contributes to survival of *P. syringae* during plant colonization, possibly due to its role in conferring maximal tolerance to conditions of low water availability.

Introduction

Water stress caused by changes in external osmolarity or desiccation is a constant threat faced by bacteria in many environments. When bacterial cells are exposed to changes in external osmolarity, cell growth may cease until a variety of changes in metabolism and gene expression occur (Jovanovich et al. 1988; Wood 1999). The most widely distributed strategy of bacterial osmoadaptation is the accumulation of compatible solutes, compounds that can accumulate to high cytosolic concentrations without disrupting normal cellular machinery. Accumulation can be through *de novo* synthesis or through transport of osmoprotectant compounds from the environment. These osmoprotectant compounds can function directly as compatible solutes, as with glycine betaine, or can serve as precursors, as occurs with choline, which is converted to glycine betaine after uptake. Accumulation via transport is generally favored, because it is far less energetically expensive than de novo synthesis.

Trehalose is a non-reducing disaccharide formed by two glucose molecules linked by an α-1,1-glycosidic bond. This versatile compound functions as a compatible solute in most prokaryotes and as an external carbon source or a component of cell wall glycolipids for some (Strom and Kaasen 1993; Horlacher and Boos 1997; Arguelles 2000; De Smet et al. 2000; Richards et al. 2002). Genes encoding trehalose biosynthesis are widely distributed in nature (Elbein 1974; Richards et al. 2002). Trehalose serves as the primary protective osmolyte in *E. coli* (Ishida et al. 1996), yet trehalose accumulation is only detectable in *P. aeruginosa* under high levels of osmotic stress, with NAGGN and glutamate being the predominant accumulated osmolytes at low to moderate osmotic stress levels (D'Souza-Ault et al. 1993).

At least five biosynthetic pathways are known for trehalose in prokaryotes. The most widely distributed pathway involves the conversion of glucose into trehalose via two enzymatic steps catalyzed by trehalose-6-phosphate synthase (TPS, or OtsA in *E. coli*) and trehalose-phosphatase (TPP, or OtsB in *E. coli*) (De Smet et al. 2000; Elbein et al. 2003). In the second pathway, the enzyme trehalose synthase (TS, or TreS) converts the α-1,4-bond of maltose to an α-1,1-bond, forming trehalose (Elbein et al. 2003). The third pathway involves the conversion of

maltodextrins such as glycogen into trehalose via two enzymatic steps catalyzed by maltooligosyl trehalose synthase (TreY) and maltooligosyl trehalose trehalohydrolase (TreZ) (Streeter and Bhagwat 1999; Elbein et al. 2003). The fourth pathway involves the reversible synthesis of trehalose from glucose 1-phosphate and glucose via trehalose phosphorylase (TreP) (Wannet et al. 1998; Schiraldi et al. 2002). Recently, a new biosynthetic pathway (TreT) was discovered in the hyperthermophilic archaeon *Thermococcus litoralis* in which trehalose is synthesized from ADP-glucose and glucose (or less efficiently from UDP-glucose and GDP-glucose) via trehalose glycosyltransferring synthase (TreT) (Qu et al. 2004; Ryu et al. 2005).

Prokaryotic species often utilize multiple trehalose biosynthetic pathways. For example, *Mycobacterium tuberculosis* and *Ralstonia solanacearum* have genes suggesting the presence of the OtsAB, TreYZ, and TreS pathways (Avonce et al. 2006). Many species possess multiple copies of the same pathway; for example, *Mesorhizobium loti*, *M. tuberculosis*, *R. solanacearum* and *Xanthomonas campestris* have two TPS genes, while *Thermoanaerobacter tengcongensis* has two genes for trehalose phosphorylase (*treP*). In addition, some genomes contain truncated gene copies that may not produce functional products, including *M. loti,* which has a truncated copy of TPS (Avonce et al. 2006). Among pseudomonads, *P. aeruginosa* strain PAO1 has genes with homology to the *E. coli treZ* and *treS* genes, while *P. putida* KT2440 and *P. syringae* DC3000 have TreZ and TreS homologs and genes with homology to *S. coelicolor treY*. All three strains appear to lack the OtsAB pathway, but functional characterization of trehalose biosynthesis has not been well documented in these species. One of the objectives of this study was to identify the functional trehalose biosynthetic loci, and thus the likely trehalose biosynthetic pathway(s), in *P. syringae*.

Trehalose clearly plays a role in protecting bacterial cells from water stress, yet the contribution made by trehalose accumulation to survival of bacteria in the phyllosphere has not been examined. The leaf surface is a harsh environment where low water availability is a constant threat to resident microbes (Hirano and Upper 1983, 1990). Bacteria that are able to colonize this habitat must be able to endure desiccation and osmotic stress brought about as surface water evaporates and remaining dissolved solutes become highly concentrated. Osmotolerance is among several fitness traits predicted to contribute to the ability of bacterial

pathogens such as *Pseudomonas syringae* to colonize leaf surfaces (Lindow et al. 1993; Beattie and Lindow 1994; Beattie and Lindow 1994). Therefore, trehalose accumulation may contribute to bacterial survival on leaf surfaces as well as within endophytic sites for pathogens on susceptible hosts. A major objective of this study was to characterize the quantitative contribution of trehalose production by *P. syringae* pv. tomato strain DC3000 in osmotolerance and in fitness during leaf colonization of both susceptible and resistant host plants as well as non-host soybean plants.

Materials and Methods

Bacterial growth media

The rifampin (Rif)-resistant phytopathogen *P. syringae* pv. tomato strain DC3000 (Moore et al. 1989) was used in this study. *P. syringae* was grown in King's B (KB) medium (King et al. 1954), MinA medium (Kagami et al. 1998) amended with 10% succinate and 10% glucose, or MinAM medium (MinA medium containing 10 mM potassium phosphate) amended with 10% succinate and 10% glucose at 28°C. Antibiotics were used at the following levels (μg/ml): rifampin, 50; tetracycline 20; and kanamycin, 50. *E. coli* was grown at 37°C in Luria-Bertani (LB) medium.

Preparation of electrocompetent DC3000 cells

Bacterial cultures that were grown in KB medium to an optical density (OD) at 600 nm of approximately 0.8 were chilled on ice for 10 min then harvested by gentle centrifugation (3000xg) for 5 min at 4°C. Cell pellets were gently resuspended in 400 ml of ice-cold, sterile nanopure water, centrifuged, and pellets resuspended in 200 ml of ice-cold, sterile nanopure water. Cells were centrifuged a third time and resuspended in 5 ml of ice-cold, sterile nanopure water containing 10% glycerol. Cells were divided into 50 ul aliquots and frozen immediately at -80°C.

Construction of bacterial mutants

The putative trehalose biosynthetic loci were deleted using a combination of gene splicing by overlap extension PCR (Choi and Schweizer 2005) and homologous recombination.

Briefly, a 1-kb region of each of the genes flanking the target operons were PCR-amplified from DC3000 genomic DNA using the primer pairs listed in Table 1. In addition, a kanamycin cassette containing flanking FRT sites was amplified from pKD4 (Datsenko and Wanner 2000) using the primer pair FRT-F (5'-ATTGTGTAGGCTGGAGCTGCTTC-3') and FRT-R (5'-CCATGGTCCATATGAATATCCTCC-3'). The three fragments were ligated together by overlap extension PCR using the original F1 and R2 primers to produce a single 3.5-kb fusion product consisting of the kanamycin cassette and the flanking genes. This single fragment was cloned into the MCS of pTOK2 (Tc^R)(Chen and Beattie, unpublished data) and sequenced for verification. To generate chromosomal deletions, pTOK2T was electroporated into electrocompetent DC3000 cells. After outgrowth in liquid KB medium for two hours at 28°C, cells were plated on solid KB medium containing Km to select for recombination events. Colonies were then screened for Tc sensitivity to identify double recombinants and the deletion mutants were confirmed by PCR.

Table 1. Chromosomal deletion mutants. Gene numbers correspond to PSPTO numbers. Underlined nucleotide bases indicate regions that complement 5'- and 3'- ends of the FRT-kanamycin cassette from pKD4.

Mutant	Target genes for deletion	Flanking genes	Primer sequences for amplifying flanking genes (5' → 3')
DCTRE1	2760-2762	2759	F1: TCTGCAGGCGGACGTCAGCAACGA
			R1: CCTGGGGCGTGAGGAGTGATGCTCGCGAGCATCACTCCTCACGCCCCAGG
		2763	F2: GAAGGTACCCAGCGAGGTCAGCGCTGACCTCGCTGGGTACCTTC
			R2: TAAAGCCAATGCATCATCACGTTCAACAG
DCTRE2	3125-3134	3124	F1: GTTGACGGGCAATTTCTTCCAC
			R1: GAAGCAGCTCCAGCCTACACAATGGTCGGTTGAACGGTCGAG
		3135	F2: GGAGGATATTCATATGGACCATGGGGCGGATTCGGCGACTACCTG
			R2: GGCAGCGAACATCTGAGCATC
DCTRE3	2760-2762	2759	Same as used for DCTRE1 and DCTRE2
	3125-3134	2763	
		3124	
		3135	

NMR spectroscopy

A modified method from Kuhlmann and Bremer (2002) was used to analyze ethanolic cell extracts from mutant strains for the presence or absence of trehalose using natural-abundance

^{13}C-nuclear magnetic resonance (NMR). Cells were grown for approximately 28 h in liquid MinA media amended with 10% succinate and 10% glucose, with or without 0.3M NaCl. Cells were harvested during late exponential phase; the final density was approximately 2 x 10^8 cells/ml for the wild-type and slightly lower for the mutants. Cells were centrifuged at 7,000xg for 2 min and washed with fresh MinA, then centrifuged again. Cells were lysed using three alternating freeze-thaw cycles in liquid nitrogen and 50°C water, then suspended in 80% ethanol. Cell lysates were centrifuged at 10,000xg for 5 min to pellet cell debris, and the remaining supernatant was decanted and evaporated in a 50°C water bath using nitrogen gas. Precipitates were resuspended in D_2O and ^{13}C-NMR spectra were recorded with a Bruker AC300 spectrophotometer operating at 75 MHz. The compounds in the extracts were identified by comparing the chemical spectral shifts with published values for trehalose (D'Souza-Ault et al. 1993), L-α-glutamate (Mikkat et al. 2000), NAGGN (D'Souza-Ault et al. 1993), and *O*-α-D-glucopyranosyl-(1→2)-glycerol (glucosylglycerol) (Mikkat et al. 2000).

Evaluation of bacterial growth in culture

Bacteria were grown overnight in MinAM liquid medium and were centrifuged and resuspended in fresh MinAM. Approximately 1.2 x 10^6 cells (75µl) were introduced into each well of a 96-well microtiter plate containing 75 µl of MinAM with or without NaCl. Plates were incubated with shaking (350rpm) at 28°C and growth was monitored using a Bio-Tek EL340 microplate reader. The ratio of the OD at 405nm to the OD at 630nm was recorded: this ratio minimized the impact of condensation on the plate lid on the estimate of relative cell density. Cell growth in individual wells was tracked, and wells that exhibited unusual growth were excluded from statistical analysis.

Evaluation of bacterial growth on plants in a growth chamber

Tomato (*Solanum lycopersicum*) cultivars Rio Grande-S (susceptible to bacterial speck) and Rio Grande-R (resistant to bacterial speck) were grown in a Conviron E15 growth chamber at 24°C and 60% or 90% relative humidity with 10-h light/14-h dark cycle. Five- to six-week-old plants were used. Bacterial cells grown overnight in liquid KB medium were centrifuged and resuspended in 10 mM $MgSO_4$ containing 0.02% Silwet to a final inoculum density of 10^8 cells/ml. Wild-type DC3000 cells were mixed with the trehalose mutant DCTRE3 in a 1:1 ratio

and bacterial suspensions were sprayed onto both adaxial and abaxial leaf surfaces until the leaves were moderately wet. Plant leaves remained moist for at least one hour before being returned to the growth chamber at the same settings as during plant propagation. The one hour drying period was performed to allow bacterial invasion before a period of rapid evaporation of leaf surface moisture following placement in the growth chamber. At select timepoints, whole leaves were harvested and homogenized in washing buffer containing peptone and 10 mM potassium phosphate, and dilutions were plated on KB agar containing Rif to enumerate the total bacterial population and on KB agar containing Rif and Km to enumerate the mutant population. Plates also contained 20 μg/ml cycloheximide to suppress fungal growth. The DC3000 population size was estimated by subtracting the mutant population from the total population.

Evaluation of bacterial growth on plants in the field

Tomato cultivars Rio Grande-R and Rio Grande-S, as well as soybean (*Glycine max*) cultivar Williams were used for this experiment. Soybean seeds were planted directly into field plots at the Iowa State University Horticulture Station near Gilbert, IA, on June 23rd, 2008. Tomato seedlings raised in a greenhouse until approximately 6-weeks old were transplanted into the field plots on July 6th. Treatments began 4 weeks later on August 3rd. DC3000 and mutant strains were grown on KB plates containing appropriate antibiotics for three days prior to inoculations, suspended in 10 mM phosphate buffer (PB) and washed 1x in 10 mM PB. Mixtures containing equal numbers of wild-type and mutant cells were prepared in 10 mM PB containing 0.02% Silwet. Bacterial suspensions were sprayed onto both adaxial and abaxial leaf surfaces using a hand-sprayer until the leaves were uniformly wet. Plants were sprayed under a mobile tent to minimize inter-plot contamination.

Whole leaves were harvested for each replicate sample at each timepoint and stored in a cooler during transport to the laboratory for processing. Leaves were homogenized in washing buffer, and dilutions were plated as described for the experiments performed in the growth chamber. High temperatures at the field plot varied between 22°C and 34°C, and low temperatures varied between 14°C and 22°C. Rainfall events occurred on days 9 and 10 post-inoculation.

Results

Identification of the candidate operons for trehalose biosynthesis

The genome of DC3000 was screened for the presence of ORFs with similarity to known trehalose biosynthetic genes. PSPTO_3128 putatively encodes a glycosyl hydrolase family protein with 30% amino acid similarity to TreY in *Corynebacterium glutamicum*. TreY encodes a maltooligosyl trehalose synthase that catalyzes the transglycosylation of the last glucose moiety at the reduced end of maltodextrins such as glycogen from an α-1,4-bond to an α-1,1-bond leading to a maltooligosyltrehalose containing a trehalose moiety at the end of the polymer. PSPTO_3126 putatively encodes an α-amylase family protein with amino acid similarity to TreZ in *Sinorhizobium meliloti* (43%) and *C. glutamicum* (39%). In those organisms, TreZ encods a malto-oligosyltrehalose trehalohydrolase that catalyses the hydrolytic release of trehalose from the maltooligosyltrehalose polymer.

PSPTO_3126 and _3128 appear to lie in an operon of five genes, PSPTO_3125-3129, based on their close proximity (the largest gap being 20 nt) and co-expression in response to water stress in a whole-genome transcriptional analysis (Chapter 3; Fig 1). In addition, qRT-PCR analysis of RNA isolated from DC3000 cells showed considerable amplification of the intergenic regions between all genes in the cluster, suggesting that the genes were originally transcribed as a single mRNA transcript (Fig 1). The first gene in this putative operon encodes glycogen synthase (GlgA: PSPTO_3125), an enzyme that catalyzes the synthesis of glycogen from monomeric UDP-glucose. In *C. glutamicum,* trehalose synthesis is dependent on glycogen synthase as *glgA* mutants are unable to synthesize trehalose in that organism (Tzvetkov et al. 2003). PSPTO_3127 putatively encodes the amylomaltase MalQ, an enzyme that hydrolyzes maltodextrins into smaller dextrins and glucose. The function of PSPTO_3129 is unknown.

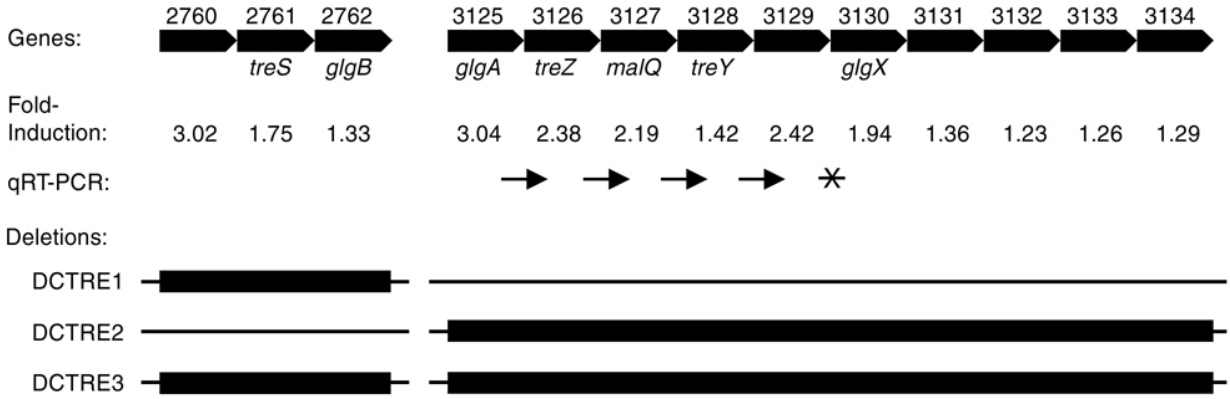

Figure 1. Organization, expression and deletion of loci putatively involved in trehalose synthesis in *P. syringae* pv. tomato DC3000. Gene numbers are listed as PSPTO numbers. The fold-induction levels are in response to a 15-min incubation with NaCl (-1 MPa), as evaluated using global gene expression analysis (Chapter 3), with all of the genes shown exhibiting significant induction ($p < 0.05$). qRT-PCR analysis demonstrated amplified (arrow) or non-amplified (asterix) intergenic regions, indicating the presence or absence or linked genes, respectively. Deleted loci are represented as black boxes for mutants DCTRE1, DCTRE2, and DCTRE3.

PSPTO_3130 contains a small domain with amino acid similarity to the TreZ homolog PSPTO_3126 (30%) and TreY homolog PSPTO_3128 (24%). This gene putatively encodes the glycogen de-branching enzyme GlgX but may have additional enzymatic functionality due to the presence of the small TreY/Z domains. *glgX* lies in another operon, PSPTO_3130-3134, which lies immediately downstream of PSPTO_3125-3129 and likely constitutes a separate operon based on the 160 nt distance between PSPTO_3129-30 and lack of qRT-PCR intergenic amplification (Fig 1).This operon was also induced by water stress (Chapter 3).

PSPTO_2761 shares 73% amino acid identity with the trehalose synthase (TreS) gene from *Pseudomonas putida*. In that organism, TreS is part of an alternate pathway where trehalose synthase converts the α1,4-bond of maltose into a α1,1-bond, forming trehalose. This gene is in a third putative operon, PSPTO_2760-62, and contains a putative enzyme with alpha amylase activity (PSPTO_2760) as well as the glycogen branching enzyme GlgB (PSPTO_2762). This operon was also induced by cellular exposure to water stress.

Loss of all three biosynthetic loci for trehalose eliminated trehalose accumulation in response to osmotic stress.

A ^{13}C NMR spectrum of DC3000 cells grown in MinA medium containing 0.3M NaCl showed the presence of peaks that correlated with peaks present in the published spectra of trehalose (90.9, 70.2, 69.8, 68.7, and 58.3), L-α-glutamate (178.8, 173.4, 52.2, 30.5, and 24.3), and NAGGN (175.5, 173.4, 172.1, 171.4, 51.0, 50.6, 28.8, 24.5, and 19.5) (Fig. 2A). There were nine unidentified signals at 71.8, 71.7, 70.4, 70.2, 68.7, 68.6, 60.3, 58.4, and 58.2 that are indicative of *O*-α-D-glucopyranosyl-(1→2)-glycerol (glucosylglycerol), a compatible solute reported in *P. mendocina* and *P. pseudoalcaligenes* (Pocard et al. 1994) but not previously reported in *P. syringae*. A ^{13}C NMR spectrum of the DCTRE3 mutant showed the absence of peaks corresponding to trehalose, but not the other compatible solutes (Fig 2B), demonstrating that trehalose was not accumulated in these cells.

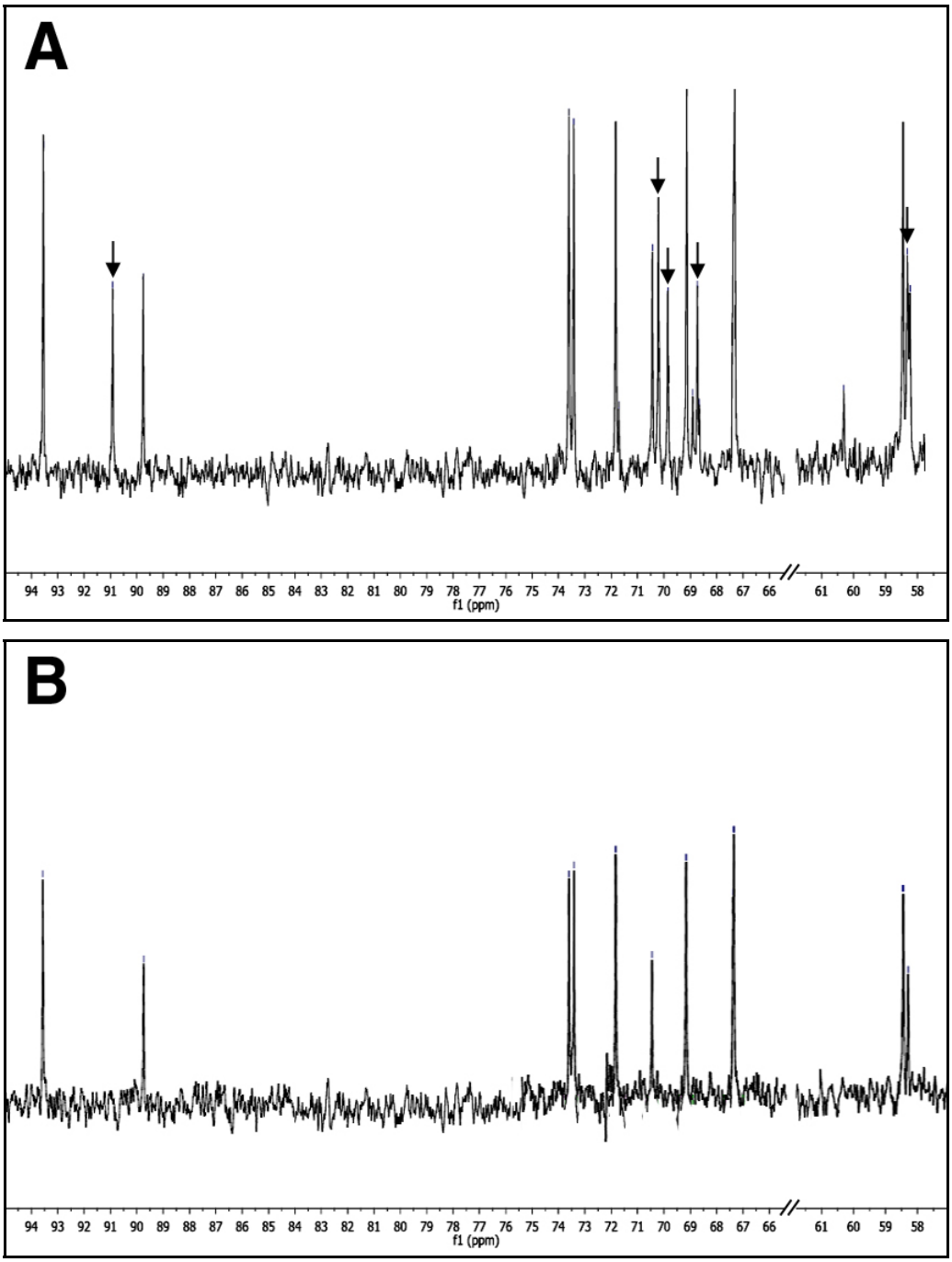

Figure 2. ^{13}C NMR spectra from (A) DC3000 and (B) DCTRE3 cells growing in MinA with 10% succinate, 10% glucose, and 0.3M NaCl. Resonances at 90.9, 70.2, 69.8, 68.7, and 58.3 arise from trehalose (arrows). The trehalose peaks are absent in the NMR spectrum of the DCTRE3 cells.

Trehalose production contributes to DC3000 osmotolerance in culture

When bacterial cells were grown in liquid Min AM media without NaCl, the mutants were indistinguishable from the wild-type over both a 27-h and 79-h time-course (Figs 3A,B). In contrast, the mutants all grew to slightly lower cell densities in the presence of 0.2M NaCl (Fig 3D), and to dramatically lower cell densities in the presence of 0.4M NaCl (Figs 3E, F). An analysis of variance (ANOVA) performed on population sizes at the final timepoint in each time-course indicated that the strains differed significantly in their final cell densities after 79 h of growth with 0.2M NaCl (Fig 3D) and after 27 and 79 h with 0.4M NaCl ($p<0.001$) (Figs 3E,F) with all of the mutants significantly lower than the wild-type ($p<0.05$, Fisher's LSD).

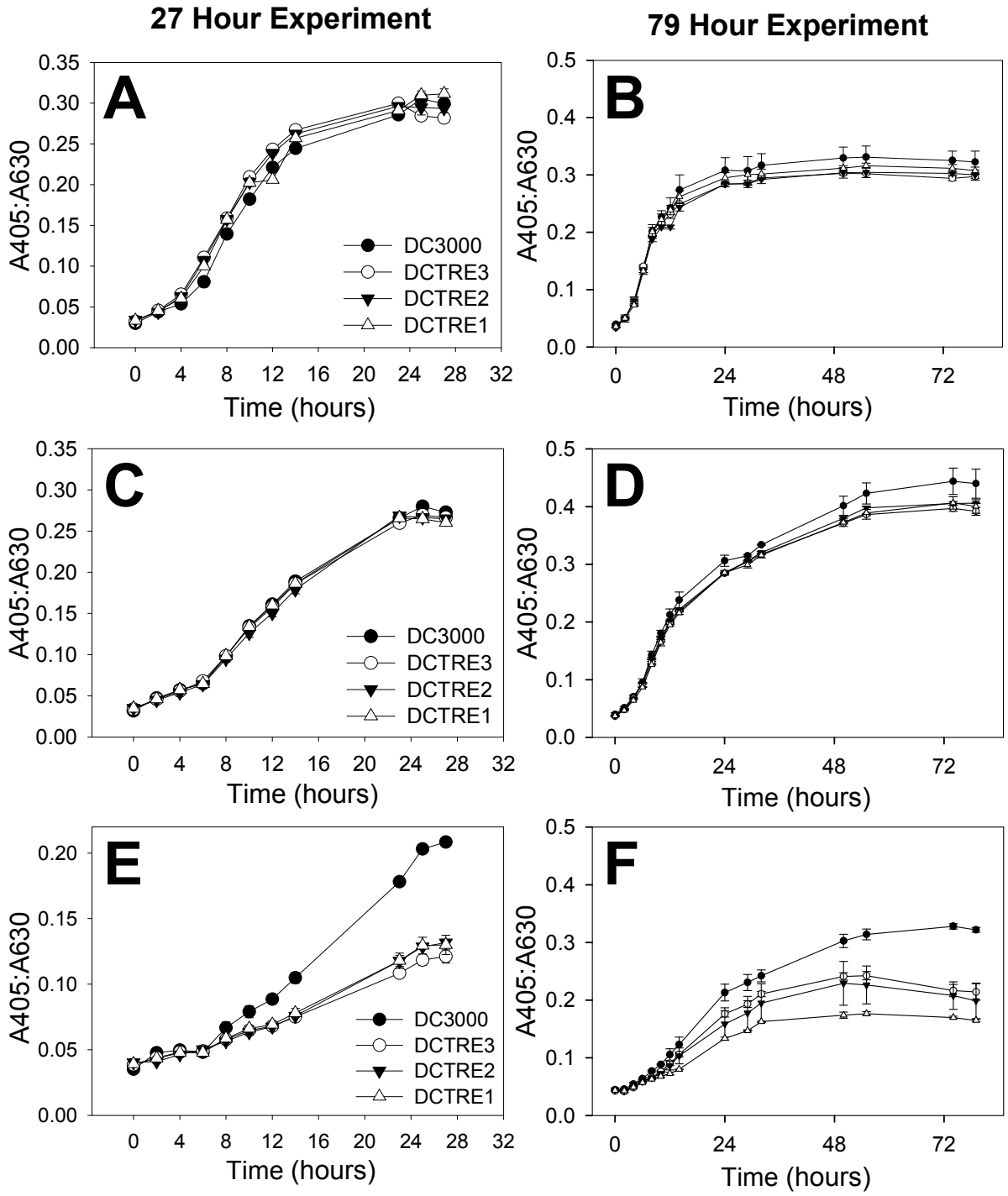

Figure 3. Effect of osmotic stress on bacterial growth in MinAM medium containing (A-B) 0M NaCl, (C-D) 0.2M NaCl, or (E-F) 0.4M NaCl inoculated with DC3000 (●), DCTRE3 (○), DCTRE2 (▼), or DCTRE1 (Δ). Experiments were performed for 27 hours (A, C, E) and 79 hours (B, D, F). Values represent the mean A_{405}:A_{630} ratio ± SEM (n=3 with two subsamples per replicate).

Trehalose production contributes to DC3000 survival on host leaves in a growth chamber.

To evaluate the impact of trehalose production on bacterial growth and survival on leaves of susceptible host plants, populations of the trehalose mutant DCTRE3 and the wild-type DC3000 were monitored after spray-inoculation onto Rio Grande-S tomato plants and incubation at two relative humidity (RH) levels for 2-3 weeks (Fig 4). At both RHs, bacterial cells reached a carrying capacity of approximately 10^6 CFU/leaf within 2 days post inoculation (dpi). At 65% RH, populations of the trehalose mutant DCTRE3 dropped rapidly between days 2 and 7 to levels significantly lower than the wild-type at both 7 dpi (p=0.001) and 14 dpi (p=0.012) based on a Student's t-test (Fig 4A). In contrast, at 90% RH, the mutant population did not decrease in size until after 7 days (Fig 4B), and was not significantly lower than the wild-type until 11 dpi (p=0.037) and 17 dpi (p<0.001). The similar growth of the wild-type and mutant during the initial stages of colonization when the populations were increasing or holding steady, but smaller populations of the mutant during the stage when the populations were decreasing, suggests that trehalose production contributes specifically to DC3000 survival and not growth during its association with leaves. The earlier decrease in DCTRE3 populations at 65% RH than 90% RH suggests that the contribution of trehalose to DC3000 survival on leaves is due to its contribution to osmotolerance.

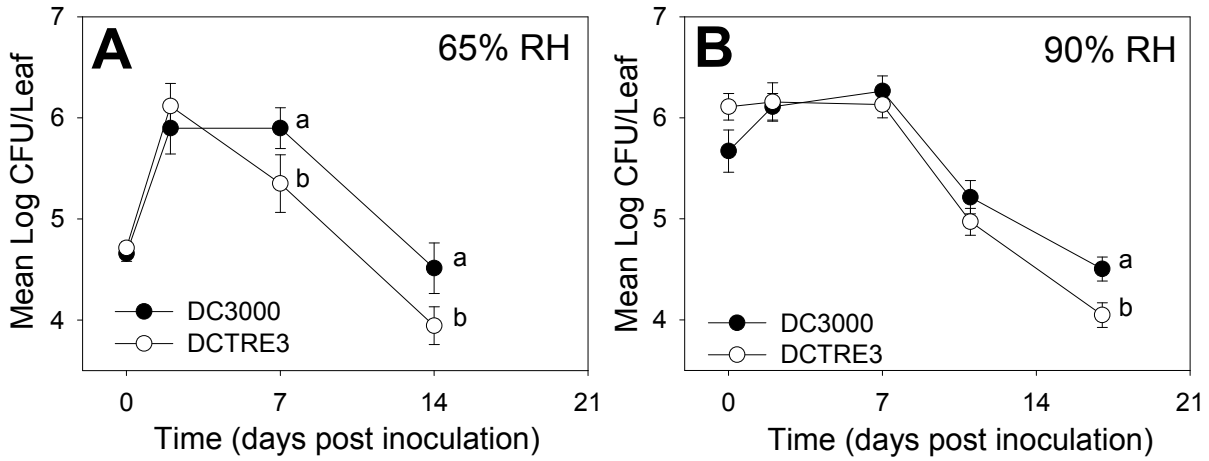

Figure 4. Population dynamics of DC3000 (●) and DCTRE3 (○) on leaves of susceptible tomato plants. Leaves were sprayed with cell suspensions (10^7 cells/ml), and plants were incubated at (A) 65% or (B) 90% relative humidity (RH) at 28°C in 10h/14h light/dark cycle. Values shown are mean log (CFU/leaf) ± SEM (n=15-20 leaves)

Field study

To assess the impact of trehalose production on the fitness of *P. syringae* on leaves under natural conditions, the population sizes of DC3000 and the DCTRE3 mutant were monitored after introduction onto tomato Rio Grande-S (susceptible) and Rio Grande-R (resistant) plants as well as onto non-host soybean (*Glycine max*) plants in field plots. As expected, populations of both DC3000 and DCTRE3 declined rapidly after inoculation onto soybean plants (Fig 5A), but the populations of DCTRE3 decreased even more than DC3000 (p=0. 04 and 0.11 at 7 and 10 dpi, respectively, Student's t-test). This decrease in relative fitness over time was also detected by calculating the percentage of the total DC3000 and DCTRE3 population comprised by the DCTRE3 population on each leaf and observing a decrease in the mean log-transformed percentage over time (Fig 5B). On soybeans, the proportional representation of DCTRE3 mutants decreased below 50% between 4 and 7 dpi and remained low thereafter (Fig 5B). Regression analysis revealed a significant decrease in the proportion of DCTRE3 mutants present in the total population over the entire ten-day experiment based on the slope of a line of the log (% mutant) values from 0 to 10 dpi (Fig 5B).

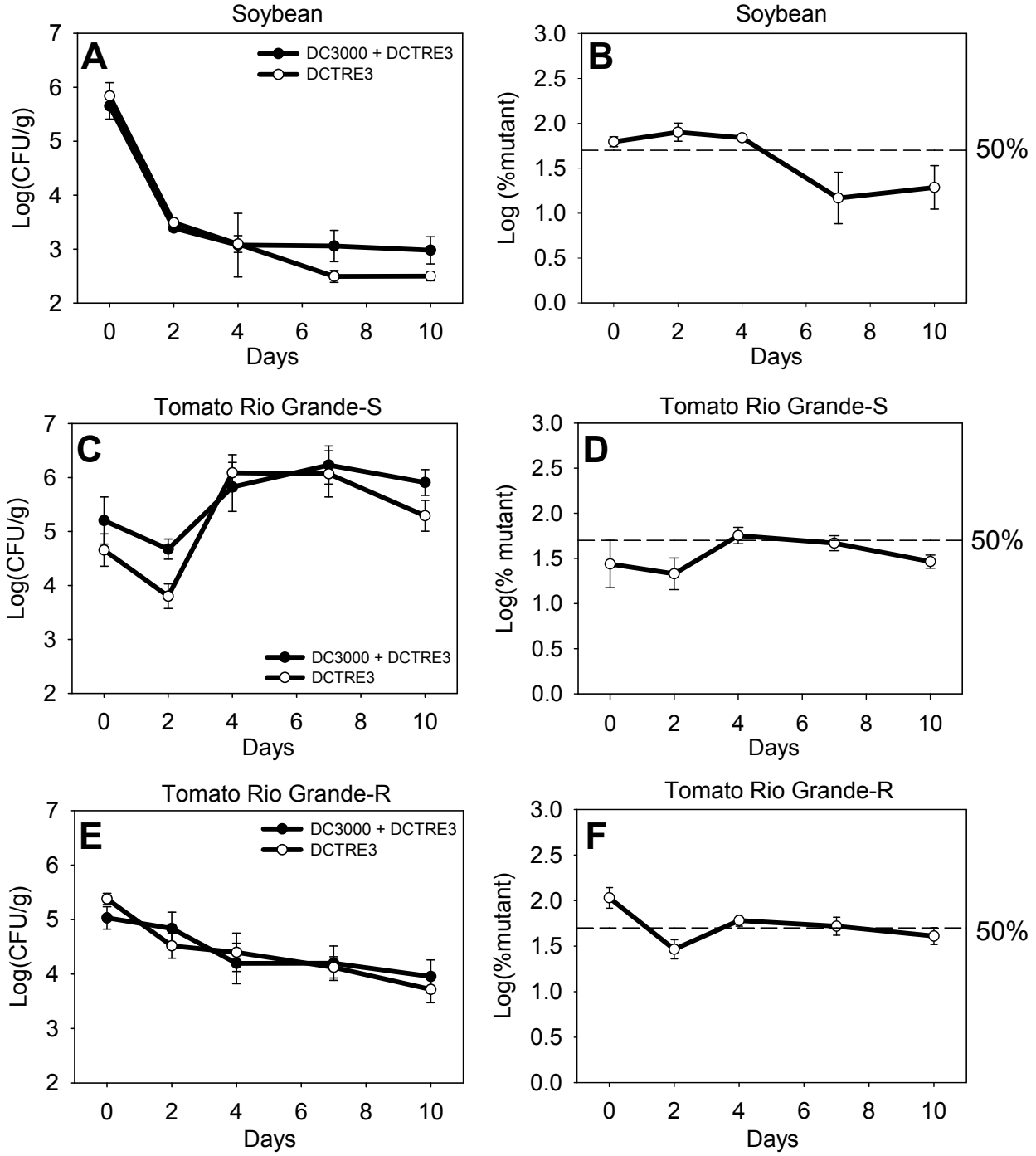

Figure 5. Epiphytic fitness of the DCTRE3 mutant relative to DC3000 on host and non-host plants in field plots. Leaves of field-grown non-host soybean (A-B) and host tomato Rio Grande-S (C-D) and tomato Rio Grande-R (E-F) were sprayed with a 1:1 mixture of DC3000 and the DCTRE3 mutant (10^7 cells/ml of each). The size of the combined populations of the two strains (●) and the DCTRE3 mutants (○) were monitored over time and were plotted as log (CFU/g

fresh wt) (A,C,E). The percentage of the total population that was comprised of the mutant was determined and the mean of the log-transformed percentage was plotted (B,D,F). The dotted line indicates a 1:1 ratio (i.e., the mutant comprises 50% of the population). Values shown are means ± SEM (n=12).

Similar to growth on soybean, DC3000 and DCTRE3 populations on resistant tomato plants (Rio Grande-R) generally declined (Figure 5E). Populations of DC3000 and DCTRE3 did not differ significantly in size at most timepoints. However, the proportional representation of DCTRE3 decreased slightly, but significantly, over the 10-day period (Figure 5F), as indicated by regression analysis (slope=-0.032, p=0.023). Because DC3000 growth on leaves of the non-host plant soybean and the resistant host Rio Grande-R is likely restricted to epiphytic sites because of the plant defense system, the continuous decrease in DC3000 populations on these hosts and the lower populations of DCTRE3 provide confirmatory evidence that DC3000 is a poor colonizer of epiphytic surfaces and trehalose production contributes to fitness on these surfaces.

In contrast to growth on soybeans and R tomato, DC3000 exhibited strong growth during its growth on susceptible tomato Rio Grande-S (Figure 4C). Although populations of DC3000 and DCTRE3 initially decreased, they then grew rapidly, likely as the result of bacterial cells invading the leaf and establishing disease-causing endophytic populations. Between days 4 and 10, populations of DCTRE3 declined by nearly 0.8 log units, whereas the wild-type strain DC3000 continued to grow 0.4 log units. Regression analysis indicated that the log (% mutant) values decreased significantly between days 4 and 10 dpi (slope=-0.05, p=0.017).

Discussion

The purpose of this study was to identify the trehalose biosynthesis genes in *P. syringae* and quantify the impact on growth and survival both in culture and when in association with living host and non-host plants. Genomic analysis suggests that *P. syringae* utilizes at least two different trehalose biosynthetic pathways, including the TreYZ pathway in which maltodextrins such as glycogen are converted into trehalose, and the TreS pathway in which maltose is

converted directly into trehalose. Three putative operons were identified based on gene proximity, coexpression analysis from the microarray experiment (Chapter 3), and qRT-PCR amplification of intergenic regions. These operons were deleted and the resulting mutants exhibited significantly decreased growth in NaCl-amended growth media within 24 h or 79 h of an osmotic up-shift to 0.4M or 0.2M NaCl, respectively. These results suggest that trehalose accumulation contributes to the osmotolerance of *P. syringae* in a concentration-dependent manner. These results are consistent with the role of trehalose accumulation in *P. aeruginosa* where the disaccharide is only synthesized in response to high osmotic stress (D'Souza-Ault et al. 1993). Trehalose biosynthesis did not influence bacterial growth in the absence of salt suggesting that trehalose is not a required metabolite in *P. syringae*. Interestingly, deletion of the single operon PSPTO_2760-2762 (DCTRE1) or the double operon PSPTO_3125-3129/3130-3134 (DCTRE2) had virtually the same impact on growth in high osmolarity medium as deletion of all three operons (DCTRE3; Figure 2), suggesting that the complete trehalose biosynthetic pathway in *P. syringae* is dependent upon enzymes produced by genes in all three operons. This is unusual and warrants further study.

Growth of the trehalose mutant DCTRE3 was significantly impaired compared with wild type DC3000 after bacteria were sprayed onto susceptible tomato plants grown in a growth chamber (Fig 3). Clearly, relative humidity had an impact on survival of both strains but drier air contributed to a more rapid decline in populations of the trehalose mutant when plants were grown at 65% RH compared with 90% RH. These results demonstrate that trehalose biosynthesis is important for *P. syringae* cells growing in association with living plant tissue, particularly under lower humidity.

Bacterial growth was also characterized after inoculation onto non-host soybean plants and both susceptible and resistant tomato plants growing outdoors in field plots. Bacterial populations declined rapidly after inoculation onto non-host soybean leaves. These bacteria are not able to invade soybean leaves or establish endophytic populations. As a result, a majority of the recovered bacteria were likely remaining surface residents that died quickly from exposure to the harsh abiotic stresses present there. Trehalose mutant populations declined more rapidly than wild-type DC3000 cells on these leaves by 7 dpi indicating that trehalose production contributed

to epiphytic population maintenance, rather than establishment, and had a greater role in late-stage survival (i.e., after the majority of the population had been killed) rather than early-stage survival (i.e., during the initial population decrease following inoculation) on soybeans.

Growth characteristics for bacteria inoculated onto host tomato plants were complex. Once sprayed onto plants in the field, the bacterial inoculum evaporated in a matter of minutes due to the hot temperatures and direct sunlight present during inoculation. A vast majority of the bacteria sprayed onto the leaf surfaces were likely not able to invade the leaf before the surface liquid evaporated, trapping most bacteria outside the leaf. As a result, only a small number of cells may have made their way into the leaf through open stomata where they eventually established small endophytic populations. Whole-leaf sections do not discriminate between these two populations, and between days 0 and 2, a vast majority of the recovered bacterial cells probably originated from the leaf surface as indicated from the rapid die-off. In contrast, the cells recovered on day 4 likely included a large number of bacteria growing endophytically within the leaf. In fact, both strains appear to have reached a carrying capacity of approximately 10^6 CFU/g within the leaf, suggesting that water is sufficiently available in endophytic leaf sites during the early stages of infection because growth of the trehalose mutant was not significantly restricted compared with the wild type strain. Diseased tomato tissues became necrotic and desiccated as the disease progressed throughout the leaf tissue between days 4 and 10, however, and during this period trehalose biosynthesis was clearly important for survival of *P. syringae* cells. In contrast to disease, bacterial cells of both strains steadily declined over the entire period when inoculated onto resistant tomatoes. Again, trehalose biosynthesis was clearly important for survival because populations of the mutant DCTRE3 declined more rapidly compared with wild type DC3000.

Acknowledgements

I thank Kelly Peterson and Chiliang Chen for help in the construction of the bacterial strains DCTRE1, DCTRE2, and DCTRE3, and along with Rina Mbofung, for help with the field experiments and bacterial enumeration. I also thank Adam Bogdanove for providing the tomato

seeds. This project was supported by the National Research Initiative of the USDA-CSREES, grant No. 2005-35319-15300.

References

Arguelles, J. C. 2000. Physiological roles of trehalose in bacteria and yeasts: a comparative analysis. Arch. Microbiol. 174:217-224.

Avonce, N., Mendoza-Vargas, A., Morett, E. and Iturriaga, G. 2006. Insights on the evolution of trehalose biosynthesis. BMC Evol. Biol. 6:109.

Beattie, G. A. and Lindow, S. E. 1994. Comparison of the behavior of epiphytic fitness mutants of *Pseudomonas syringae* under controlled and field conditions. Appl. Environ. Microbiol. 60:3799-3808.

Beattie, G. A. and Lindow, S. E. 1994. Survival, growth, and localization of epiphytic fitness mutants of *Pseudomonas syringae* on leaves. Appl. Environ. Microbiol. 60:3790-3798.

Choi, K. H. and Schweizer, H. P. 2005. An improved method for rapid generation of unmarked *Pseudomonas aeruginosa* deletion mutants. BMC Microbiol. 5:30.

D'Souza-Ault, M. R., Smith, L. T. and Smith, G. M. 1993. Roles of N-acetylglutaminylglutamine amide and glycine betaine in adaptation of *Pseudomonas aeruginosa* to osmotic stress. Appl. Environ. Microbiol. 59:473-478.

Datsenko, K. A. and Wanner, B. L. 2000. One-step inactivation of chromosomal genes in *Escherichia coli* K-12 using PCR products. Proc. Natl. Acad. Sci. U.S.A. 97:6640-6645.

De Smet, K. A., Weston, A., Brown, I. N., Young, D. B. and Robertson, B. D. 2000. Three pathways for trehalose biosynthesis in mycobacteria. Microbiology 146:199-208.

Elbein, A. D. 1974. The metabolism of alpha,alpha-trehalose. Adv. Carbohyd. Chem. Biochem. 30:227-256.

Elbein, A. D., Pan, Y. T., Pastuszak, I. and Carroll, D. 2003. New insights on trehalose: a multifunctional molecule. Glycobiology 13:17R-27R.

Hirano, S. S. and Upper, C. D. 1983. Ecology and epidemiology of foliar bacterial plant pathogens. Annu. Rev. Phytopathol. 21:243-269.

Hirano, S. S. and Upper, C. D. 1990. Population biology and epidemiology of *Pseudomonas syringae*. Ann. Rev. Phytopathol. 28:155-177.

Horlacher, R. and Boos, W. 1997. Characterization of TreR, the major regulator of the *Escherichia coli* trehalose system. J. Biol. Chem. 272:13026-13032.

Ishida, A., Otsuka, N., Nagata, S., Adachi, K. and Sano, H. 1996. The effect of salinity stress on the accumulation of compatible solutes related to the induction of salt-tolerance in *Escherichia coli*. J. Gen. Appl. Microbiol. 42:331-336.

Jovanovich, S. B., Martinell, M., Record, M. T. and Burgess, R. R. 1988. Rapid response to osmotic upshift by osmoregulated genes in *Escherichia coli* and *Salmonella typhimurium*. J. Bacteriol. 170:534-539.

Kagami, Y., Ratliff, M., Surber, M., Martinez, A. and Nunn, D. N. 1998. Type II protein secretion by *Pseudomonas aeruginosa*: genetic suppression of a conditional mutation in the pilin-like component XcpT by the cytoplasmic component XcpR. Mol. Microbiol. 27:221-233.

King, E. O., Ward, M. K. and Raney, D. E. 1954. Two simple media for the demonstration of pyocyanin and fluorescin. J. Lab Clin. Med. 44:301-307.

Kuhlmann, A. U. and Bremer, E. 2002. Osmotically regulated synthesis of the compatible solute ectoine in *Bacillus pasteurii* and related *Bacillus* spp. Appl. Environ. Microbiol. 68:772-783.

Lindow, S. E., Andersen, G. and Beattie, G. A. 1993. Characteristics of insertional mutants of *Pseudomonas syringae* with reduced epiphytic fitness. Appl. Environ. Microbiol. 59:1593-1601.

Mikkat, S., Galinski, E. A., Berg, G., Minkwitz, A. and Schoor, A. 2000. Salt adaptation in pseudomonads: characterization of glucosylglycerol-synthesizing isolates from brackish coastal waters and the rhizosphere. Syst Appl Microbiol 23:31-40.

Moore, R. A., Starratt, A. N., Ma, S. W., Morris, V. L. and Cuppels, D. A. 1989. Identification of a chromosomal region required for biosynthesis of the phytotoxin coronatine by *Pseudomonas syringae* pv. tomato. Can. J. Microbiol. 35:910-917.

Pocard, J. A., Smith, L. T., Smith, G. M. and Lerudulier, D. 1994. A prominent role for glucosylglycerol in the adaptation of *Pseudomonas mendocina* Skb70 to osmotic stress. J. Bacteriol. 176:6877-6884.

Qu, Q., Lee, S. J. and Boos, W. 2004. TreT, a novel trehalose glycosyltransferring synthase of the hyperthermophilic archaeon *Thermococcus litoralis*. J. Biol. Chem. 279:47890-47897.

Richards, A. B., Krakowka, S., Dexter, L. B., Schmid, H., Wolterbeek, A. P., Waalkens-Berendsen, D. H., Shigoyuki, A. and Kurimoto, M. 2002. Trehalose: a review of properties, history of use and human tolerance, and results of multiple safety studies. Food Chem. Toxicol. 40:871-898.

Ryu, S. I., Park, C. S., Cha, J., Woo, E. J. and Lee, S. B. 2005. A novel trehalose-synthesizing glycosyltransferase from *Pyrococcus horikoshii*: molecular cloning and characterization. Biochem. Biophys. Res. Commun. 329:429-436.

Schiraldi, C., Di Lernia, I. and De Rosa, M. 2002. Trehalose production: exploiting novel approaches. Trends Biotechnol. 20:420-425.

Streeter, J. G. and Bhagwat, A. 1999. Biosynthesis of trehalose from maltooligosaccharides in *Rhizobia*. Can. J. Microbiol. 45:716-721.

Strom, A. R. and Kaasen, I. 1993. Trehalose metabolism in *Escherichia coli*: stress protection and stress regulation of gene expression. Mol. Microbiol. 8:205-210.

Tzvetkov, M., Klopprogge, C., Zelder, O. and Liebl, W. 2003. Genetic dissection of trehalose biosynthesis in *Corynebacterium glutamicum*: inactivation of trehalose production leads to impaired growth and an altered cell wall lipid composition. Microbiology 149:1659-1673.

Wannet, W. J., Op den Camp, H. J., Wisselink, H. W., van der Drift, C., Van Griensven, L. J. and Vogels, G. D. 1998. Purification and characterization of trehalose phosphorylase from the commercial mushroom *Agaricus bisporus*. Biochem. Biophys. Acta. 1425:177-188.

Wood, J. M. 1999. Osmosensing by bacteria: signals and membrane-based sensors. Microbiol. Mol. Biol. Rev. 63:230-262.

Chapter 5. Conclusions and future directions

Bacteria are ubiquitous in the phyllosphere where many species are able to colonize leaf surfaces and influence plant health. The phyllosphere is a harsh environment where low water availability can significantly influence bacterial populations. Epiphytic population sizes are often strongly correlated with disease incidence and severity, and differences in bacterial stress tolerance can significantly influence these populations during periods of water stress. Further, changes in leaf hydration are known to occur during both disease and plant defense responses. Therefore, leaf water status may play a significant role in determining the outcome of bacterial-plant interactions. In this study, we demonstrated that leaf hydration can be significantly altered by the presence of potential bacterial pathogens and populations of resident microbes can be altered by changes in leaf water status.

We characterized early physiological changes in plants challenged with pathogenic and non-pathogenic bacteria, and found that leaf vascular activity is virtually completely halted in just the first three hours following inoculation with an HR-inducing strain. The vascular restriction preceded or was simultaneous with reductions in stomatal conductance, leaf transpiration, and photosynthesis, and resulted in significant water loss in affected leaves. A major finding of this work is that bacterial growth suppression in plant tissues during gene-for-gene mediated resistance could be completely reversed by halting leaf water loss; water loss was halted by blocking transpiration using either petroleum jelly or continuous incubation at high RH. This finding, in conjunction with our previous observation that *P. syringae* cells sensed inhibitory levels of water stress in resistant *A. thaliana* plants (Wright and Beattie 2004), supports the possibility that the gene-for-gene mediated resistance response suppresses the growth and spread of bacterial populations by limiting water availability to the bacteria and thus effectively starving them of water. In addition, we found that coronatine-mediated stomatal opening (Melotto et al. 2006) is only transient and is quickly followed by stomatal closure that is mediated by one or more T3SS effectors. Changes in leaf physiology, as monitored using a LI-6400 photosynthesis system, were shown to be highly dynamic following *P. syringae* inoculation. Such physiological data are critical to complement the accumulating wealth of

knowledge on the signal transduction cascades and transcriptional changes associated with resistance and pathogenesis.

In this study, we also performed whole-genome microarray experiments to elucidate differences in gene expression between two closely related pathovars of the bacterial plant pathogen *Pseudomonas syringae* in response to osmotic water stress. We found considerable differences in the expression of many pathogenesis-related genes between *P. syringae* pv. tomato strain DC3000 and pv. syringae strain B728a, including genes in the Hrp type III secretion system, type III effectors, and the type VI secretion system. The nature of the changes in gene expression suggest that osmotic stress may attenuate the virulence or growth of DC3000 while having little influence, or even a positive influence, on the virulence or growth of B728a. In addition, B728a exhibited stronger induction of alginate and NAGGN biosynthetic genes. This may translate into greater survival of B728a in response to an equivalent level of water stress compared with DC3000, especially over the long-term. Validation analysis using qRT-PCR showed that NAGGN gene expression peaked early but declined by 1 hour, in contrast to trehalose gene expression which tended to gradually increase over time, suggesting that NAGGN is a short-term response to water stress while trehalose production is a long-term adaptation strategy.

Trehalose is an important compatible solute synthesized by bacteria in response to water stress. The trehalose biosynthetic pathway has not been previously characterized for *P. syringae*, and the contribution of trehalose biosynthesis to population growth has not been evaluated in this species. In this study, we identified three putative trehalose biosynthetic operons in *P. syringae* pv. tomato DC3000 based on gene homology to functionally-characterized trehalose biosynthetic genes in other bacterial species. These putative operons were deleted individually and collectively from the genome, and the resulting mutants all exhibited significantly decreased growth compared to wild-type DC3000 cells within hours of an osmotic upshift to 0.2M or 0.4M NaCl when grown in liquid culture. Growth of the triple-operon-deletion mutant DCTRE3 was significantly impaired compared with wild-type DC3000 when grown in association with host and non-host plants grown under controlled environmental conditions as well as in field plots. Collectively, these results demonstrate that trehalose biosynthesis contributes to growth and

survival of *P. syringae* cells in response to hyperosmotic stress and when growing in association with living plant tissue.

Future directions

The mechanism of vascular restriction remains a mystery. Water-conducting tracheids and vessels can be blocked by a variety of pathogen-induced and plant-derived processes. The formation of tyloses or secretion of gummosis seems unlikely given the rapid nature of the response. Xylem water movement is known to be easily disrupted by cavitation, the formation of air bubbles that become trapped in leaf veins and block water flow. Physical disruption of the air-tight bundle sheath surrounding xylem elements that may occur during cell suicide and tissue collapse could allow air to become trapped within the xylem, blocking it. In addition to vascular restriction, it is not clear how localized leaf drying can occur without water moving passively from adjacent, well-hydrated regions back into the desiccated lesion. Following the hypersensitive response, cells lining the periphery of affected lesions exhibit significant changes in gene expression and physiology. Cellular processes including the down-regulation of aquaporins or electrolyte uptake may help retain water in living cells and prevent plasmolysis.

The extent to which other incompatible pathogens can trigger HR-associated vascular restriction is not well known. Vascular restriction has been reported primarily for non-bacterial pathogens during gene-for-gene mediated resistance (Hammond-Kosack et al. 1996; Chaerle et al. 1999). Vascular restriction was reported on *Nicotiana benthamiana* when challenged with non-host *P. syringae*, but this was a basal defense response (Wright et al. 2000). A variety of pathovars of *P. syringae* are known to elicit non-host HR on *Nicotiana tabacum*, including pathovars syringae, tomato, phaseolicola, and pisi (Mysore and Ryu 2004). *N. tabacum* could be challenged with these bacteria in order to quickly determine whether vascular restriction occurs in other pathosystems.

In order to better assess whether leaf drying directly restricts bacterial growth by starving cells of water, bacterial pathogens could be genetically modified that are more highly resistant to water stress. Microarray analysis of *P. syringae* suggested that mechanisms such as osmoprotectant transporters and compatible solute synthesis were critical for this organism to

adapt to water stress (Chapter 3). Isogenic strains could be developed that over-express these systems and then tested for increased resistance to osmotic water stress and desiccation. These strains could then be used to trigger the hypersensitive response *in planta*. Increased survival of these strains compared to wild-type cells would be strong evidence that leaf water loss directly inhibits bacterial growth during gene-for-gene mediated resistance.

References

Chaerle, L., Van Caeneghem, W., Messens, E., Lambers, H., Van Montagu, M. and Van Der Straeten, D. 1999. Presymptomatic visualization of plant-virus interactions by thermography. Nat. Biotechnol. 17:813-816.

Hammond-Kosack, K. E., Silverman, P., Raskin, I. and Jones, J. 1996. Race-specific elicitors of *Cladosporium fulvum* induce changes in cell morphology and the synthesis of ethylene and salicylic acid in tomato plants carrying the corresponding *cf* disease resistance gene. Plant Physiol. 110:1381-1394.

Melotto, M., Underwood, W., Koczan, J., Nomura, K. and He, S. Y. 2006. Plant stomata function in innate immunity against bacterial invasion. Cell 126:969-980.

Mysore, K. S. and Ryu, C. M. 2004. Nonhost resistance: how much do we know? Trends Plant Sci. 9:97-104.

Wright, C. A. and Beattie, G. A. 2004. *Pseudomonas syringae* pv. *tomato* cells encounter inhibitory levels of water stress during the hypersensitive response of *Arabidopsis thaliana*. Proc. Natl. Acad. Sci. U.S.A. 101:3269-3274.

Wright, K. M., Duncan, G. H., Pradel, K. S., Carr, F., Wood, S., Oparka, K. J. and Cruz, S. S. 2000. Analysis of the N gene hypersensitive response induced by a fluorescently tagged tobacco mosaic virus. Plant Physiol. 123:1375-1386.